Structural and Ecophysiological Pattern in the Xero-Halophytic C_4 Grass, *Sporobolus rigens* (Tr.) Desv.

By TYGE W. BÖCHER and PETER OLESEN

Det Kongelige Danske Videnskabernes Selskab
Biologiske Skrifter **22**:3

Kommissionær: Munksgaard
København 1978

DET KONGELIGE DANSKE VIDENSKABERNES SELSKAB
udgiver følgende publikationsrækker:

THE ROYAL DANISH ACADEMY OF SCIENCES AND LETTERS
issues the following series of publications:

	Bibliographical Abbreviation
Oversigt over Selskabets Virksomhed (8°) *(Annual in Danish)*	Overs. Dan. Vid. Selsk.
Historisk-filosofiske Meddelelser (8°)	Hist. Filos. Medd. Dan. Vid. Selsk.
Historisk-filosofiske Skrifter (4°) *(History, Philology, Philosophy, Archeology, Art History)*	Hist. Filos. Skr. Dan. Vid. Selsk.
Matematisk-fysiske Meddelelser (8°) *(Mathematics, Physics, Chemistry, Astronomy, Geology)*	Mat. Fys. Medd. Dan. Vid. Selsk.
Biologiske Skrifter (4°) *(Botany, Zoology, General Biology)*	Biol. Skr. Dan. Vid. Selsk.

Selskabets sekretariat og postadresse
The address of the Academy is:

Det Kongelige Danske Videnskabernes Selskab,
Dantes Plads 5,
DK-1556 Copenhagen V.
Denmark.

Selskabets kommissionær
The publications are sold by the agent of the Academy:

MUNKSGAARDS BOGHANDEL,
6, Nörregade,
DK-1165 Copenhagen K.
Denmark.

Structural and Ecophysiological Pattern in the Xero-Halophytic C_4 Grass, *Sporobolus rigens* (Tr.) Desv.

By TYGE W. BÖCHER and PETER OLESEN

Det Kongelige Danske Videnskabernes Selskab
Biologiske Skrifter **22**:3

Kommissionær: Munksgaard
København 1978

Synopsis

Sporobolus rigens is a xero-halophytic grass species of the C_4 type. Six stages in the development and differentiation of the leaf blade tissues are described. The fifth is the stage of optimal photosynthetic activity; during the sixth stage chloroplasts and cytoplasmic material disintegrate.

Branching of the rootstock is initiated by buds of endogeneous origin; green parts are differentiated into cortical or endodermoid cells. The mucus of the root tips contains abundant bacteria; epidermal cells near the root tips have thick mucilaginous outer walls and cytoplasm of glandular tissue type. Two types of roots are produced: rather weak, mainly absorbing roots and strong anchorage roots. In older roots, the innermost cortex layer is transformed into an additional endodermoid layer. The cortex becomes lacunose, and sometimes weak, absorbing root branches grow downwards in the lacunae.

The mesophyll cells develop into arm cells: they branch and form internal wall ridges. The chloroplasts show normal grana development, they contain a peripheral reticulum, and their stroma contains electron-dense tubular structures that increase in number. Bundle-sheath cells form a modified, split Kranz sheath. The development of grana equals that in mesophyll chloroplasts, but the number of stroma thylakoids is less in bundle-sheath chloroplasts. During senescence, dense, two-phase vacuolar bodies containing phenolic substances develop in bundle-sheath cells.

In minor bundles, a special type of transfer cells and cells from which commissural strands issue are developed in the mestome sheath. The epidermis contains sunken stomata with particularly large subsidiary cells, which contain abundant lytic enzymes during senescence. At regular intervals short cells with specialized wall structure occur; these are interpreted as unicellular salt glands.

Emphasis has been laid on characters related to the C_4 type of photosynthesis and transport pathways in leaves. Evidence is presented that xero-halophytic C_4 grasses have primarily evolved adaptations related to perennation and resistance.

Key words: *Xero-halophytic, C_4 plant, root dimorphism, chloroplast ultrastructure, organogeny and differentiation, senescence.*

TYGE W. BÖCHER and PETER OLESEN
Institute of Plant Anatomy and Cytology
University of Copenhagen
83 Sølvgade, DK-1307 Copenhagen K.

Printed in Denmark by Bianco Lunos Bogtrykkeri A/S. ISBN 87-7304-063-0

Contents

Abbreviations: LM, light microscope; TEM, transmission electron microscope; SEM, scanning electron microscope; MS, mesophyll; BS, bundle sheath; ER, endoplasmic reticulum.

Introduction

Sporobolus rigens (Tr.) Desv. is in many respects an exceptional plant. The anatomy and morphology of its leaves were described in a previous paper (*Böcher* 1972) which, however, contained many unsolved questions of great interest. It is, therefore, necessary and tempting to present a monographic treatment, dealing not only with leaf differentiation and the structure of mature leaf blades, but also with the anatomy of roots, stems and leaf sheaths.

Sporobolus rigens is a typical xerophyte and at the same time a halophyte. It is highly specialized and has reached a high ploidy level. Its long, often slightly spiralled leaf blades exhibit a structure which has the characteristics of plants utilizing the C_4-dicarboxylic acid pathway in photosynthesis. The leaves have elongated cylindrical distal parts. The central cores in these leaves are made up of large, probably water-storing cells, while the peripheral parts contain many bundles arranged in a cylinder. The bundles have chloroplast-containing sheaths and an interfascicular mesophyll composed of arm cells. The sunken stomata are confined to epidermal stripes covering thee arm cell mesophyll. Some specialized short-cells in the epidermis are tentatively interpreted as salt glands, while other specialized cells in the mestome sheaths have properties indicating a function comparable to that suggested for transfer cells.

Sporobolus rigens occurs in Argentina on salt steppes or on shores of salt lakes. Ecological details are found in *Böcher, Hjerting* & *Rahn* (1972), *Werner* (1972, 1974) and *Ruthsatz* (1977).

In the present work a division of labour was practised so that essentially the LM work was done by T. W. Böcher whereas the TEM and SEM work was done by P. Olesen. Both authors, however, collaborated in the preparation of the manuscript resulting from mutual discussions of the observations.

Material and Methods

The present study is based on observations of material from plants raised from seeds of *Sporobolus rigens* (Tr.) Desv. kindly provided by Dr. *Fidel Antonio Roig*, Mendoza, Argentina; the seeds originated from Dorrego, Prov. Buenos Aires. In a few cases observations were made on leaf material collected and preserved in alcohol by the senior author during a journey in W. Argentina in 1955. Plants were grown in greenhouses in the Botanical Garden of the University of Copenhagen or in a controlled environment chamber (Fenger, Copenhagen).

For light microscopy (LM), fixation and embedding was either according to the paraffin technique (*Jensen* 1962) or to the glycol methacrylate technique (*Feder* & *O'Brien* 1968). Sections cut on rotary microtomes (steel or glass knives) were stained with Fast green-safranin, Sudan IV, *Johansen*'s quadruple stain (*Jensen* 1962), Periodic acid-Schiff (PAS), Toluidine blue (*Feder* & *O'Brien* 1968) or Aniline-blueblack (*Fisher* 1968). Furthermore, fresh sections cut by hand or on a freezing microtome were stained with ClZnI, $FeCl_3$, J-KJ, Sudan IV and Ruthenium red (*Jensen* 1962).

The photochemical activity of the chloroplasts in fresh hand sections of leaves was investigated with Tetranitro blue tetrazolium chloride (TNBT) and 3-(3.4-Dichlorophenyl)-1.1-dimethylurea (DCMU) as described by *Dyar* (1953) and *Olesen* (1974).

In a histochemical investigation of the localization and activity of acid phosphatase the technique of *Barka* & *Anderson* (1962) using 1-Naphthyl-phosphate or Naphthol-AS-phosphate as substrate was performed on fresh hand or cryostat sections. As control, incubation media without substrate were used.

For transmission electron microscopy (TEM), thin slices or small cubes of root and leaf tissue were fixed in different ways. The primary fixation was in (1) 3–5 % glutaraldehyde in 0.1 M Na-K-phosphate buffer pH 6.8 overnight at room temperature, or (2) 2 % para-formaldehyde and 2.5 % glutaraldehyde in 0.1 M Na-cacodylate buffer pH 7.0 for 4–6 hours at room temperature, or (3) as in (2) but with 4 % tannic acid added. In all cases the tissue was rinsed in 2–3 changes of buffer and post-fixed in 2 % OSO_4 in the same buffer as that used during the primary fixation. After post-fixation (4–6 hours at room temperature or overnight at 0–2 °C) the tissue was rinsed in buffer, dehydrated through ethanol, and embedded in low-viscosity epoxy resin (*Spurr* 1969) via propylene oxide. Because of the very hard and tough nature of this plant (most cell walls are conspicuously thickened and rather impermeable) it was very difficult to obtain adequate fixation and embedding; as a matter of fact it was only possible after prolonged time schedules at room temperature and the use of continuous rotation or agitation during fixation, dehydration and embedding. With mature and slightly senescing tissue it proved necessary to prolong the embedding procedure to one week or more, and to use vacuum infiltration.

Semi-thin sections (0.5–2 µm) of TEM tissue blocks were used for LM after staining with 0.05 % Toluidine blue at pH 8.3 and Safranin or Thionin (*Sievers* 1971) in combination with Mercuric bromphenol blue (*Mazia* et al. 1953). For TEM, tissue blocks were sectioned on a LKB Ultrotome with glass or diamond knives. Thin sections mounted on carbon-coated Parlodion or Formvar films were double stained with uranyl acetate and lead citrate as usual, or double stained without drying before staining and between uranyl and lead ("wet staining", *Mollenhauer* 1974). Sections were studied and photographed in a JEM T-7 electron microscope; magnification was calibrated with a cross grating replica.

For scanning electron microscopy (SEM), tissue blocks were fixed following the procedures for TEM (see above) with or without post-fixation in osmium. Dehydration was through water-ethanol, and the tissue was dried either by freeze-drying from benzene using an Edwards tissue drier or by critical point drying from amyl acetate and CO_2 with a Polaron E 5000 apparatus. After coating with carbon and gold in a conventional Edwards vacuum evaporator or sputter coating with gold (Polaron E 3000 sputter), specimens were viewed and photographed using Cambridge Stereoscan 600, Cambridge Stereoscan Mk II and Jeol JSM P-15 scanning electron microscopes.

In a preliminary survey of transpiration and photosynthetic rates in the genus *Sporobolus* (a comparison between species with cylindrical and flat leaves, respectively) the carbon dioxide compensation point for *Sporobolus rigens* was determined by *H. S. Heide-Jørgensen*. An infra-red gas analyser (IRGA, Grubb-Parsons, UK) was used in a closed gas exchange system with the leaf chamber placed in a controlled environment growth cabinet (Weiss, Giessen, West Germany). Values of 7–9 ppm CO_2 were measured.

Acknowledgements

This study was supported by the Danish Natural Science Research Council (grant nos. 511–1809, 511–6847 and 511–6975). The authors are indebted to *Marianne Philipp* for slides used for the chromosome countings and to *Henning Heide-Jørgensen* for determinations of the CO_2-compensation point. For excellent technical assistance we thank *Ella Buck*, *Lisbeth Thrane Haukrogh*, *Kirsten Pedersen* and *Svend Åge Svendsen*. We also thank *Bent W. Rasmussen* and *Hans J. Fuglsang* for operating the SEM's at the Zoological Museum and at the Institute of Historic Geology and Palaeontology, University of Copenhagen, respectively.

Results

A. Rootstock and basal stem internodia

Sporobolus rigens has a firm, tussocky growth form. Lateral rhizomatous shoots issue near the base of the primary ones and soon ascend or become erect. The rootstock usually carries many such lateral shoots which, however, rarely terminate in flowering culms. The majority of the basal shoots proceed vegetatively with distichuous leaves. The first and lowest leaves consist of sheaths only. They are followed by leaves with long, more or less green sheaths encircling the next leaves which terminate in blades. At the base the latter are hollow adaxially (crescent-shaped in cross sections), but become cylindrical distally (Fig. 9). Lateral shoots of the second order issue from the bases of first order shoots and likewise develop leaves in two alternate ranks, but the axes between two successive leaves are turned about 90° in relation to the axes of the mother shoots. Subbasal short internodia are sometimes formed. They may be without encircling sheaths and are green when exposed to light.

The anatomy of the rootstock is remarkable. The central narrow pith is surrounded by collateral vascular bundles in 3–4 strata. The abaxial bundles are surrounded by a thick sclerenchymatous cylinder in which the smaller outer bundles are embedded. Outside the cylinder follows an endodermis with secondary thickenings of the interior and radial walls. The thick walls are traversed by densely spaced pit canals. The mature rootstock endodermis resembles that described later in adventitious anchorage roots.

The xylem differentiates with the protoxylem placed towards the center. In the central strata with larger bundles the protoxylem tends to form a single row of vessels. This row becomes shorter in the peripheral bundles and is reduced to a few or no cells in those bundles which lie in the sclerenchymatous cylinder. Metaxylem develops on both sides of the protoxylem row. In peripheral bundles the wide metaxylem vessels may be the only functional xylem elements. The phloem parts are surrounded by semicircular sclerenchymatous areas.

The parenchyma between the bundles forms a regular network, but the regular pattern is broken by radial bundles accompanied by radially stretched parenchyma. The radially arranged cells form broad tissue areas resembling rays. They are found inside lateral buds which have an endogenous origin and resemble primordia of lateral roots. The sclerenchymatous cylinder and the endodermis disappear outside the radial "rays" which continue to the bud with its cap-shaped leaf primordia. The bundles continue in procambial strands terminating at the bases of leaf primordia (Fig. 1).

Longitudinal sections reveal an intricate system of vascular bundles. The axial main bundles are interconnected with radial bundles. Branching of main bundles occurs and the radial bundles often exhibit a deviating compound structure, being temporary unions of two or more collateral ones. Several anastomosing bundles are also found. The compound bundles may be bipolar (with two opposite protoxylem groups) or may occasionally approach a leptocentric structure.

There are several points of resemblance to the vascular system in stems of *Pandanaceae* (*Zimmermann, Tomlinson & le Claire* 1974).

Inside the rootstock endodermis in *Sporobolus* follows a pericycle of 1–3 cell rows. The living cells have thick walls which, however, after tangential stretching and division may appear rather thin.

The cortex has two distinct zones. The adaxial zone has tangentially stretched cells, many intercellular spaces and pits on short arms. The abaxial zone has shorter, often radially stretched cells dividing periclinally. Sometimes the cortex contains small veins or fibrous strands.

The epidermis is composed of short cells with thick cuticular flanges on abaxial parts of the anticlinal walls. In longitudinal sections, however, the cells are longer with interspaced short silica cells and few guard cells which are not sunken.

The green basal stem internodia deviate anatomically from the rootstock by a continuous endodermoid sheath encircling an atactostele with vascular bundles in three strata around a pith which gradually breaks down. As in the rootstock, the smallest abaxial bundles are embedded in a sclerenchymatous cylinder. Other sclerenchymatous areas occur in the cortex and are widest where the cortical chlorenchyma is absent. The latter occurs in connection with epidermal stomata which are not sunken.

The photosynthetic cells are organized in two interconnected groups. The spaces between the groups are occupied by parenchyma and sclerenchyma. The endodermoid cells have larger roundish cells either with few or no chloroplasts, or filled with chloroplasts which are conspicuously larger than those in the adjacent cortex chlorenchyma. The endodermoid green cells store abundant starch. Thus the layer appears as a starch sheath (Fig. 2).

Similar endodermoid layers with large chloroplasts were described by *Volkens* (1887: Plate XVII 1–2 pp. 56 and 149) in *Panicum turgidum* as a "Mantel von Sammelzellen". It is remarkable that the bundles in *Panicum*, as in *Sporobolus* where they are situated inside the endodermoid layer, have no bundle sheaths. Thus the endodermoid layer in such stems appears to be homologous to the bundle sheaths in leaves, wcich feature will be discussed later.

B. Root structure and development

Being a typical xerophyte, *Sporobolus rigens* exhibits several anatomical characteristics corresponding to those described in desert grasses, e.g. by *Henrici* (1929), *Goosens* (1935) and *Hansen* et al. (1976).

Root tip mitosis

Squash preparations made by *Marianne Philipp* showed that *Sporobolus rigens* has approximately 144 very small chromosomes. The exact 2n number was impossible to establish. Some of the chromosomes appeared larger than the rest or were not clearly distinguishable. The number may exceed 144 slightly. However, considering that 36 is the most common number in the genus, 144 would fit well in a series starting with 36.

Cytology of mucilaginous root tips

Root tips from potted plants always have a mucilage layer surrounding the cap and extending along the root surface distal to the root hair zone. The mucus which contains abundant ellipsoidal bacteria is produced mainly by the cap cells but also by the epidermal cells next to the cap (Fig. 3). During this production the outer cap cells loosen and occur as islands in the mucus. Concomitant to the release of peripheral cap cells, the wall chemistry changes, as observed after staining with toluidine blue, and often becomes invaded by bacteria. The protoplasts of the released cells disintegrate gradually, but curiously enough the plasmodesmata in their walls are maintained.

The mucilage itself appears doubly refractive but does not react with ClZnJ. In TEM the mucilage apparently has a homogeneous texture with no signs of a fibrillar structure. The cap cells exhibit ultrastructural features characteristic of glandular tissues, e.g. hypertrophic dictyosomes, long parallel cisternae of rough ER and numerous small vacuoles and vesicles. It is a question whether the mucilage is produced during the disintegration of released cap cells or is secreted by the coherent cap tissue. The presence of mucilage along epidermal cells between the cap and the root hair zone

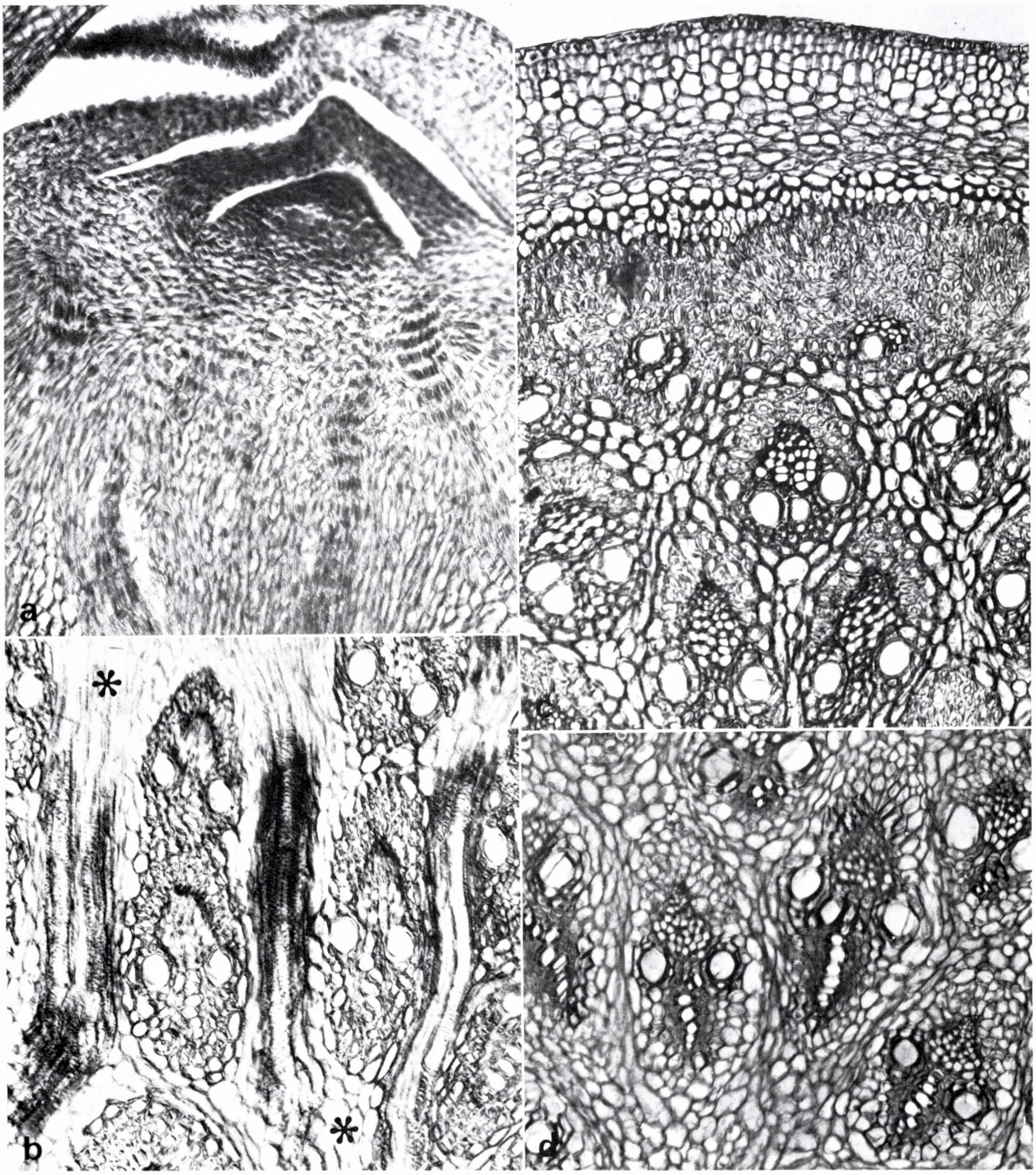

Fig. 1. Transverse sections of rhizome (× 333). – *a.* Initiation of lateral shoot showing cap-shaped leaf primordia and procambial strands. – *b.* Area inside lateral bud showing tissue areas resembling rays (*) and containing radial bundles, furthermore cross sections of several collateral bundles. – *c.* Outermost part with epidermis, cortex, endodermis, pericycle and stele with parenchyma network and peripheral bundles. – *d.* Interior part: bundles containing wide metaxylem vessels and rows of protoxylem.

and the fact that the epidermal cells structurally resemble a glandular tissue suggest that these cells participate in mucilage production. In LM a gradual transition between the epidermal outer wall and the mucilage is evident. The outer surface of the mucilage is apparently limited by a thin film to which soil particles and cell remains adhere. It is obvious that the epidermal cells undergo frequent anticlinal divisions.

The nuclei in the secreting epidermal cells are conspicuous and occupy a central position. Numerous vacuoles with a loose fibrillar or granular content are found in outwards and inwards directions. Most cells contain proplastids with starch grains and a dark staining dense granular matrix (Plate I). In some cells vacuoles contain a dark region with a similar dark granular texture. The structural difference found between cells with few and many vacuoles indicates a correlation between, on one hand, few vacuoles and abundant proplastids with starch and, on the other hand, many vacuoles containing a fibrillar material concentrated in the center and few proplastids. A theory involving autolytic breakdown of starch and whole proplastids leading to the production of vacuoles with granular or fibrillar contents appears probable. In the outer half of the cells the cytoplasm is densely spaced with ER cisternae of the rough type, dictyosomes and mitochondria. The dictyosomes are particularly frequent in the outermost zone where they appear associated with vesicles containing a dense fibrillar material (Plate Ib).

The outer boundary of the epidermal cells appears very irregular showing numerous various-sized projections of wall material into the cytoplasm. The very thick wall is slightly stratified except in the innermost zone which displays a homogeneous texture and density similar to that found in the dictyosome vesicles.

The plasmalemma is appressed to the wall except for wall areas projecting into the cytoplasm where a light, empty zone is inserted between plasmalemma and the wall material. This light zone may represent remains of vacuoles discharged through the plasmalemma. In between the projections numerous microtubules are found close to the plasmalemma, whereas they are absent from the projections themselves. The anticlinal walls are thickest near the outer wall where they show small projections similar to those in the outer wall.

The ecological significance of the mucilage is not sufficiently understood. It was discussed by *Goosens* (1935), who assumed a dual function in protecting the root tip against water loss as well as in facilitation of water absorption from the soil. Other unsolved problems concern a possible role of the bacteria occurring in the mucilage around the root cap. The structural similarity between the outer epidermal cells walls and the wall ingrowths found in transfer cells is evident (see further pp. 22 and 24).

Root dimorphism

Sporobolus rigens produces two types of roots (A and B) which are distinguished by the different development of endodermis and the pericyclic tissues. Type A continues to have rather thin endodermal and pericyclic walls (Fig. 4c). The primary stage of development is prolonged or maintained. In cases where the root attains a greater diameter, the walls become thicker but they never reach the tertiary stage. In young roots the majority of endodermal cells soon get a suberin lamella all around, but no Casparian strips. Typical passage cells are not developed, but a number of cells are without suberin lamellae and are placed outside the protoxylem groups. Many cells in the cortex layers also develop suberin lamellae and the cells next to the endodermis often have thickened tangential walls which lignify. The passage areas in the endodermis appear to continue as irregular, radial cortical cell rows without wall thickenings (Fig. 7). The majority of roots of the A-type are small and lateral. Some develop in cortex lacunae in larger roots of the B-type.

Type B. Already in young roots the endodermis reaches the tertiary stage (Fig. 5). The tangential and radial walls thicken as does the pericycle which becomes sclerenchymatous. In transverse sections

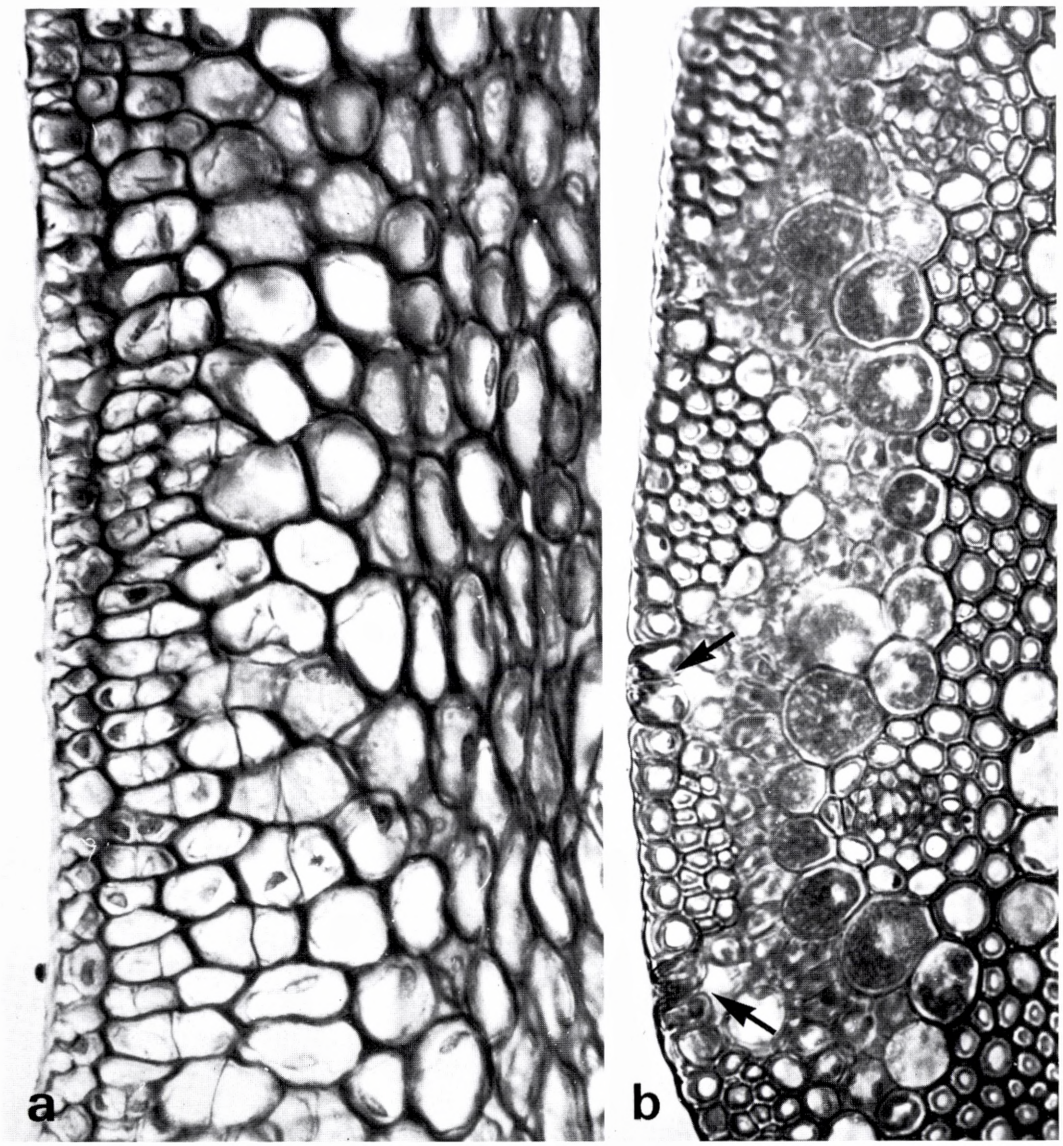

Fig. 2. a. Transection of subterraneous rhizome: epidermis with conspicuous cutinized flanges in anticlinal walls. Cortex in two different strata; the outer with numerous new periclinal walls, the interior with some tangential stretching of the cells (× 500).– *b.* Transection of green basal stem internodium. Arrows show stomata surrounded by sclerenchyma and leading into chlorenchyma. The latter consists of small outer cells and a conspicuous endodermoid layer of larger cells with abundant starch-containing large chloroplasts (× 500).

the central core in young roots resembles a star and shows up brightly in polarized light. The thick walls consist of lignified cellulose. The tertiary layers in the endodermis react with phloroglucinol-HCl, but the latest deposited layer sometimes remains unstained. On the other hand, it does react with ClZnJ. The suberin lamella is continuous and easy to demonstrate with Sudan IV and appears as bright lamellae in TEM micrographs (Fig. 6). No passage areas were detected. The outer part of the radial walls in the endodermis remains thin, making possible tangential connections between the endodermal cells.

The walls of the cortex layer next to the endodermis develop continuous suberin lamellae and behave as an additional endodermis. Tertiary thickenings are formed early. Sometimes such thickenings and suberin lamellae are formed even in the second cell layer outside the endodermis. In older roots the tertiary endodermal thickenings increase and the pit canals which reach the suberin lamella become longer. Some of them, however, do not reach the cell lumen but are blocked, being overtopped by the latest formed wall lamellae (Fig. 5).

A final stage in old roots is characterized by very thick tertiary deposits on the tangential walls in two layers, the genuine endodermis and the additional one of more flat cortex cells. The thick tertiary deposits on the inner tangential walls appear stratified which, as shown by TEM, is due to a different orientation of the component fibrillar material.

Tertiary thickenings of the same type occur in the interiorly persisting cortex layers in *Sporobolus fimbriatus* and *S. indicus* studied by *Goosens* (1935). In *Aeschynanthus* they are described by *Guttenberg* (1943) but here the genuine endodermis is without thickenings. In *Zea* and *Saccharum* tertiary endodermal thickenings are described by *Kroemer* (1903). They resemble those in *Sporobolus rigens* although in the latter the deposits in the middle parts of the cells are so thick that they form wall humps (Fig. 4, 5).

The pit canals in *Sporobolus rigens* have funnel-shaped widenings opposite similar widenings in the canals of the adjacent pericyclic cells. Plasmodesmata between the widenings of a pit-pair were impossible to detect in LM because the suberin lamella which they have to penetrate is as dark as the plasmodesmata themselves. In TEM, however, the plasmodesmata evidently traverse the pit membranes and continue unbroken through the suberin lamella, but they exhibit a distinct constriction in the area of contact with the suberin lamella. The pit canals are densely spaced and the cells on both sides of the pit-pair keep living. It is therefore likely that the pit system enables water uptake, but that water contained in the thick walls can only enter the stele through the plasmodesmata. The occurrence of two endodermoid layers with strong wall thickenings and pericyclic sclerenchyma points towards a mechanical primary function. In roots of the B-type the conducting tissues are protected from water loss even in cases where the cortex and epidermis are injured.

The cortex exhibits a clear stratification. In the interior layers next to the endodermoid layer the cells are tangentially flattened and form regular rows. They have relatively thick walls and many narrow intercellular spaces. Some radial walls are particularly thick and brownish.

The middle cortex also has regular radiating cell rows. However, the cells are larger and have thin walls. At certain intervals the cells are dissolved and cavities are formed. The cavities may be very wide and separated only by narrow tissue columns which abaxially are connected with the outer cortex layers. In the beginning these are collenchymatous and thus without intercellular spaces. Later the cells develop into sclerenchyma, their walls becoming uniformly thickened and lignified.

The middle cortex thus develops into a kind of spongy parenchyma. However, in the surroundings of lateral roots which penetrate the cortex no cavities are formed. Such roots are demarcated by thick and lignified walls towards the cortex of the older maternal root. *Henrici* (1929) and *Goosens*

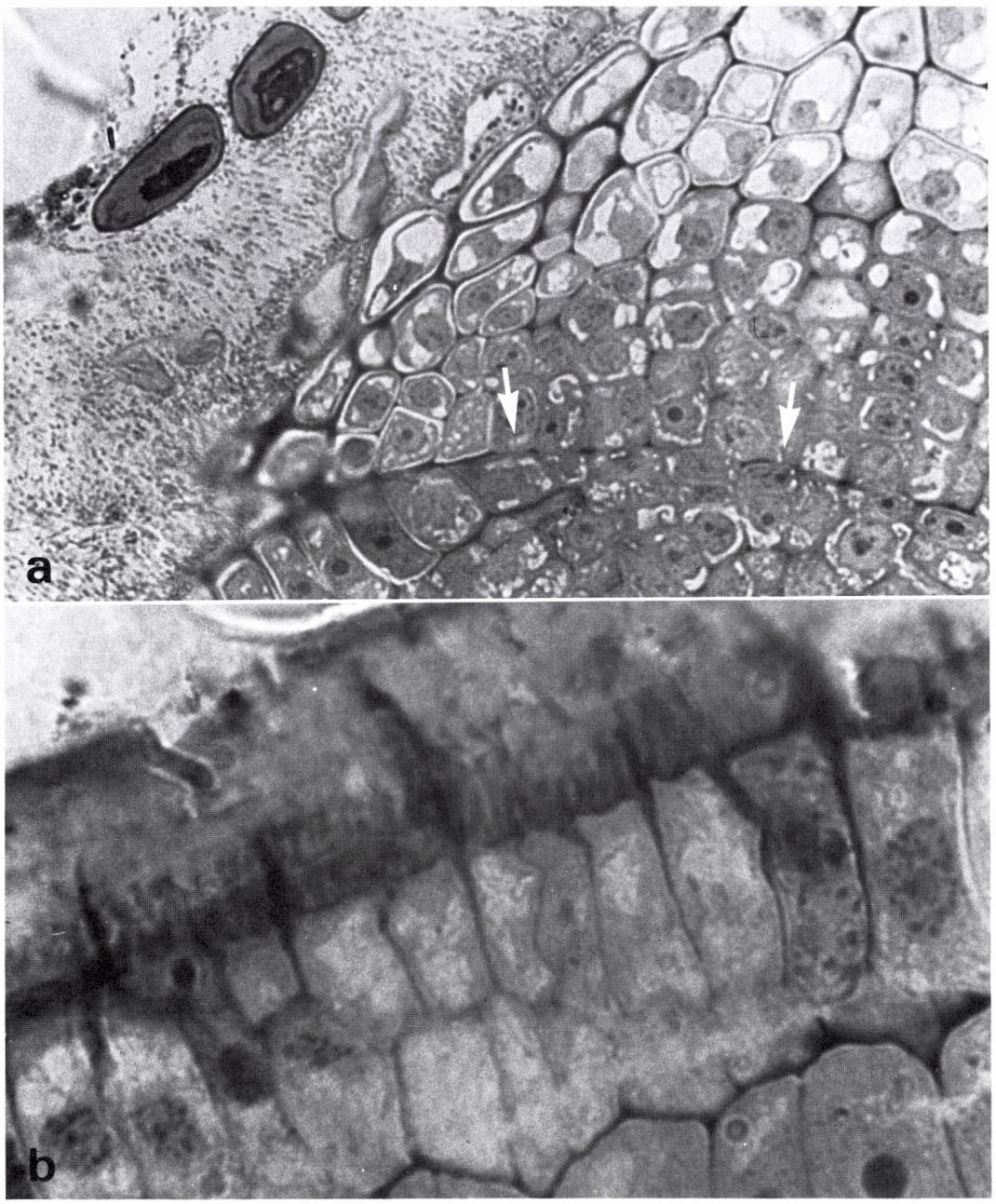

Fig. 3. Longitudinal sections of root tip. Toluidine Blue. – *a.* Root cap producing mucilage which contains abundant bacteria and discharged cap cells. Boundary between cap and tip meristem indicated by white arrows (× 1,200). – *b.* Mucilage producing epidermal root cells near the tip. Interior part of the thick mucilaginous wall with many parallel, radiating dark structures (× 1,800).

(1935) found similar lysigenous cavities in the root cortex of South African xerophytic grasses. They interpret the lacunose tissue as an aerenchyma of importance for the oxygen supply and state that roots without spaces die presumably as a result of suffocation. However, *Henrici* also believes that a perforated middle cortex may act as a sponge from which water may be taken up.

In old roots of *Sporobolus rigens* it is not unlikely that water may rise by capillarity in the spongy cylinder between the outer and interior cortex and pass to the endodermoid layer and the endodermis where a further uptake is controlled by these layers of living cells . In some of the roots the cavities contain small roots of the A-type (Fig. 7). These small roots are weak lateral roots which when reaching the firm outer cortex turn and grow into one of the cavities. They may fill a cavity which was already formed or in some cases contribute to its formation. In one case a narrow root of this kind issued from another of the A-type which presumably had stopped its growth near the surface of the mother root. The narrow root could be followed in a longitudinal section of the mother root; it was slightly bent inside the cavity and produced no root hairs. In many cases the small roots issue from globular primordia formed at the end of a vascular core or on its sides as swellings surrounded by endodermis. On the surface such primordia appear as small outbulgings. Sometimes their growth is hampered and they are transformed into small localized cork tumours. Different procaryotic cells sometimes occur abundantly in or along the partly decomposed margins of the cortex bordering the lacunous middle layers.

Rootlets of the A-type resemble those described from many species inhabiting wet soil (see e.g. *Freidenfelt* 1904). They may be adapted to higher moisture in the surrounding medium (shores of salt lakes), but how they really function remains unknown.

The occurrence of two root steles within a common cortex sheath was described by *Henrici* and *Goosens* in the South African grass *Pogonarthria squarrosa*. Figure 7 in *Goosens*' paper shows that the small root in the cortex of the mother root even produces root hairs. But in this case no root dimorphism was ascertained. Recently *Goller* (1977) has shown that in *Stipa joannis* up to twelve lateral roots take a parallel course down the cortex forming a "cable" together with the stele of the parent root.

The conditions which determine the development of the root types A and B in *Sporobolus rigens* need to be clarified. We know about differences found between apices of long and short roots in *Euphorbia* (*Raju* et al. 1964). In *Sporobolus* we assume similar differences between weak A-roots, mainly assisting in uptake of water and ions, and strong B-roots responsible for the anchorage of the plants and root penetration into soil areas previously unutilized.

C. Anatomy of the leaf sheaths

Transverse sections of vegetative shoots usually show two central blades. The upper (youngest) is almost cylindrical and placed in the hollow of the leaf blade base of the second-youngest leaf. Together they fill out a cylindrical core and are encircled by sheath parts of one or two leaves below (Fig. 9).

The outermost sheath differs from the interior younger one mainly in two ways. (1): The subepidermal outer part of the sheath is sclerenchymatous, i.e. it consists of vascular bundles with abundant sclerenchyma alternating with and occasionally merging with pure sclerenchymatous strands. Subepidermal fibers strengthen the interior surface of the sheath. (2): In the middle part of the sheath wide lysigenous cavities occupy large parts of the mesophyll.

The interior sheath may encircle the central core twice. Sclerenchyma is found exclusively on the outer sides of the bundles. Lysigenous cavities are small or missing.

Following a leaf sheath from its basal part to the blade, continuous changes in the distribution and quantities of tissues and cavities can be ascertained:

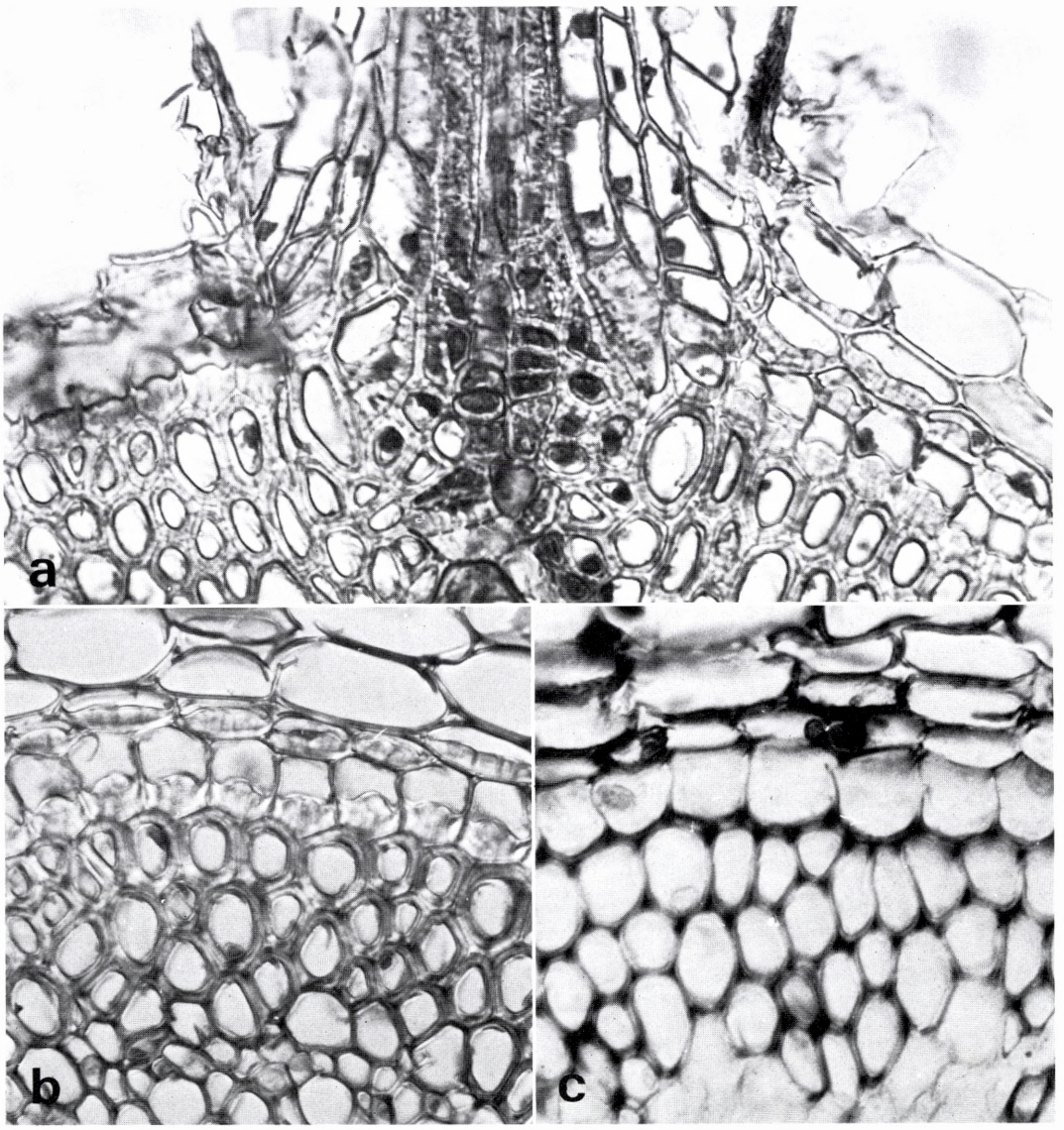

Fig. 4. Transections of roots showing details of endodermis and formation of lateral root. – *a*, *b*. Strong anchorage roots (B-type) with additional endodermoid layers. Semipolarized light (× 500). – *c*. Roots of type A with weakly thickened endodermal walls (× 640).

pure sclerenchymatous strands decrease, cavities become smaller and less frequent. In the basal parts, bundle sheaths of thick-walled cells surround the adaxial xylem part in the bundles and sometimes contain starch grains or chloroplasts. In the upper parts, chloroplasts in the bundle sheath increase in number. In areas between the bundles, empty cavities gradually become replaced by chlorenchyma of the arm cell type. These chlorenchyma stripes have a few connections to stomata in the adjacent outer epidermis. In a single case in the basal part an air-filled cavity was connected with a stoma by a funnel of wide empty cells with large simple pits in their walls. Such a funnel was believed to function as a lenticell.

In the uppermost part of the sheath a regular alternation between bundle areas and green arm cell mesophyll begins. This structure continues in the blades. Where the leaf sheath contains green tissue stripes, they may anatomically resemble stem internodia. However, the latter have a continuous endodermoid layer, while in the leaf sheaths the bundle sheaths, in cross sections, form semicircles around bundle areas issuing on both sides of the bundle fiber plates.

In cases where chlorenchyma separates a small vein and a larger bundle, the sheath belonging to the latter is green in the part bordering the chlorenchyma but thick-walled and empty elsewhere (Fig. 8).

D. Differentiation of the leaf blade tissues

In longitudinal sections of young leaf bases it is hardly possible within the intercalary meristems to distinguish between procambial and non-procambial cells. On both sides of the meristematic zone, however, a location of procambial strands becomes obvious by the maturation of protoxylem elements, but a clear distinction between bundle sheath primordial cells and other primordial cells was not possible in the meristem itself. A striking question is, how can the apical zone and the first leaf primordia be supplied with water and nutrition without direct vascular connections? As in e.g. *Triticum* (cp. *Sharman* & *Hitch* 1967) we assume that the growth is ensured by general diffusion.

The stages mentioned in the following are not clearly demarcated. Transition from one stage to the next is completely smooth, but for convenience the differentiation is described in discrete steps. A survey of the mature leaf blade anatomy is found in a previous paper (*Böcher* 1972).

Stage 1. In the youngest blades inside the encircling sheaths a differentiation soon becomes obvious between epidermis, bundle areas and inter-bundle areas. The latter are parenchymatous and pass smoothly into the central parenchyma of larger cells which resembles a pith (Fig. 9a). At this stage guard cell precursors are differentiated as somewhat larger cells with conspicuous nuclei situated outside inter-bundle areas.

Bundle sheath cells (in the following BS cells) can be traced as the first layer of enlarged cells on both sides of the bundle areas. The outermost BS cells are smaller and reach the epidermis. The layer inside the BS precursors is the mestome sheath initials. They are not differentiated from the procambial cells or the cells which later develop into fiber plates. However, in transections of small veins it is possible in a few cases to detect one or two deviating cells among the mestome sheath initials. These cells had particularly large nuclei and densely stained cytoplasm. They were believed to be precursors for transfer cells (cp. p. 22) or mother cells for commissural strands which always issue from cells placed opposite transfer cells (*Böcher* 1972, Fig. 3A).

Stage 2. A pronounced increase in the size of the BS cells has taken place. These cells contain larger nuclei than the cells on their sides. The inter-bundle parenchyma is now differentiated usually in three rows of cells between the BS cell rows. The central row has fewer and wider cells than the two rows next to the BS rows (Fig. 10a).

At this stage cells in the inter-bundle parenchyma develop into arm cells which in the following are referred to as mesophyll cells (MS cells). The

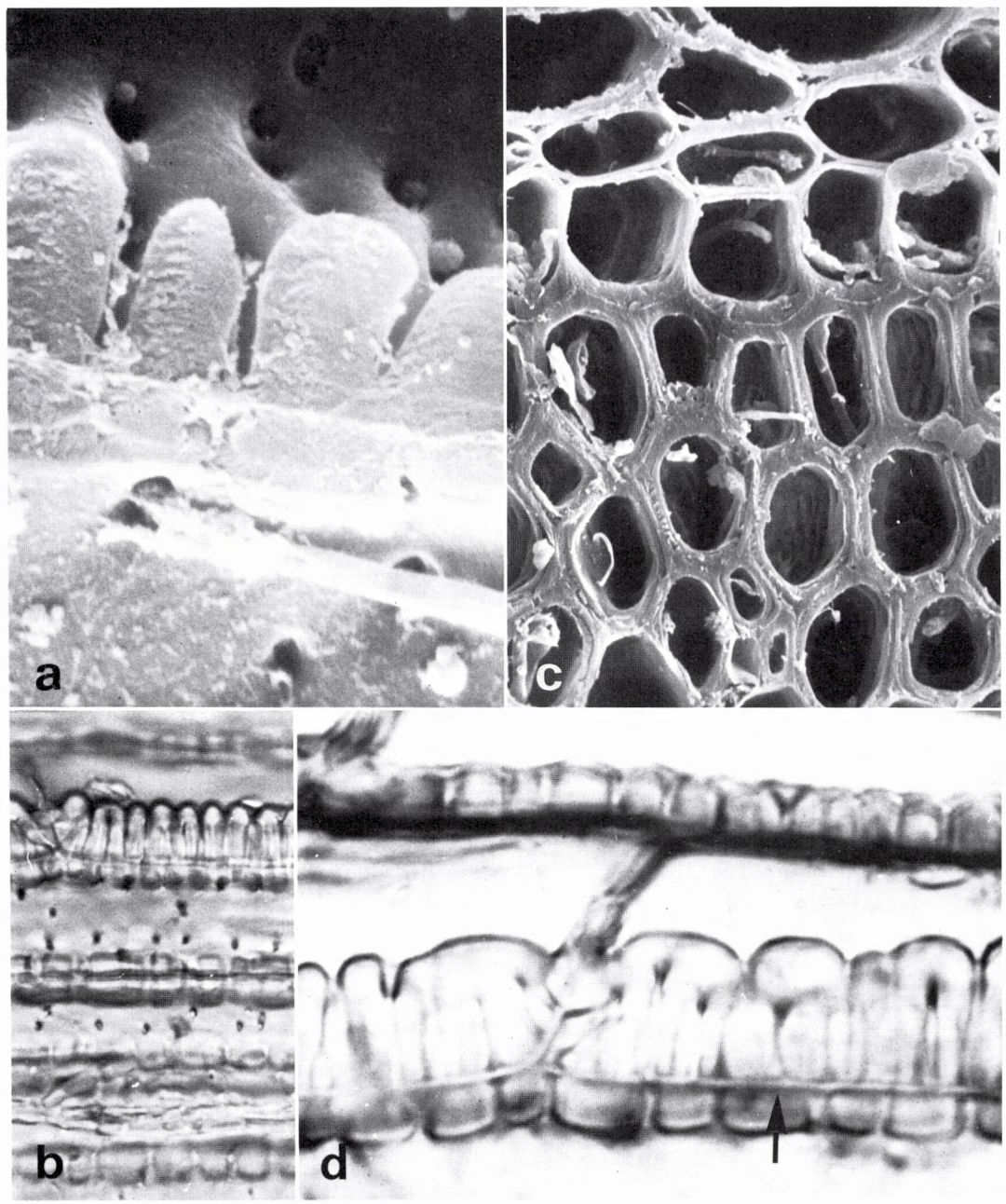

Fig. 5. Endodermis in roots (a, b, d B-roots and c A-root). – *a.* SEM of inner tangential wall with pit canals (× 5,650). – *b.* Longitudinal section of endodermis and pitted pericyclic cells (× 800). – *c.* SEM of endodermis and adjacent layers in weak root (× 1,150). – *d.* Details of endodermis and additional endodermoid layer showing overlayering of branched pit canals by thick tertiary deposits. Conspicuous suberin lamella (arrow) (× 2,000).

development into arm cells is characterized by an incipient formation of intercellular spaces resulting from a localized dissolution of the middle lamella and formation of small ingrowths in the longitudinal walls (Fig. 9b and Plate IV). The localization of these wall ingrowths, which are particularly frequent in walls abutting BS cells, is determined by a band of 15–25 microtubules running just inside the plasmalemma as shown in cross and paradermal sections, Plate IV. The ingrowths are in fact internal ridges which partly partition the cells. Their growth is accomplished by deposition of new wall material accompanied by a withdrawal from the neighbouring cells, resulting in the formation of new tubular intercellular spaces.

The participation of microtubules in the development of internal ridges was also noted in armed mesophyll cells of *Pinus strobus* by *Harris* (1971). A similar role of microtubules is well-known from wall-thickenings in xylem elements (*Pickett-Heaps* 1967) and has also been demonstrated in hyalocytes in leaves of *Sphagnum* (*Schnepf* 1973). Thus, the development of armed mesophyll cells of different origin provides further evidence for the general importance of microtubules during the development of wall-thickenings.

The development of air spaces and internal ridges commences just inside the substomatal cavities and proceeds further into the MS areas. In the epidermis, stomatal complexes with guard cells and subsidiary cells become differentiated (Fig. 10) as well as regular alternation between short and long cells. A few of the short cells are already differentiated as silica cells.

The BS cells never reach the epidermis. A subepidermal layer of smaller cells separates the BS cells from the epidermis. Later the smaller cells develop into cells which are intermediate between BS cells and fibers. They have pit connections with BS, MS, fiber and epidermal cells. Typically these cells are located between the outermost BS cells and specialized epidermal short cells which may function as salt glands (see p. 24).

In the basal part of the blade the smaller bundles near the margin of the concave adaxial surface are sometimes completely surrounded by BS cells (Fig. 13c), but in a vast majority of cases the green BS cells appear as two one-layer cell plates on each side of the bundle with its mestome sheath and fiber plate.

The BS cell plates bring about a compartmentation of the peripheral part of the blades. Later the division becomes even more pronounced when the inter-bundle parenchyma develops into arm cell mesophyll (MS).

At stage 2, full-grown chloroplasts are absent from both tissues which later become responsible for maximum photosynthesis.

TEM studies, however, reveal that small proplastids in BS and MS develop few thylakoids and have small starch grains (Plate II).

In the BS cell rows the mitotic activity ceases but appears to continue in the MS rows, perhaps particularly in the lateral ones where the divisions are inclined to be unequal. In larger bundles the protophloem is maturing as are the fibers next to it.

Stage 3. As a result of further intercellular space formation and growth of internal ridges, the MS cells undergo a complicated branching and finally they appear as plicate mesophyll or arm cell tissue. The internal ridges form walls projecting far into the lumina of the cells. In their innermost parts these wall projections split and thereby surround loop-like cavities which undoubtedly become part of a continuous air space system (Fig. 12b). The central parts of the cells with the nuclei maintain a cylindrical form and in median cross section it appears as if this central part had become separated from the arms by a cylindrical (circular) wall (Fig. 12a). The interpretation of this phenomenon led to the erroneous suggestion of a formation of cylindrical holes in the MS cells (*Böcher* 1972).

The BS and MS cells develop numerous chloroplasts which are placed along the walls. They are usually oval or spindle-shaped, rarely spherical. The BS chloroplasts are significantly larger than those in the MS. The formation of thylakoids is rather advanced and distinct grana are developed.

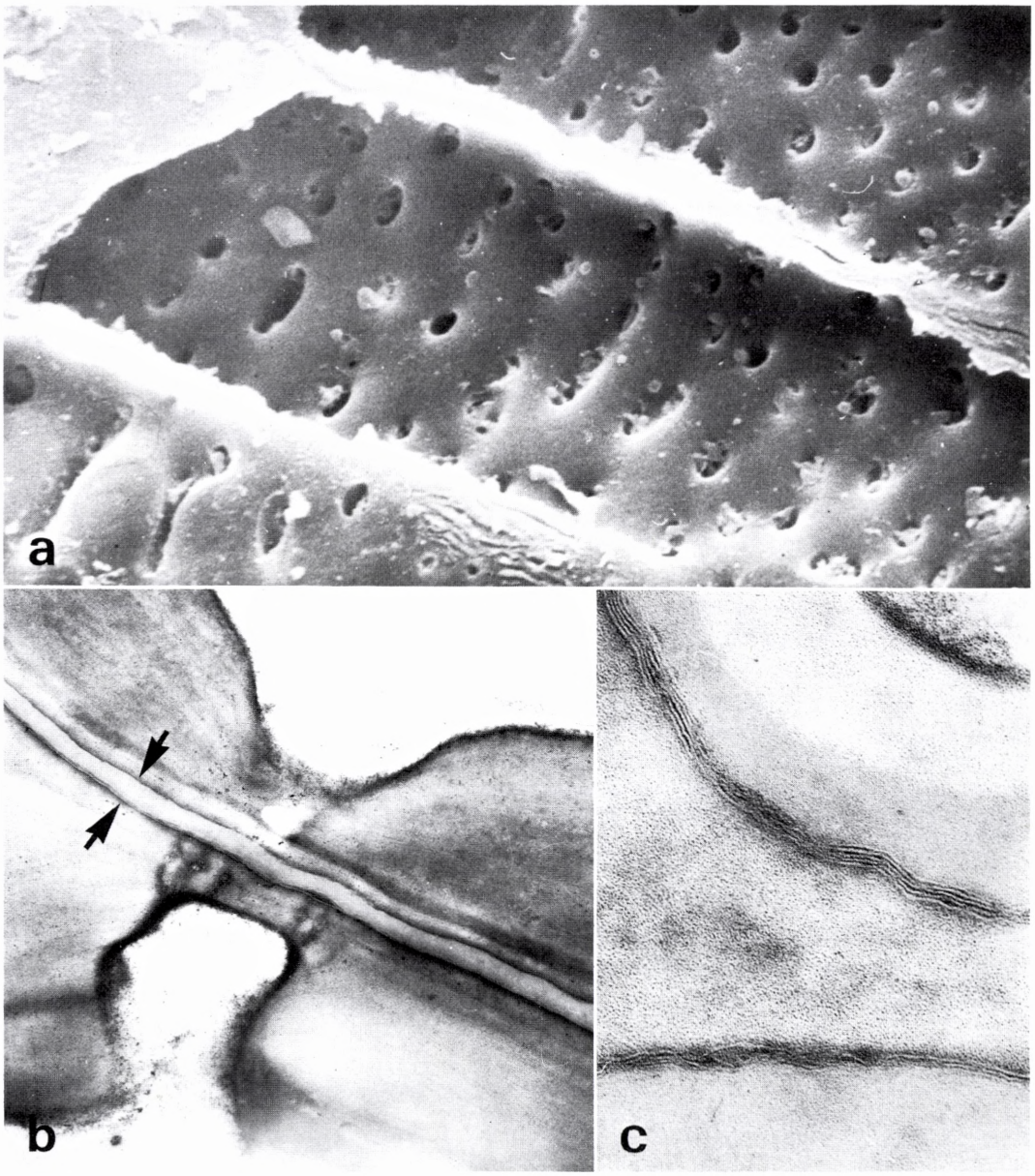

Fig. 6. Electron micrographs of endodermis in strong roots (B-type). – *a*. SEM of entrances of pit canals seen from the lumen of endodermal cells (× 3,300). – *b*. TEM of pit pair with plasmodesmatal connections seemingly stopping at the suberin lamella (arrows) (× 18,150). – *c*. TEM showing details of suberin lamellae (× 83,250).

Starch grains are still present but their number has decreased (Plate II).

At stage 3, the BS cells often exhibit outbulgings in the walls separating the sheath cells. The outbulgings resemble folds in endodermal radial walls in the areas where Casparian strips are formed (Fig. 11b, c). These wall structures, however, disappear as soon as the walls become thicker. The folds may represent an artefact created during fixation and dehydration (cp. *Clarkson* et al. 1971), but the fact remains that the BS cells temporarily show a structural phenomenon characteristic of endodermal cells.

During stage 3, the fiber plates become clearly differentiated, but the walls in the fiber cells are still fairly thin and nuclei remain present. In the larger bundles the phloem and the metaxylem are fully developed.

The outer epidermal walls increase in thickness and cutinize. The guard cells and the salt gland short cells are further differentiated (Plate V). The latter are placed regularly near stomatal openings but are separated from the subsidiary cells by one or a few normal epidermal cells. The salt gland cells differ from normal epidermal cells by the maintenance of a large central nucleus and a much lower degree of vacuolization. In the dense cytoplasm a kind of proplastids with homogeneous granular contents appear in increasing numbers, as well as mitochondria and dictyosomes. The development of a characteristic stratigraphy of the outer walls has commenced (see p. 24).

Stage 4. During this stage chloroplasts of a roundish shape develop in both types of photosynthetic cells. They occur in all parts, although mainly along the walls. The walls of the BS cells increase considerably in thickness apart from the numerous pits which become particularly conspicuous in the walls towards the MS cells and the transfer cells and between adjacent BS cells. The nuclei of the latter have not yet assumed their final position at the walls towards the MS cells (Fig. 13).

In the phloem the cell walls increase conspicuously and become heavily stained with toluidine blue, indicating contents of pectic substances or hemicellulose. A similar cell wall increase takes place in the transfer cells. Here the walls become traversed by fairly long pit canals. The nuclei of these cells are always placed in a central position and reach a remarkable size (Fig. 16a). Also the cell walls in fibers and in epidermis increase by adding several new wall layers which show up brightly in polarized light.

Stage 5. The final arrangement of the BS chloroplasts takes place. Further they attain their final size and shape which can be characterized as thickened discs. Their size is at least twice that of the MS chloroplasts (Plate III). The arrangement proceeds gradually and is finished first in the cells which are closest to the epidermis. The two rows of BS cells belonging to the same bundle show the same sequence at the same time, but the development in all bundle sheaths in the same leaf is not simultaneous. The cells placed nearest to the central parenchyma maintain a scattered position of the chloroplasts, while the chloroplasts in the adjacent cells are moved towards the walls of the bundle side. The nuclei move to the opposite side at the walls towards the MS cells. Generally the chloroplasts are densely spaced along the wall facing the bundle (Plate VIIa) and a large central vacuole occupies the space between the chloroplasts and the nucleus. The disciform chloroplasts seem always orientated with their flattened sides parallel to the leaf surface, e.g. against the light. During stage 5, the chloroplasts continue their growth and undoubtedly reach their maximal photosynthetic capacity. Concomitantly large numbers of well-developed elongated mitochondria accumulate between the chloroplasts. The highest concentration of mitochondria is found in the area adjacent to the wall facing the bundle.

At the same time as the chloroplasts reach their final shape and size, they complete the differentiation of the internal lamella system. Well-developed grana are separated by relatively few stroma thylakoids (Plate IIIb). The peripheral

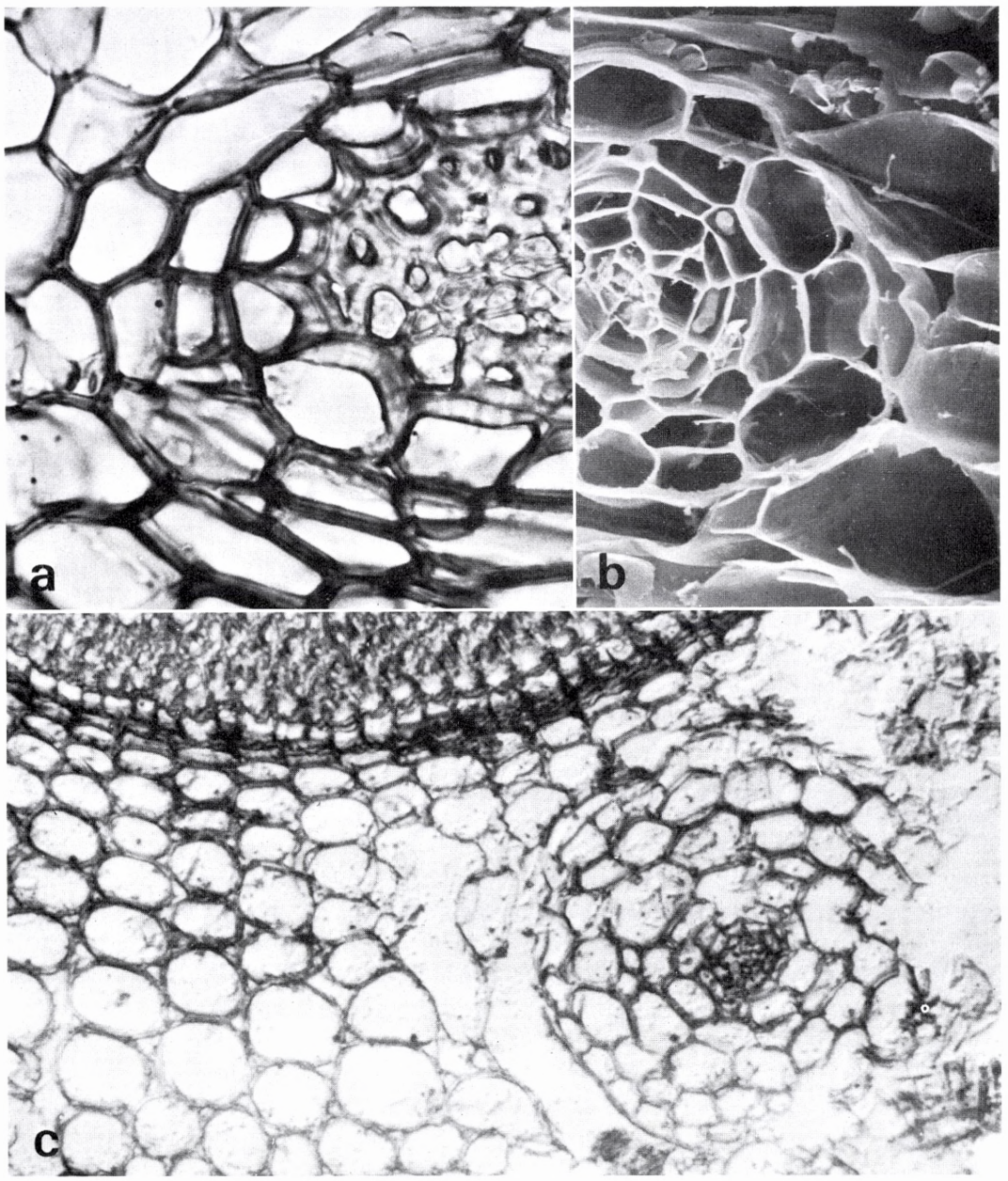

Fig. 7. Transections of young roots. – *a*. B-root in semipolarized light (× 500). – *b*. SEM of A-root (× 540). – *c*. A-root penetrating cortex in older A-root where the cortex cells are arranged in regular radial rows (× 250).

reticulum characteristic of C_4-plants is poorly developed in the BS chloroplasts.

The chloroplasts in the MS cells appear quite normal in shape, size and thylakoid arrangement, but here the peripheral reticulum is well-developed (Plate IIIc, d). An interesting feature of MS chloroplasts is the inevitable presence of semi-crystalloid aggregates of electron-dense tubules (Plate IIIc, d). These tubules measure 150 Å in outer diameter and are placed hexagonally with a center to center spacing of 200 Å. At high magnification it appears that the tubules are composed of more or less globular subunits much like the situation known from cytoplasmic microtubules (Plate VIIIc, d). The number of these subunits is 5–7 compared to 13 protofilaments in cytoplasmic microtubules. The interpretation of hollow tubules composed of subunits is further stressed by micrographs obtained after fixation with tannic acid (*Olesen* 1978, Figs. 13–16) and our Plate VIIIe.

A comparison of MS and BS chloroplasts indicates that the development of grana in BS cells is at least equal to that in MS cells. Thus it appears as a deviation from the situation normally encountered in C_4-plants. A closer examination of the thylakoid configuration and the degree of grana formation in the two types of chloroplast (Table 1) clearly supports this assumption. The analysis shows that the total amount of grana thylakoids is equal, while the ratio of grana thylakoids to stroma thylakoids is significantly higher in BS chloroplasts. A demonstration of a higher degree of thylakoid stacking in BS chloroplasts relative to MS chloroplasts has never been mentioned in previous treatises of chloroplast structure in C_4-plants.

The two parts (sides) of the thick walls separating MS and BS cells exhibit an interesting difference after staining with toluidine blue. The thin parts belonging to the MS cells attain a dark bluish-violet colour, while the thicker BS cell parts show a pale bluish tint indicating some lignification.

Table 1. Analysis of thylakoid configuration and the degree of grana formation in mesophyll and bundle sheath chloroplasts in *Sporobolus rigens*.

	Grana thylakoids (G) mm/mm²	Stroma thylakoids (S) mm/mm²	G/S ± S.D. (n = 10)
Mesophyll chloroplasts	0.33 ± 0.17	0.19 ± 0.09	1.7 ± 0.3
Bundle sheath chloroplasts	0.39 ± 0.12	0.08 ± 0.01	4.7 ± 0.4

Ten distinct electron micrographs were selected for each type of chloroplast and the length (mm) of grana thylakoids (G, thylakoids with at least one of the sides forming part of a partition*) and stroma thylakoids (S, thylakoids separated from other thylakoids by stromal material) was determined and related to chloroplast area (mm²). *A partition is here defined as the electron-dense line between two appressed thylakoids in a granum.

As in many other grasses (cp. *Brown* 1975), the green BS cells are separated from the vascular tissues by a mestome sheath consisting of very long thick-walled sclerenchymatous cells with numerous pits (Plate VII). As shown by *O'Brien* & *Carr* (1970) in Festucoid grasses, some of these mestome cells develop a suberin lamella. In *Sporobolus* similar two-layered lamellae occur (Plate VIId) in mestome cells which thereby resemble endodermal cells (cp. Fig. 6c). As mentioned in connection with stage 1 (p. 20) some mestome sheath cells deviate early from the remaining cells. The cells in question develop into transfer cells located as a single row in longitudinal direction on each side of the smaller veins. In transverse sections these cells are invariably placed just outside the border between xylem and phloem (Plate VIIc). In some cases commissural strands issue from these cells (*Böcher* 1972 Fig. 3A, our Fig. 11a). What we here designate transfer cells deviate from the typical transfer cells described by *Gunning* et al. (1968) by the absence of wall invaginations. On the other hand, their plasmalemma surface is considerably increased through the presence of many densely spaced, deep pit canals. In this way wall areas between pits often appear as broad flanges or

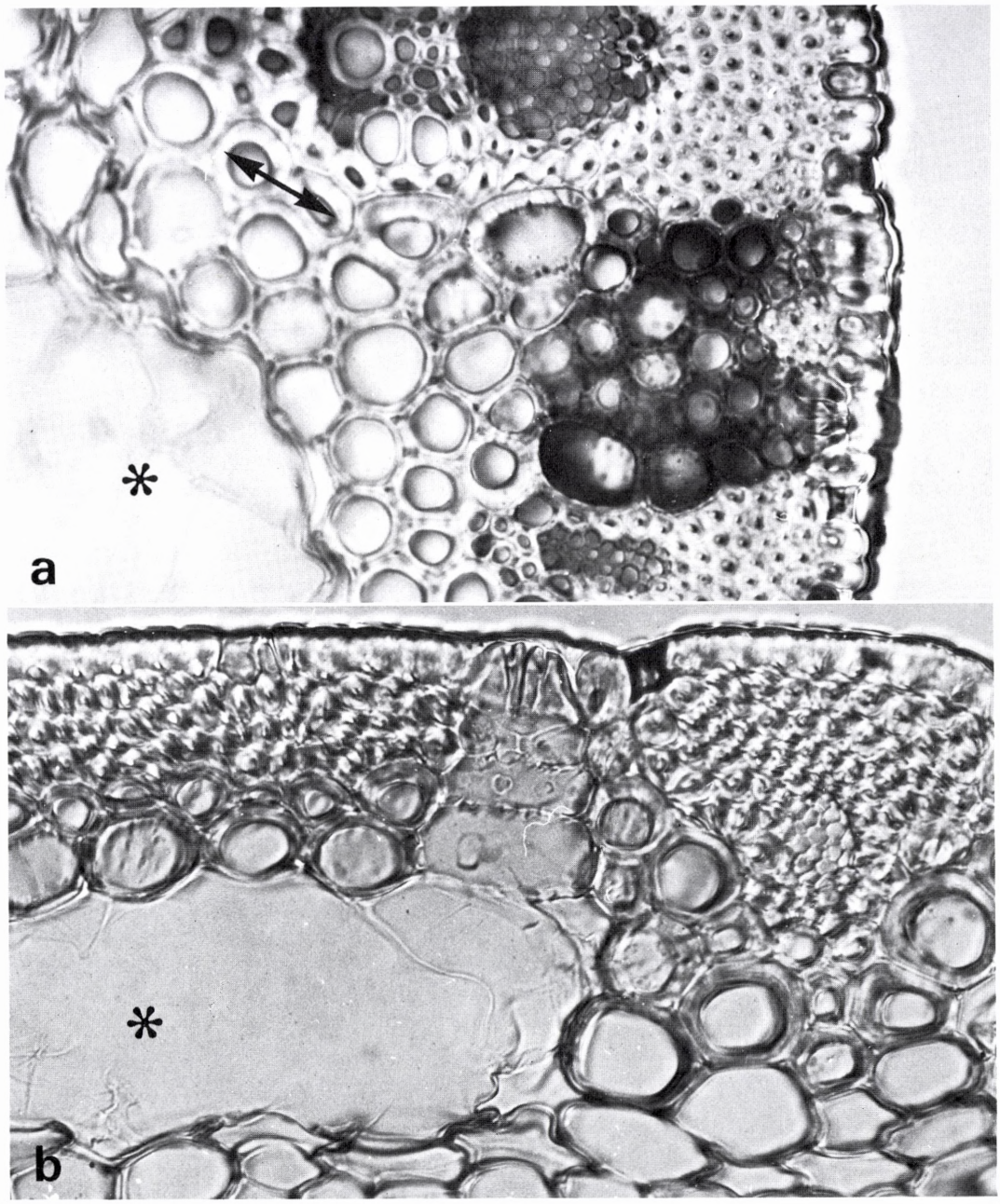

Fig. 8. Anatomy of outer leaf sheaths. Transverse sections, semipolarized light (× 500). – *a.* Chlorenchymatous area and stoma surrounded by sclerenchyma associated with vascular bundles. Arrow indicates thick-walled cells homologous to bundle sheath. Lysigenous air space (*). – *b.* Schlerenchymatous sheath area with thin-walled connecting duct between stoma and lysigenous air space (*).

trabeculae, which is a typical feature in transfer cells in many grass species (*Zee* & *O'Brien* 1971). Histochemically, the transfer cells in *Sporobolus* deviate from the other mestome cells by: (1) a strong reaction for acid phosphatase, (2) a considerably higher staining capacity with several dyes (Toluidine blue, Aniline blue black, PAS). The protoplast contains a hypertrophied central nucleus (Fig. 16a), abundant mitochondria and dense cytoplasm. Abundant plasmodesmata are observed in the pits between transfer cells and BS cells and phloem parenchyma cells (Plate XIc). When the transfer cells are in direct contact with sieve elements, however, their interface contains very few plasmodesmata.

The mestome sheath gradually merges into fiber plates between the bundles and epidermis. The continuity between xylem elements, mestome cells, fibers and epidermal cells without intervening intercellular spaces provides a conspicuous apoplastic pathway for water transfer to the epidermis. Thus, although originating from the mestome sheath, the fiber plates may functionally be interpreted as bundle sheath extensions (cf. *Wylie* 1952).

The epidermal cell pattern contains normal cells with thick outer walls and thick cuticular layers, stomatal complexes and with regular intervals short cells, which are either silica cells or which develop into specialized cells previously considered as salt glands.

The stomata are sunken and the walls of the antechambers are furnished with a multitude of wax configurations which tend to overarch the entrances and thus may be considered as an antitranspirant structure (Fig. 15). Similar wax rods are particularly well-developed at the entrances to the conspicuous antechambers in *Bredemeyera colletioides* (*Böcher* & *Lyshede* 1968). In the case of *Sporobolus* the wax rods may also prevent water filling of the stomata during flooding in the early spring. Seen from inside, the dumbbell-shaped guard cells and the very large subsidiary cells are prominent in SEM pictures obtained after sectioning and freeze-drying (Fig. 18).

The silica cells are most abundant in the leaf sheaths and in the proximal, hollow parts of the blades where they are restricted to the adaxial surface. In the cylindrical, distal parts silica cells are few and scattered. In these parts the salt gland cells become numerous. They occur with great frequency in the cell rows adjacent to rows containing stomata, but are occasionally found outside the fiber plates. As pointed out earlier (*Böcher* 1972: 350), their location adjacent to stomata coincides with the position of a complex of small MS cells and the outermost BS cells. In most cases these short cells occur singly separated by epidermal long cells, but occasionally they occur in groups of two or three. In surface views (Fig. 15) they appear rectangular and in section it is evident that like silica cells they are slightly sunken relative to the surrounding epidermal cells (Fig. 16). The wall staining patterns indicated a clear demarcation from other epidermal cells (*Böcher* 1972) and invited to further studies. As shown in Plate VI this demarcation results from the presence of a cutinized wall layer in the anticlinal walls which is a character common to salt glands in e.g. *Tamarix* and *Spartina* (*Thomson* 1975). The thickness of this wall layer decreases inwards and may even be traced along the interior wall (Plate VIb). In the anticlinal walls the cutinized layer appears granular, i.e. electron-dense irregular granules embedded in a lighter matrix, and ts is separated from the protoplast by a thin electron-translucent non-granular lamella (Plate VIa, b). The granular component of the cutinized wall varies considerably and is most conspicuous in the outermost part, whereas the innermost part (i.e. against the electron-translucent layer) appears more fibrillar. The granular component stains with Sudan IV and the inner zone probably comprising the electron translucent layer stains intensely with PAS (Figs. 16, 17). The cutinized wall structure continues in the interior part of the outer wall. At the junction between the anticlinal and the outer wall this layer is connected to the common cuticular layer present in all epidermal cells. In the middle part

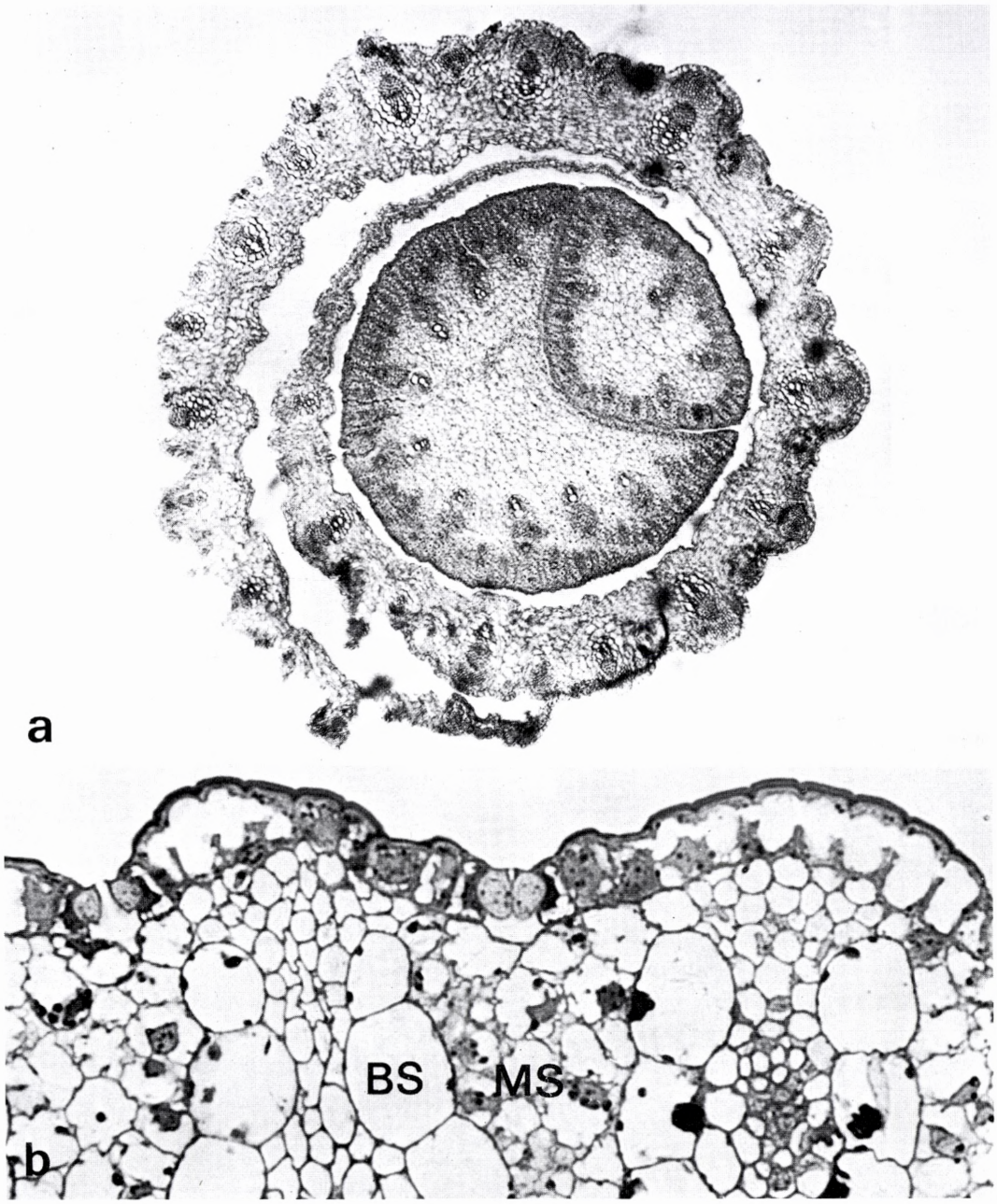

Fig. 9. *a.* Transection of entire shoot. The sheath encircles two leaf blades, the lower (older) being crescent. Developing bundle areas (at stage 1) surround a central pith-like parenchyma (× 50). – *b.* Detail of later stage (stage 2–3) showing young stomata, bundle sheaths (BS) and arm cell mesophyll (MS) (× 720).

of the outer wall an electron-transparent non-fibrillar and non-granular zone occurs between the inner granular cutinized layer and the cuticular layer (Plate VIb, d). Thus in TEM this zone appears empty, but in LM it is recognizable by its strong affinity for stains like toluidine blue and ruthenium red. The protoplast of the salt gland cells is always denser than that of the surrounding cells, and during the development strongly stainable plastids (cp. p. 18) increase in number and size. At maturity some vacuolization takes place but the cells retain their dense cytoplasm and organelle content. A characteristic feature is the presence of a complex lamellar structure between the anticlinal walls and the centrally placed nucleus (Plate VIc). This structure is composed of tortuous cisternae delineated by very distinct trilaminate membranes which apparently are connected to the plasmalemma in this wall region. The thickness, trilaminate appearance and connection with the plasmalemma correspond to the partitioning membranes described in salt glands of *Spartina* (*Levering* & *Thomson* 1971). Thus the presence of these membranes indicates a function comparable to that in the basal cells of *Spartina* salt glands. *Liphschitz* & *Waisel* (1974) investigated salt glands in 25 grass species and found in all of them that the glands were bicellular: a basal collecting cell and a cap cell assumed to be the secreting one. Furthermore they found a variation in the localization of the basal cell which may be half embedded in the photosynthetic tissue or included in the epidermis. In *Sporobolus rigens* the glands appear unicellular and the presence of an apparently empty zone in the outer wall complex indicates that this double wall structure has evolved from a bicellular condition. Thus this zone, which varies considerably in size and stains as mentioned above, may represent a reduced cap cell. The cutinized layer in the anticlinal and outer walls corresponds to the cutinized part (bordering the neighbouring epidermal cells) of the basal cell wall in bicellular glands (*Liphschitz* & *Waisel* 1974). The granular appearance of this wall is similar to the wall between basal and cap cells in *Spartina* (*Levering* & *Thomson* 1971). A striking fact is the apparent structural identity between the salt gland cells in *Sporobolus rigens* and the cork cells found in the cork-silica-cell pairs in grasses (e.g. in *Avena*, *Kauffman*, *Petering* & *Smith* 1970). The need of additional investigations in order to clarify this resemblance seems obvious.

Stage 6. Stage 5 undoubtedly represents an optimal cell condition. It is followed by a stage characterized by degeneration of chloroplasts and cytoplasmic material. The cells senesce and during the entire stage, which ends with the death of the cells, autophagic activity plays an important role. The dead cells finally become empty. The senescing processes are not synchronized in the different photosynthetic areas in the blades. Usually, however, a degeneration of the MS cell areas is followed by a decay of BS cells.

The first sign of degeneration is an increase in the number of tubules in semicrystalline aggregations in MS chloroplasts. They occur in low numbers at stage 4–5, but now they multiply and gradually occupy a major part of the chloroplast volume (Plate VIII). At the same time the thylakoids become disorganized, i.e. the regular grana configurations disappear and very often the thylakoids are placed in parallel, forming long curved clusters around the tubular aggregates.

Concomitant to the increase in the amount of chloroplast tubules, the contrast of the thylakoids in MS chloroplasts decreases. Later a similar decrease in electron density appears in BS chloroplasts but here, as opposed to the situation in the MS cells, this decrease is not synchronized between individual cells. The final dissolution of the chloroplasts generally occurs earlier in MS cells than in BS cells. The plastoglobuli increase in size and density and may accumulate as irregularly formed dense bodies surrounded by the remains of thylakoids and chloroplast envelopes (Plate IX).

In the BS chloroplasts the sequence of events during degeneration differs considerably from that described above (1) The orientation of grana

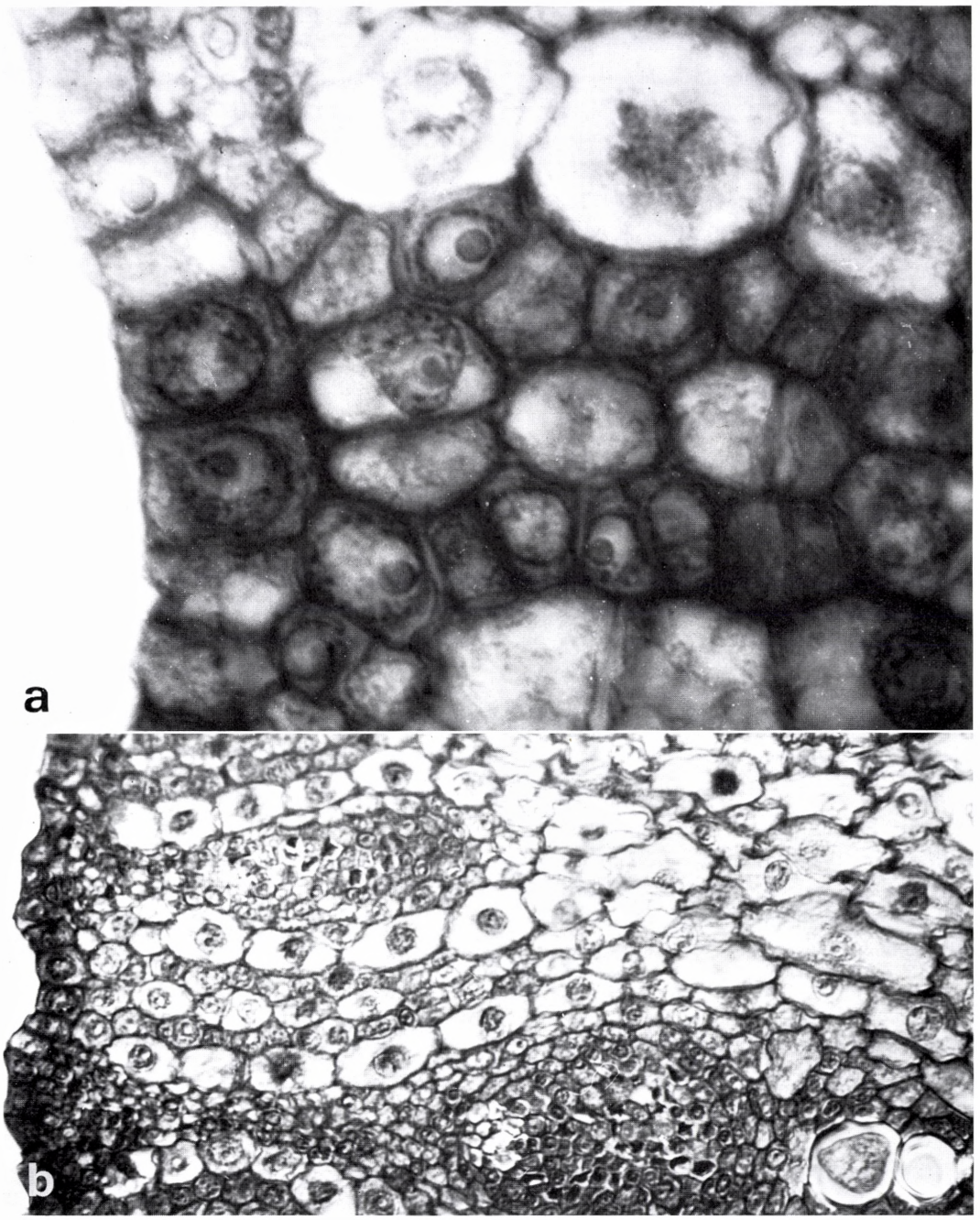

Fig. 10. Differentiation at stage 2. – *a*. Large bundle sheath cells and three rows of inter-bundle parenchyma which later becomes armed mesophyll. In the epidermis two guard cell precursors with large nuclei indicate the position of a later developing stomatal complex (× 2,000). – *b*. Survey of inter-bundle area surrounded by a small and a larger vascular bundle. The development of protoxylem elements is restricted to the latter. (Semipolarized light, × 50).

changes from being parallel to the longitudinal axis to a disturbed appearance as shown in Plate IXa. At the same time the chloroplasts swell, become more roundish and may adhere. (2) Semicrystalline tubules, as described in MS, are very infrequent and always disappear before complete dissolution. (3) In the few stroma thylakoids present a swelling takes place and gradually the swollen parts become filled with a very electron-dense material (Plate IXb). (4) The number of thylakoids in the grana decreases and gradually the grana disappear, i.e. the partitions are dissolved. (5) After the disintegration of the grana the remaining thylakoids show a tendency to form long concentric lamella bands parallel to the chloroplast surface (Plate IXc). In many preparations these lamellae appear swollen and develop into tubular or vesicular structures. These structures show a striking resemblance to peculiar membranous modifications in sieve element plastids in *Spinacia* leaves affected by virus diseases and containing associated mycoplasm-like organisms (*Esau* 1977). (6) Concomitant to the changes in thylakoid configurations, the chloroplasts decrease considerably in volume, the plastoglobuli occupy a greater proportion and often appear at lower contrast. (7) During the final dissolution of the thylakoids very electron-dense irregular lamellae often appear in contact with plastoglobuli. In fact, micrographs such as Plate IXc, d strongly suggest that the dense lamellae are formed from plastoglobuli during dissolution of the latter. Similar thick and dense lamellae are characteristic features of chromoplasts developing carotenoid pigment bodies, e.g. carotene bodies in carrots (*Ben-Shaul* et al. 1968) and lycopene bodies in tomatoes (*Ben-Shaul* & *Naftali* 1969).

During maturation of the green tissue electron-dense spherosome-like bodies accumulate in both MS and BS cells. Presumably these bodies represent lipid droplets. In MS cells they persist during senescence and show an increase in size whereas in BS cells they participate in the formation of peculiar "vacuoles" inside the tonoplast. In *Böcher* (1972: 358) these "vacuoles" were referred to as coated vacuoles because their surfaces were stained by Aniline blue black. Similar vacuolar bodies were found in mesophyll and BS cells in *Spartina alterniflora* by *Akers* et al. (1977a, b). In *Sporobolus* the vacuolar bodies are initiated by an increase in size of the numerous lipid droplets which accumulate in the vicinity of the pit fields between MS and BS cells (Plate Xa).

Concomitant to the first signs of BS chloroplast degeneration (see above), the lipid droplets increase further in size and develop into two-phased structures as shown in Plate Xa, b. The exterior phase appears finely granular with medium electron density and is separated from an interior amorphous lighter phase by a very narrow dense layer. The proportion of the total volume occupied by either phase varies considerably.

At a later stage similar and very enlarged bodies appear inside the tonoplast of the central vacuole which typically produce branches in between the chloroplasts. Direct evidence of the passage of the two-phase structures into the central vacuole is lacking, but micrographs such as Plate Xc clearly indicate that such events take place. Presumably the actual passage through the tonoplast is a very dynamic process which is very difficult to fix adequately.

Our interpretation of the vacuolar bodies as derived from cytoplasmic spherosomes is substantiated by the findings of *Smith* (1974). He demonstrated that the material in the vacuoles of the cotyledon cells in *Crambe abyssinica*, from which the aleurone grains subsequently develop, is supplied via spherosomes crossing the tonoplast. This vacuolar material is very electron-dense, acid phosphatase active, and appears much like intermediary stages of the vacuolar bodies in *Sporobolus*, cp. our Plate VI with Fig. 5c, d in *Smith* (1974).

In the vacuolar bodies the interior phase now changes from an amorphous to a dilute granular appearance (Plate Xc, e). At the same time the vacuolar bodies grow in two ways: (1) Several two-phase structures coalesce into greater entities. (2) Small, slightly denser droplets accumulate

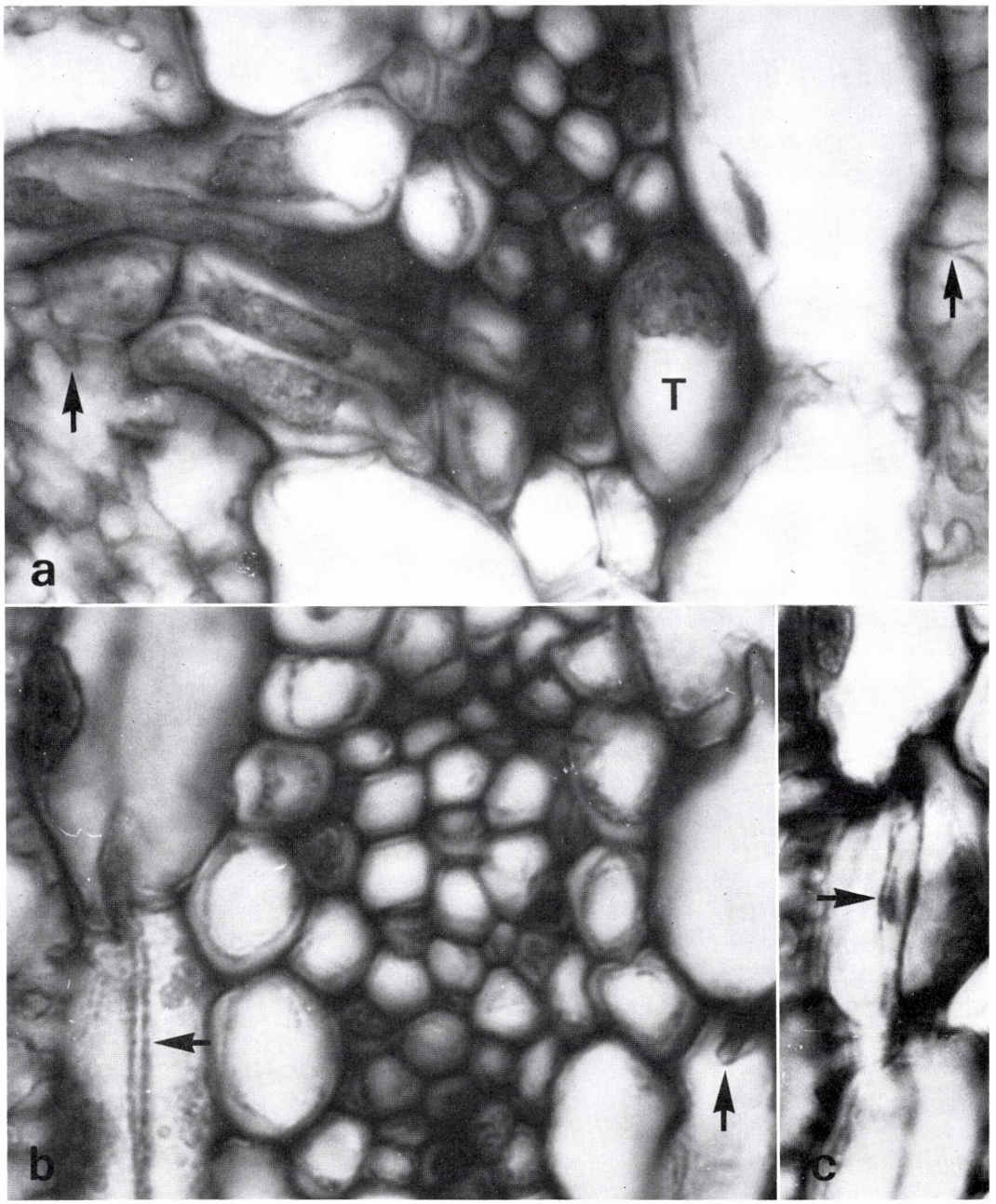

Fig. 11. Stage 3 (× 2,000). – *a.* Commissural strand issues from mestome sheath cells located opposite to specialized cell which later becomes a transfer cell (T). In the mesophyll conspicuous internal ridges and arms have developed (arrows). – *b, c.* Outbulgings in walls of bundle sheath cells resembling Casparian strips (arrows).

along the periphery of the growing bodies and fuse with them.

During the continued growth the vacuolar bodies attain a considerable size, up to 1/5 of the cell volume (Plate XI). In some preparations the exterior phase appears thin and labile with amoeboid contours, while in others it is thicker and apparently surrounds several compartments of the interior phase (Plate Xc, d).

During the last stages of chloroplast disintegration the exterior phase of the vacuolar bodies becomes tough, very electron-dense and more coarsely granular, whereas the interior phase now appears empty (Plates X–XI). The exterior tough phase may collapse at a late stage (cp. Fig. 7A–B in *Böcher* 1972).

E. Histochemistry of vacuolar bodies

The vacuolar bodies are stained with Aniline blue black in the exterior phase and attain a blue-green colour with Toluidine blue. With Nile blue they appear reddish, but with alcoholic solutions of Sudan IV they are rapidly dissolved, leaving very small red-stained globules. Tests for acid phosphatase showed a non-specific reaction typical for cells with a high content of polyphenols. All standard tests applied for proteins and tanniferous substances, however, proved negative. In the fluorescence microscope the vacuolar bodies exhibit a strong yellow-orange autofluorescence which disappeared in sections stained with Nile blue. In this stain, however, the lipid droplets in MS and BS cells showed an autofluorescence typical of spherosomes. From this evidence about the vacuolar bodies one may conclude that they contain phenolic substances and that some lipid component is involved at least during their early development. These observations in *Sporobolus* are in agreement with results of *Akers* et al. (1977b) who concluded that substances contained in the vacuolar bodies in *Spartina* could be identified as phenolic aldehydes. The correlation between the development of the vacuolar bodies and the increasing degeneration of the chloroplasts in *Sporobolus* indicates a connection between the chemical reorganisation of chloroplast material and the accumulation of phenolics. Thus the phenols may represent important end-products from, e.g., the decomposition of chloroplasts.

In order to elucidate the degree of lytic activity during senescence the localization of acid phosphatase was investigated (cf. *Matile* 1975). The most spectacular reactions were found in the cell walls (or the space between walls and plasmalemma) of the large subsidiary cells which sometimes even contained bodies (vacuoles?) filled with reaction products (Fig. 18c). Another general feature was the clear reactions connected with pits (plasmodesmata) and the plasmalemma in BS, MS and transfer cells. Furthermore, some reaction was found in walls of young phloem cells and xylem parenchyma cells in larger bundles.

Considering the striking sequence of events during degeneration of the BS cell contents (see above), it is remarkable that no clear reaction of acid phosphatase was established in any stage during this disintegration. In the vacuolar bodies, however, a non-specific reaction typical of polyphenol-storing cells was found. In MS cells the strongest phosphatase reaction occurred round the substomatal cavities: the intensity of the reaction product decreased towards the interior of the blade. Also in the BS cells a tendency towards a stronger reaction just below the epidermis was observed. The concentration of acid phosphatase activity in the large subsidiary cells and the neighbouring green cells suggests that the subsidiary cells are involved in the production of lytic enzymes.

A possible explanation of this enzyme localization and activity may be found in the fact that conspicuous changes in wall structure and chemistry were observed in the areas in question. Concomitant to the disintegration of protoplasts, the walls increased in thickness, stainability and electron density. The inter bundle-areas are effectively separated and behave like independent compartments; the senescing processes are not syn-

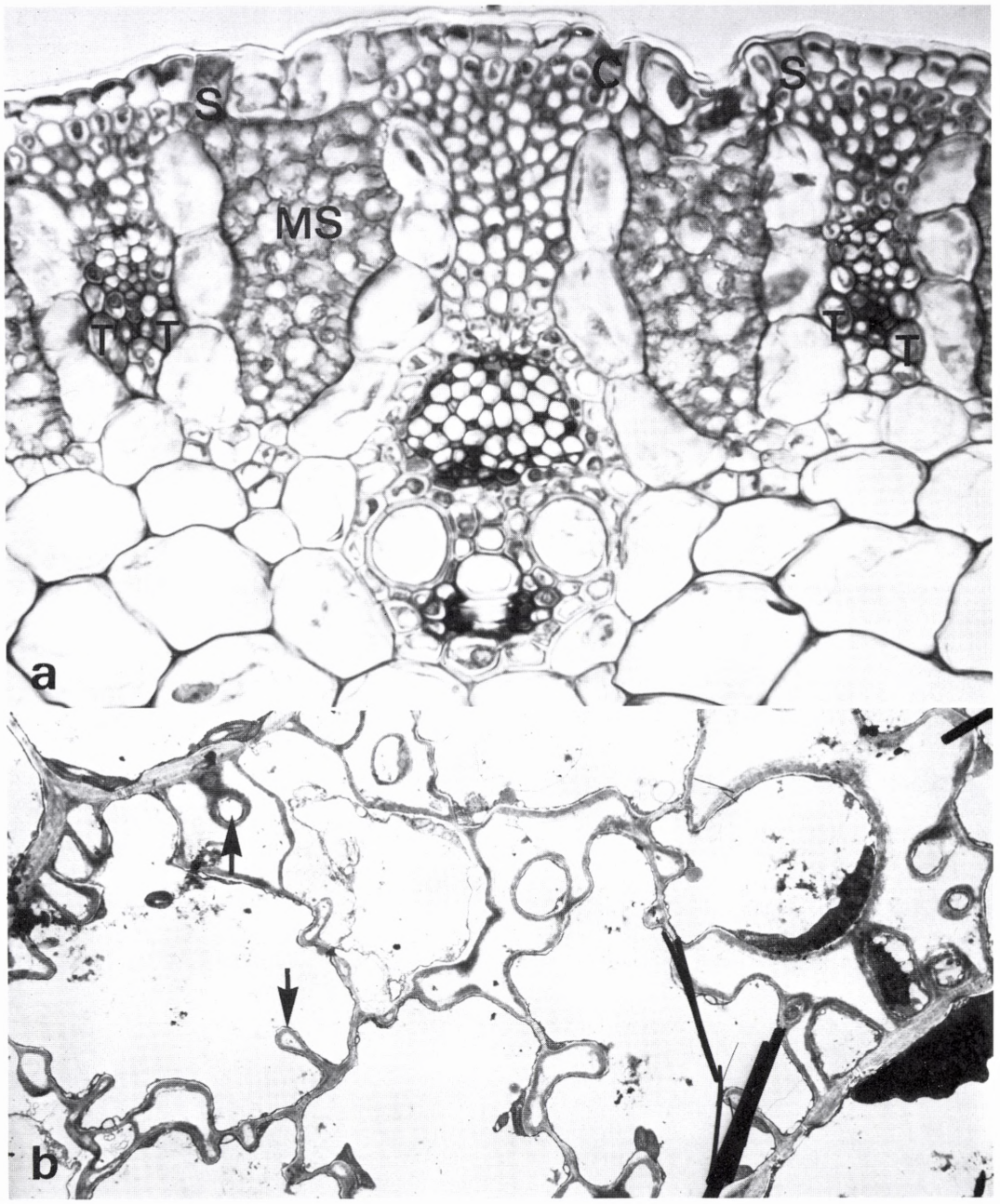

Fig. 12. Stage 2–3. – *a.* Survey of large bundle with well-developed phloem, meta- and protoxylem. In the two small bundles no metaxylem has developed and the mestome sheath contains transfer cells (T). Arm cell mesophyll (MS). In the epidermis two salt gland cells (S) and one silica cell (C) (× 500). – *b.* TEM demonstrating pronounced branching and loop formation (arrows) in arm cell mesophyll (× 3,600).

chronized, thus the changes in wall thickness and stainability and the activity of acid phosphatase may reflect a closure of early senescing compartments thereby isolating them from the remaining living compartments. On the other hand, the inactive compartments with their multitude of empty cell lumina may have a function comparable to lenticells.

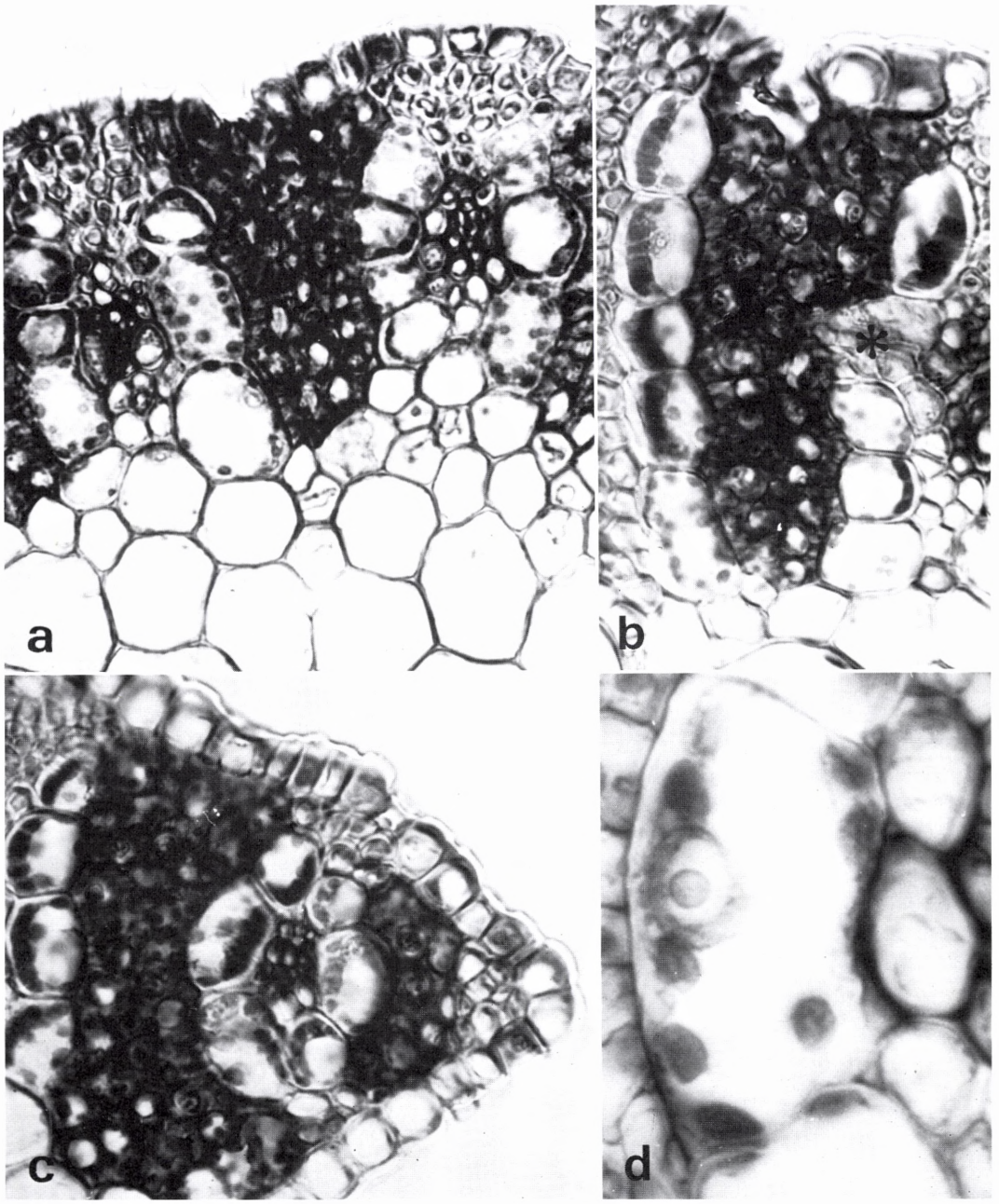

Fig. 13. Stage 4, chloroplast shape and orientation. – *a*. Scattered, roundish chloroplasts decreasing in number in bundle sheath cells towards the interior (× 500). – *b*. Bundle sheath chloroplasts assembling along bundle side of the cells; note the difference in size and arrangement of chloroplasts between outer and interior bundle sheath cells. Nuclei in central parts of arm cells and commissural strand penetrating a bundle sheath (*) (× 500). – *c*. As b but bundle sheath closed and continuous around marginal bundle (× 500). – *d*. Bundle sheath and mestome sheath cells, nucleus in bundle sheath large and still placed at the mesophyll side (× 2,000).

Discussion and Conclusions

A work of this kind that approaches a monographic treatment of the vegetative structure of an ecologically specialized species inevitably appears somewhat heterogeneous since various structural features do not necessarily call for, e.g., ultrastructural investigations. In the discussion the structural adaptations are discussed from ecophysiological rather than strict anatomical viewpoints.

A. Xerophytic Features

An obvious adaptation is the leaf blade reduction which in *S. rigens* has reached a maximum by total loss of the blade and maintenance of the midrib region. The latter is composed of a large parenchymatous tissue resembling a pith and possibly serving as a water-storing tissue; it is surrounded by a cylindrical part containing the photosynthetic tissues and associated bundles. This marginal area functions in the same way as the green cortex in apophyllous species. Thus, the total structure (i.e. central pith-like area and the photosynthetic cylinder) represents a clear case of analogous convergence (*Böcher* 1972, 1977).

The leaf epidermis shows several xerophytic characters: sunken stomata, thick cuticle and cuticular layers, and epicuticular wax in and around stomatal pores.

The whole cylindrical bundle area and epidermis is characterized by the abundance of sclerenchymatous cells. The cells of xylem, phloem, mestome sheath, bundle sheath and mestome sheath extension (fiber plate) all contain conspicuously thickened wall layers. The abundance of sclerenchyma also characterizes the leaf sheaths and the rootstock where cell walls in the pericyclic area are thickened and heavily lignified.

Among the root characters which may be interpreted as xeromorphic are the development of thick-walled cortical cells into additional endodermoid layers and the specialized structure of the epidermis showing a very thick mucilaginous outer wall.

B. Halophytic Features

Characters which can be considered as mainly adaptive to high salt concentrations in the soil are difficult to distinguish clearly from some of the xerophytic ones, but the following are evident.

The central pith-like parenchyma in the leaves brings about some succulence and permits the accumulation of great amounts of salt taken up from the soil. Virtually, salt crystals are abundant over cells of this central parenchyma in fresh cuttings left for desiccation. This compartmentation of excessive salt presumably protects the photosynthetic tissues from too high salt concentrations. The adaptive value of such an arrangement is stressed by the fact that enzymes of most halophytes are as sensitive to inorganic salts as are non-halophytes (*Greenway* & *Osmond* 1972). In the light of the widespread occurrence of salt glands in salt-tolerant grasses, e.g. *Spartina* and *Distichlis* (*Hansen* et al. 1976) and other species of *Sporobolus* (*S. pungens*, *Zemke* 1939 and *S. laetevirens*, unpublished data) it is striking that we have not been able to observe salt exudation from the epidermis of *S. rigens*. The epidermal short cells which we have considered to be salt glands are clearly reduced in relation to the majority of salt glands studied in other grasses (*Levering* & *Thomson* 1971; *Liphschitz* & *Waisel* 1974). Thus, there seems to be a correlation between the absence of salt exudation, the

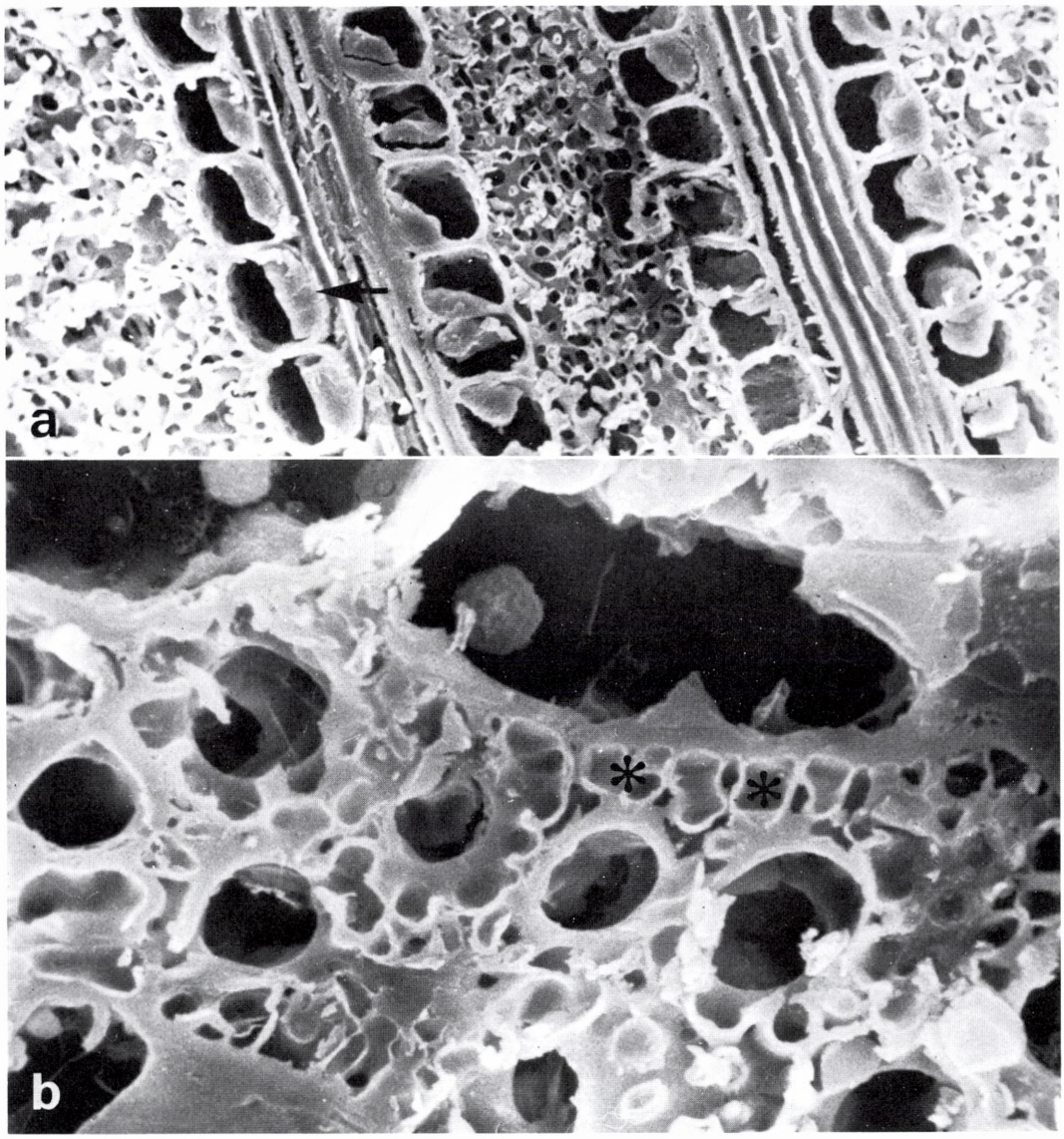

Fig. 14. Stage 5. SEM micrographs of freeze-dried material. – *a*. Survey showing alternating bundles with associated sheaths and intervening armed mesophyll. Arrow pointing towards chloroplast stack (× 300). – *b*. The same at higher magnification: narrow, peripheral arms (*) towards the bundle sheath; single chloroplast in bundle sheath cell (× 1,800).

succulence, and the reduced condition of the salt glands. However, we assume that during severe salt stress these reduced glands may function in maintaining a suitable salt concentration in the green, peripheral tissues.

Stelzer & *Läuchli* (1977) pointed to the possibility that well-developed aerenchyma and the occurrence of a second endodermis in roots afford increasing salt- and flooding-tolerance in *Puccinellia peisonis*. In *S. rigens*, which in most habitats in the spring grows on flooded or water-logged ground near salt lakes, we have found exactly the same structural features.

C. Anatomy in Relation to Other C_4 Grasses

Since *Sporobolus rigens* has a modified Kranz anatomy, dimorphic chloroplasts (peripheral reticulum only in MS chloroplasts which are two to three times smaller than BS chloroplasts) and a carbon dioxide compensation point of 7–9 ppm CO_2, there seems to be little doubt that it employs the C_4 pathway of photosynthesis.

Depending on the reaction sequence for C_4 acid decarboxylation in the bundle sheath cells, three variations of C_4 photosynthesis, which seem to be species-specific, are currently recognized (*Gutierrez* et al. 1974; *Hatch* et al. 1975): group I or NADP-ME species (high levels of NADP-malic enzyme in BS), group II or NAD-ME species (high levels of NAD-malic enzyme in BS) and group III or PCK species (high levels of PEP-carboxykinase in BS). In grasses a correlation exists between this grouping, carboxyl transfer mechanisms, and various ultrastructural features of BS cells. Thus, group I species are "malate formers" (*Downton* 1971) and often have reduced grana in BS chloroplasts, whereas group II and III species can be characterized as "aspartate formers" which always have well-developed grana in BS chloroplasts. Groups II and III can be distinguished by the location of the chloroplasts in BS cells; i.e. centripetal (group II) or centrifugal (group III). Recently *Hattersley* & *Watson* (1976) were able to demonstrate a perfect correlation between group I species and the absence of a mestome sheath, whereas group II and III species always have some mestome sheath cells intervening between metaxylem vessel elements and laterally adjacent BS cells. The presence or absence of mestome sheath cells is attributable to the fact that in different grasses BS cells can develop from the parenchyma sheath, the mestome sheath, and even within the veins (*Brown* 1975).

Table 2 summarizes data from two previous ultrastructural studies including a few species of *Sporobolus* (*Carolin* et al. 1973; *Coombs* & *Greenwood* 1976) together with biochemical and anatomical evidence from the literature (*Gutierrez* et al. 1974; *Hattersley* & *Watson* 1976) and our own unpublished results.

Table 2. Classification of C_4 species in the genus *Sporobolus* on the basis of biochemical[1], anatomical[2], and ultrastructural[3] evidence.

Group II species (NAD-ME type)
Sporobolus airoides[1a], *S. cryptandrus*[1a], *S. giganteus*[3b], *S. laetevirens*[3e], *S. rigens*[3e]
Group III species (PCK type)
Sporobolus poiretii[1a], *S. airoides*[3b], *S. fimbriatus*[1d], *S. africanus*[3c]
Group II or III species[2f]
Sporobolus diander, *S. elongatus*, *S. indicus*, *S. molleri*, *S. pyramidalis*, *S. wrightii*

[a]*Gutierrez* et al. (1974); [b]*Coombs* & *Greenwood* (1976); [c]*Olesen*, unpublished; [d]*Hatch* et al. (1975); [e]the present study; [f]*Hattersley* & *Watson* (1976).

Two conclusions can be drawn from Table 2. Firstly, *S. rigens* can be classified as a group II species on the basis of the presence of a typical mestome sheath, the centripetal position of the BS chloroplasts, and the conspicuous grana development in the latter. Secondly, some inconsistency exists in that *S. airoides* has been reported in both groups II and III. This intraspecific varia-

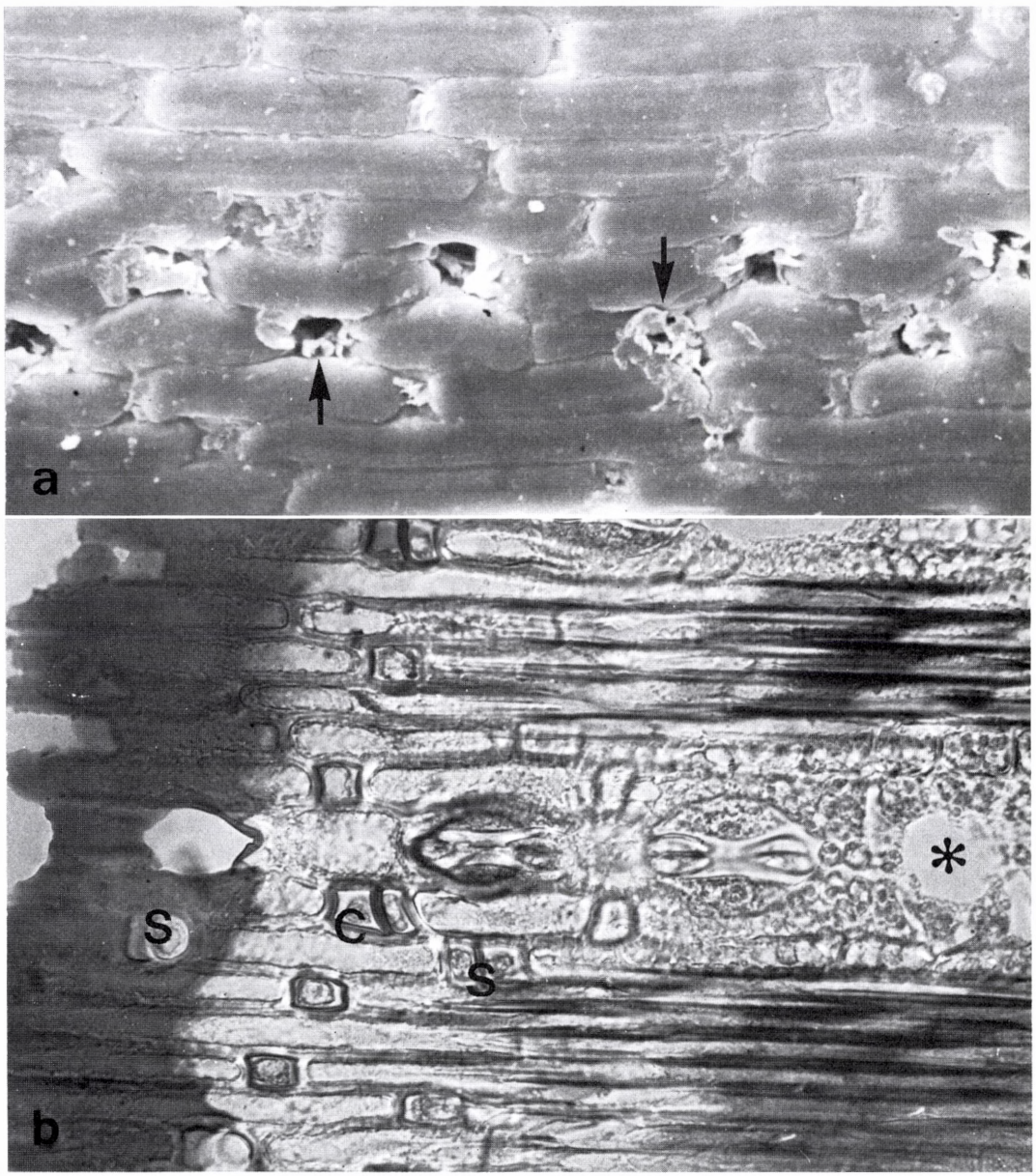

Fig. 15. *a.* SEM surface view of leaf blade. Wax figures (arrows) around stomatal pores (× 500). – *b.* Oblique, paradermal section, Sudan IV stains cuticular layer on the left and walls of stomatal entrances, silica cells (C) and salt gland cells (S). Substomatal cavity (*) (× 1,000).

tion together with the variation within the genus may have evolutionary relevance. If, as suggested by various authors, the loss of grana in BS chloroplasts should be considered an evolutionarily advanced situation in C_4 grasses, a possible evolutionary pathway would be from group II species (centripetal BS chloroplasts) to group III species (predominantly centrifugal BS chloroplasts) to group I species with varying degrees of grana reduction in the centrifugal BS chloroplasts (*Gutierrez* et al. 1974), e.g. *Zea*, *Saccharum* and *Sorghum* spp. Presumably such an evolutionary pattern can be demonstrated in the genus *Panicum* which, besides comprising C_3 species and species intermediate between C_3 and C_4, is represented by species in all three groups of C_4 plants (*Gutierrez* et al. 1974; *Brown* 1976). If this hypothesis proves correct, the evidence in Table 2 would be indicative of an evolutionary pattern in the genus *Sporobolus* from group II species to group III species.

S. rigens is a perennial xerophytic grass adapted to arid or saline environments much like *Triodia irritans* (*McWilliam* & *Mison* 1974; *Craig* & *Goodchild* 1977). Despite their disjunct distribution (*T. irritans* in Australia and *S. rigens* in South America), these grasses have a number of unusual structural modifications of the photosynthetic tissues in common: (1) highly lignified cylindrical leaves, (2) the linear arrangement of the BS cells denotes a radical deviation from the classical Kranz anatomy of C_4 plants, (3) the mesophyll is not radial but appears as pockets or islands of tightly packed arm cell tissue in contact with BS cells, and (4) sunken or otherwise protected stomata. The most conspicuous difference between the two, however, is that in *T. irritans* the cylindrical leaf form seemingly has developed through permanent infolding whereas in *S. rigens* it results from the loss of lateral regions.

D. Modifications of the Photosyntetic Apparatus in Sporobolus rigens

Ecological adaptations other than the reduction of grana in BS chloroplasts (presumably part of an adaptation to maximum photosynthetic efficiency in high temperature and high light intensity environments) are likely to manifest themselves in biochemical as well as anatomical and ultrastructural characteristics of C_4 grasses. Thus, it might be significant that *S. rigens* and *S. laetevirens*, both inhabitants of xeric and saline environments, seem to be group II species with conspicuous xerophytic and halophytic structural adaptations (see above). Therefore, we assume that in these environments natural selection has favoured the evolution of such characters of which the adaptive value is more self-evident than, e.g., the reduction of grana development and centrifugal location of BS chloroplasts. In fact, BS chloroplasts of groups II and III species possess well-developed grana (*Gutierrez* et al. 1974), which can be demonstrated also in species of *Sporobolus* (*Coombs* & *Greenwood* 1976; *Olesen* unpublished), and presumably these plants are primarily adapted to environments not characterized by extremely high light intensities. In the case of *S. rigens* the degree of thylakoid stacking (grana development) is even higher in BS chloroplasts than in MS chloroplasts (Table 1). In fact, these chloroplasts bear some resemblance to chloroplasts of shade plants which could be the result of the shading effect of the very thick-walled epidermis, BS cells, and dense MS tissue possibly combined with the vertical position of the blades. By extreme development of grana the BS chloroplasts possibly achieve a higher density of light-harvesting structures, and therefore a more efficient collection of light quanta like the situation in shade plants (*Boardman* et al. 1974).

The conspicuously branched mesophyll cells interconnect by way of cytoplasm-filled arms. The areas between adjacent cells and between the many arm bridges form an air space continuum with the substomatal cavity; this architecture creates a

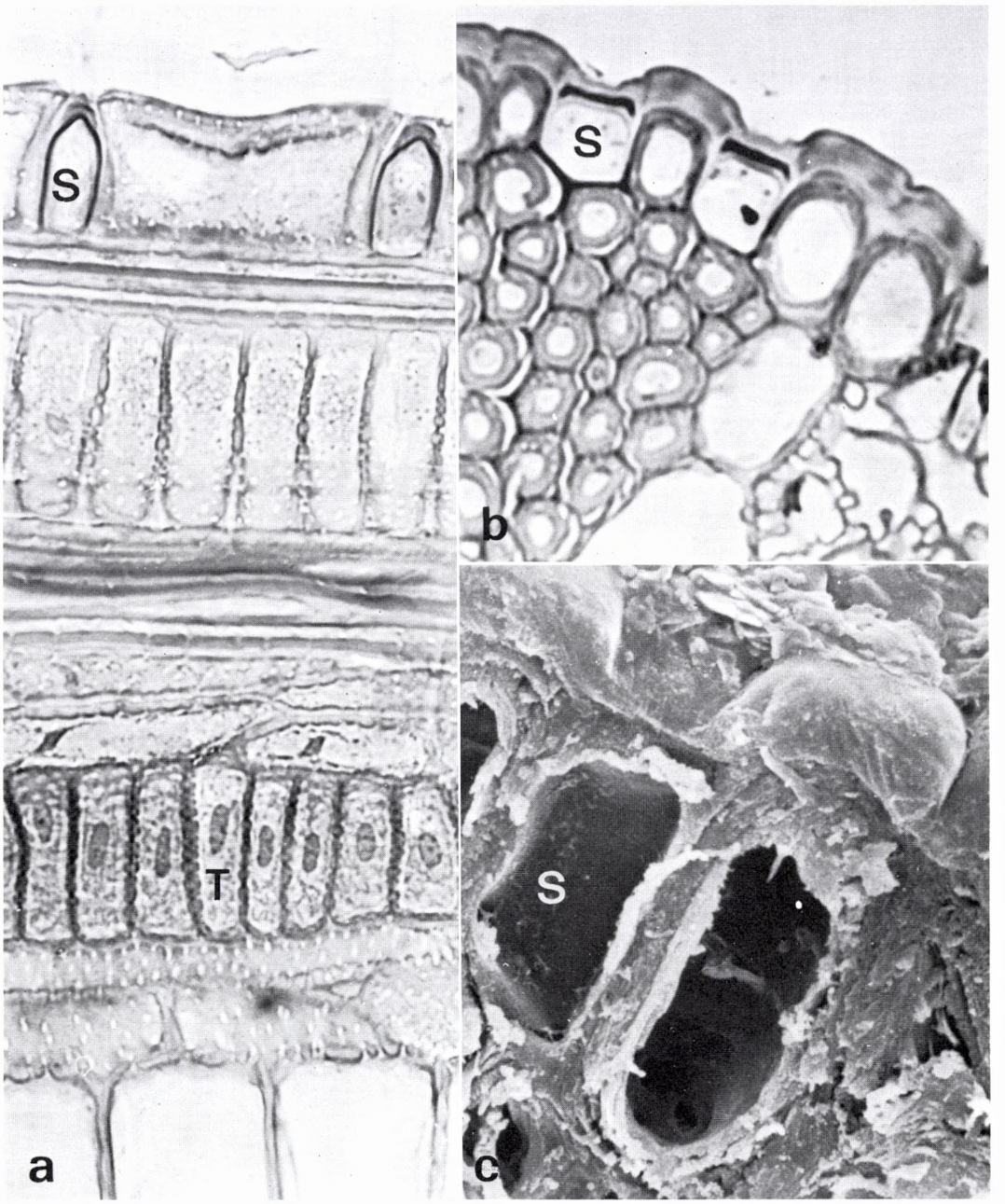

Fig. 16. Epidermal salt gland cells. – *a.* Longitudinal section stained with PAS. Salt gland cells (S) tapering and with PAS-positive walls. The section passes through the mestome sheath in minor bundle: row of transfer cells with large central nuclei and densely pitted walls (× 690). – *b.* Transection showing two salt gland cells (S) with dark stained peripheral areas possibly representing reduced outer gland cells (× 1,080). – *c.* SEM after freeze-drying showing depression outside salt gland (S) (× 2,400).

very large MS surface area. The MS chloroplasts are placed very close to the wall throughout these cells including the cross bridges. The complex air space continuum provides a highly conducting gas pathway even to the innermost cells in the dense MS tissue as well as to the interior of each arm cell. The principal advantage of this cell structure is the minimum possible resistance to CO_2 diffusion in the liquid phase which is about 10,000 times slower than in air (*Wiebe* & *Al-Saadi* 1976).

E. Transport Pathways in Leaves of Sporobolus rigens

Plasmodesmata are abundant between MS cells (at the interface between the arms) and, especially, in the dense pit-fields between MS and BS cells which point to a symplastic pathway for assimilate flux (cf. *Olesen* 1975). BS cells communicate mutually and with mestome sheath cells through a few pit-fields. From a structural viewpoint the principal pathway for the translocation of photosynthates from BS to the phloem is via the modified, transfer-cell-like mestome sheath cells found in small and intermediary but not larger bundles.

Unlike the other mestome sheath cells, these cells contain no suberin lamellae in their walls, are not lignified, stain intensely with Toluidine blue, Aniline blue black and PAS and exhibit high activities of acid phosphatase. Although they lack the most conspicuous characteristic of transfer cells, i.e. wall invaginations, the above-mentioned features substantiate the interpretation of these cells as functional transfer cells active in phloem loading. Compared to the extensive interface between MS and BS cells with very high frequencies of plasmodesmata, the area of contact between BS and transfer cells is very small and the plasmodesmatal frequency is by no means greater than between MS and BS; the area of contact between transfer cells and phloem cells contains even fewer plasmodesmata. Thus, it seems quite unlikely that phloem loading via these transfer cells takes place in the symplast only. On the contrary, by means of the deep pit canals the plasmalemma area is considerably increased, and the whole nature of the transfer cells indicates that phloem loading is partly accomplished by active transport processes located in these cells, i.e. apoplast transport is involved.

This function is in agreement with the function of phloem transfer cells or phloem parenchyma cells in dicotyledonous plants (*Pate* & *Gunning* 1969; *Geiger* 1975). Thus, in *Sporobolus rigens* the transfer cells can be visualized as "passage cells" in the endodermoid, lignified and suberized mestome sheath acting as active "pumping cells" located between the symplast of the photosynthetic tissue and the phloem symplast.

This seems to be the first demonstration of functional transfer cells in minor bundles of grass leaves where some authors (*O'Brien* & *Carr* 1970; *Ellis* 1976) have suggested that transfer cells would be unnecessary if assimilate transport into the bundles was purely symplastic. *Kuo* et al. (1974) demonstrated a marked difference in number and area of pit-fields and plasmodesmatal frequencies among mestome sheath cells in *Triticum*, where the bulk of the plasmodesmata is found in the mestome sheath cells that abut on the phloem. These cells, however, have no structural or chemical features of transfer cells. Further, these authors calculated that 85% of the total number of plasmodesmata between mesophyll and vascular tissues are confined to small and intermediate bundles. Therefore, *Kuo* et al. (1974) favoured a symplastic pathway for assimilate flux through the mestome sheath into the vascular tissue where some sort of sugar pump is thought to be located (*Geiger* 1975). The function of such a pump is presumably to pass the assimilates into the apoplast before they are loaded back into the symplast of the phloem. This active, but transient, change-over to the apoplast allows the maintenance of a low assimilate concentration at the outside of the loading surface which is necessary for symplast transport from the mesophyll.

In *S. rigens* we may view the evolutionary development of functional transfer cells as a response to selection pressures such as the rate limitation of

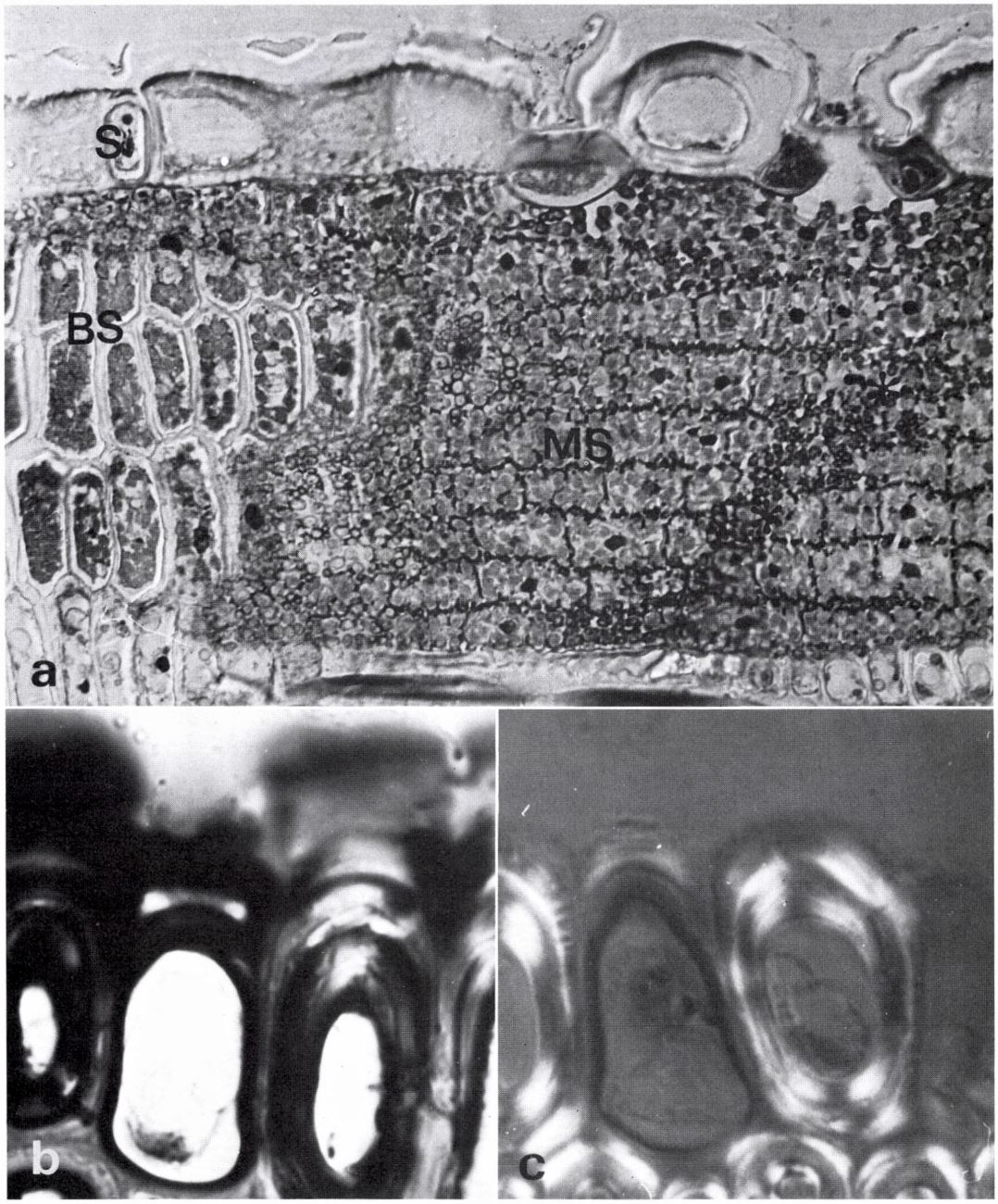

Fig. 17. a. Oblique longitudinal section. Salt gland (S), two stomata, bundle sheath cells (BS) densely packed with chloroplasts, area of contact between bundle sheath and mesophyll cells with cross sections of abundant narrow arms, central parts of mesophyll cells (MS) with nuclei and chloroplasts, area of arm-contacts between mesophyll cells (*) (× 500). – *b.* Salt gland showing light area in outer wall possibly representing reduced outer gland cell. PAS, semipolarized light (× 2,000). – *c.* The same in polarized light, note weak birefringence in outermost wall of salt gland cell (× 2,000).

translocation of assimilates into the phloem caused by thickened and lignified walls of BS and mestome sheath cells and increased amounts of photosynthates resulting from C_4 photosynthesis. The development of mestome sheath cells abutting on the phloem into transfer cells often in direct contact with sieve elements ensures efficient and rapid phloem loading, while the suberin lamellae of adjacent mestome sheath cells, together with the pumping activity of the transfer cells, may function in preventing backflow from the apoplast as suggested by *Kuo* et al. (1974) for *Triticum*. This suggestion is further substantiated by the developmental appearance of the suberin lamellae in *Triticum* (*O'Brien* & *Kuo* 1975).

Leaf structure in *S. rigens* is in agreement with the idea that in grass leaves there is an effective separation between the inwardly directed translocation of assimilates and the outwardly directed, much larger flux of water. Thus, in *Triticum*, *Kuo* et al. (1974) calculated that 85% of the assimilate translocation occurs in smaller bundles (based on plasmodesmatal frequencies in the mestome sheath) while 99% of the water flux takes place from the larger bundles (based on size of the xylem elements). In *S. rigens* the conspicuous fiber plates or bundle sheath extensions provide a direct apoplastic pathway between the mestome sheath and the thick-walled epidermal cells, which in the larger bundles is not interrupted by active transfer cells. The idea that the bulk of water transport in leaves does not occur directly through the mesophyll tissue is stressed by the observation of *Crowdy* & *Tanton* (1972) and *Byott* & *Sheriff* (1976) that a major evaporating surface in leaves is located in epidermal walls, especially those lining the substomatal cavity. In *S. rigens* a similar pathway for the transpiration stream is indicated by the fact that a subepidermal layer of small, thick-walled cells lying intermediately between BS and fiber cells separates the BS from the epidermis and borders on the substomatal cavity. These cells are located just below the unicellular salt glands in the epidermis which therefore may have a dual function as a kind of "security valve" involved both in salt secretion and in the elimination of water; especially in young, developing leaves such a hydathode function appears likely.

F. Xero-halophytic features – a synthesis

The present study reveals that *Sporobolus rigens* is a unique representative of the *Gramineae* that exhibits a number of structural and ecophysiological adaptations hardly seen before in one single species. In addition to a few classical studies (*Volkens* 1887; *Goosens* 1936), a number of papers relating single or a few structural adaptations to different environments have been published in recent years (e.g. *Hansen* et al. 1976; *Akers* et al. 1977a, b; *Stelzer* & *Läuchli* 1977). As a matter of fact, almost every specialized structure described in these papers can be found in *S. rigens*; the respective authors have considered them as adaptations to xeric and saline environments, permanent or transient flooding, soil texture, light intensity, etc. As mentioned above, it is often difficult to assign a given structural adaptation to one particular feature of the environment. For instance, it seems impossible to decide whether the conspicuous root dimorphism found both in dry desert grasses (*Goosens* 1936), temporarily flooded salt steppe grasses (e.g. *S. rigens*) and permanently flooded salt marsh grasses such as *Spartina* (*Anderson* 1974) has envolved in response to aridity, salinity or flooding. Attempts to understand the significance of the pseudovacuoles found in bundle-sheath cells in mature leaves of *S. rigens* and *Spartina* sp. (*Anderson* 1974) and the additional endodermal layers in roots of *S. rigens* and *Puccinellia* sp. (*Stelzer* & *Läuchli* 1977) are hampered by similar problems.

In the light of these circumstances we propose to use the terms xero-halophytes and xero-halophytic features or adaptations in dealing with the structure and ecophysiology of plants such as *S. rigens* and other specialized grasses. This terminology also applies to, e.g., the syndrome of structural adaptations common to *S. rigens* and *Triodia irritans* dis-

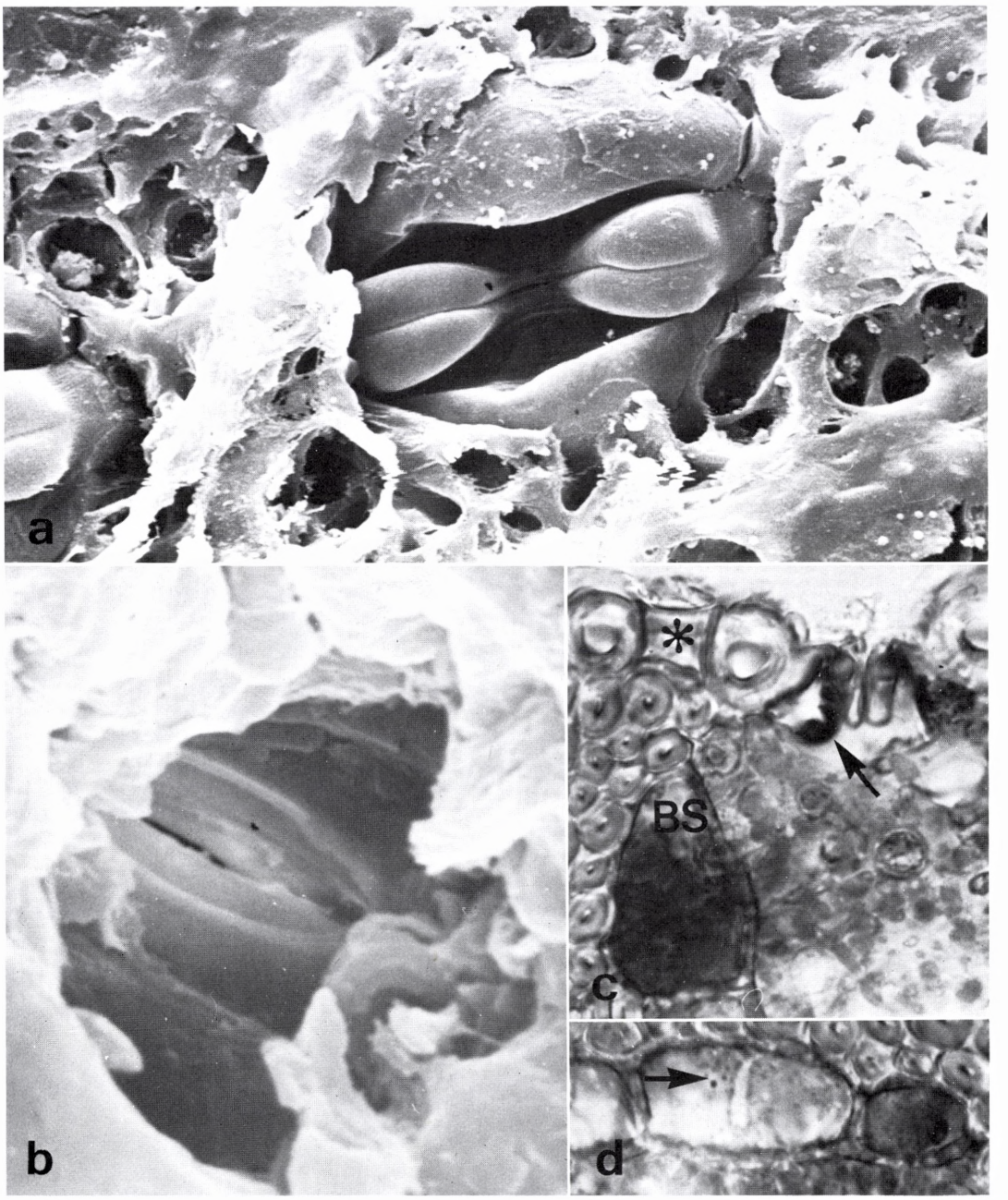

Fig. 18. a. SEM of stomatal complex observed from inside (× 4,000). – *b.* SEM of stoma observed from outside, wax configurations lining the antechamber (× 10,000). – *c.* Acid phosphatase reaction in large subsidiary cells (arrow) and in outer bundle sheath cell (BS). Silica cell (*) (× 500). – *d.* Acid phosphatase reaction in pits of bundle sheath cells (arrow) (× 500).

cussed above. Thus, we assume that the perennial lifeform of these xero-halophytic C_4 grasses has favoured the evolution of characteristics related to survival and resistance (e.g. increased xeromorphy), whereas annual C_4 grasses such as *Zea mays* have evolved adaptations to intensified, short-time activity (e.g. specialized chloroplasts and elimination of the mestome sheath).

Although the situation in grasses is by no means clarified, much evidence indicates that major differences in tissue arrangement like the distribution of sclerenchyma and radiate contra non-radiate chlorenchyma are correlated with ecological factors (*Ellis* 1976). Similar correlations can be expected between chloroplast localization and grana reduction in bundle sheath cells and, e.g., varying light intensities (diurnal rhythm and differences between habitats). This, in turn, questions the wide-spread use of such structural adaptations as diagnostic characters (*Metcalfe* 1960; *Johnson* & *Brown* 1973) with phylogenetic significance.

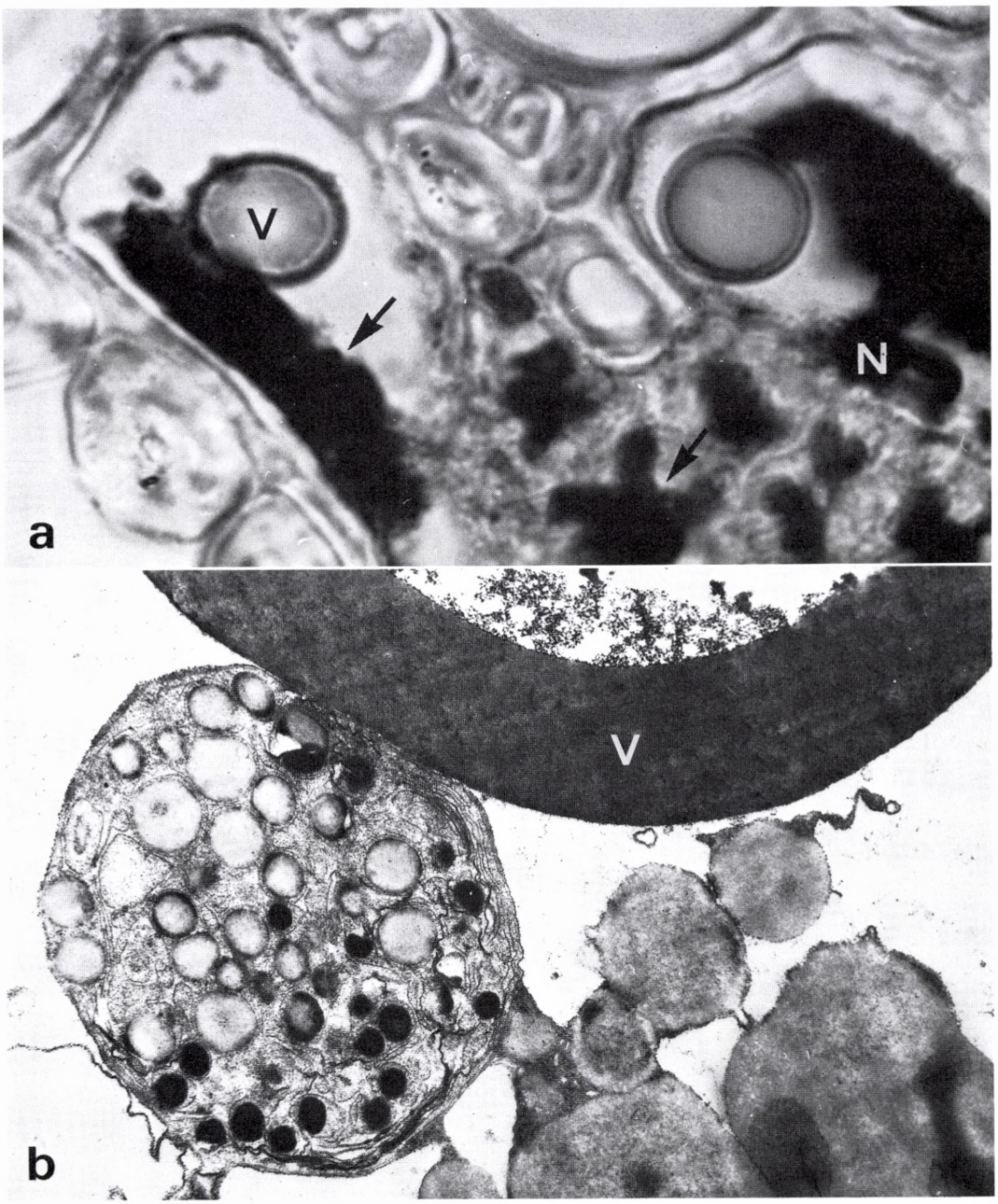

Fig. 19. Vacuolar bodies (V) in degenerating bundle sheath cells. – *a*. Dark areas representing degenerating chloroplasts (arrows) and nucleus (N). Aniline Blue Black (× 2,000). – *b*. TEM of vacuolar body in contact with degenerating chloroplasts.(× 20,000). Further details in Plates IX–XI.

Literature

Akers, S. W., C. E. Anderson & U. Blum, 1977a: Characterization of vacuolar bodies in *Spartina alterniflora*: I. Formation, development, morphology, and ultrastructure. – Amer. J. Bot. *64*: 635–640.

– 1977b: Characterization of vacuolar bodies in *Spartina alterniflora*: II. Some physical and chemical properties. – Amer. J. Bot. *64*: 641–648.

Anderson, C. E., 1974: A review of structure in several North Carolina salt marsh plants. – Ecology of halophytes (Ed. R. J. Reimold & W. H. Queen), pp. 307–344. Academic Press, New York.

Barka, T. & P. J. Anderson, 1962: Histochemical methods for acid phosphatase using hexazonium pararosanilin as coupler. – J. Histochem. Cytochem. *10*: 741–753.

Ben-Shaul, Y. & Y. Naftali, 1969: The development and ultrastructure of lycopene bodies in chromoplasts of *Lycopersicum esculentum*. – Protoplasma *67*: 333–344.

– T. Treffry & S. Klein, 1968: Fine structure studies of carotene body development. – J. Microscopie *7*: 265–274.

Boardman, N. K., O. Björkman, J. M. Anderson, D. J. Goodchild & S. W. Thorne, 1974: Photosynthetic adaptation of higher plants to light intensity: Relationship between chloroplast structure, composition of the photosystems and photosynthetic rates. – Proc. Third Int. Cong. Photosynthesis (Ed. M. Avron), pp. 1809–1827. Elsevier, Amsterdam.

Brown, R. H., 1976: Characteristics related to photosynthesis and photorespiration of *Panicum milioides*. – CO_2 metabolism and plant productivity (Ed. R. H. Burris & C. C. Black), pp. 311–325. University Park Press, Baltimore.

Brown, W. V., 1975: Variations in anatomy, associations, and origins of Kranz tissue. – Amer. J. Bot. *62*: 395–402.

Byott, G. S. & D. W. Sheriff, 1976: Water movement into and through *Tradescantia virginiana* (L.) leaves. II. Liquid flow pathways and evaporative sites. – J. Exp. Bot. *27*: 634–639.

Böcher, T. W., 1972: Leaf anatomy in *Sporobolus rigens* (Tr.) Desv. (Gramineae). – Bot. Notiser *125*: 344–360.

– 1977: Convergence as an evolutionary process. – Bot. J. Linn. Soc. *75*: 1–19.

– J. P. Hjerting & K. Rahn, 1972: Botanical studies in the Atuel Valley Area, Mendoza Province, Argentina. – Da. Bot. Ark. *22, 3*: 193–351.

– O. B. Lyshede, 1968: Anatomical studies in xerophytic apophyllous plants I. – Biol. Skr. Dan. Vid. Selsk. *16, 3*: 1–44.

Carolin, R. C., S. W. L. Jacobs & M. Vesk, 1973: The structure of the cells of the mesophyll and parenchymatous bundle sheath of the Gramineae. – Bot. J. Linn. Soc. *66*: 259–275.

Clarkson, D. T., A. W. Robards & J. Sanderson, 1971: The tertiary endodermis in barley roots. Fine structure in relation to radial transport of ions and water. – Planta (Berl.) *96*: 292–305.

Coombs, J. & A. D. Greenwood, 1976: Compartmentation of the photosynthetic apparatus. – The intact chloroplast (Ed. J. Barber), pp. 1–51. Elsevier, Amsterdam – New York – Oxford.

Craig, S. & D. J. Goodchild, 1977: Leaf ultrastructure of *Triodia irritans*: a C_4 grass possessing an unusual arrangement of photosynthetic tissues. – Aust. J. Bot. *25*: 277–290.

Downton, W. J. S., 1971: Further evidence for two modes of carboxyl transfer in plants with C_4-photosynthesis. – Can. J. Bot. *49*: 1439–1442.

Dyar, M. T., 1953: Studies on the reduction of a tetrazolium salt by green plant tissue. – Amer. J. Bot. *40*: 20–25.

Ellis, R. P., 1976: A procedure for standardizing comparative leaf anatomy in the Poaceae. I. The leaf-blade as viewed in transverse section. – Bothalia *12*: 65–109.

Easu, K., 1977: Membranous modifications in sieve element plastids of spinach affected by the aster yellows disease. – J. Ultrastruct. Res. *59*: 87–100.

Feder, N. & T. P. O'Brien, 1968: Plant microtechnique: Some principles and new methods. – Amer. J. Bot. *55*: 123–142.

Fisher, D. B., 1968: Protein staining of ribboned epon sections for light microscopy. – Histochemie *16*: 92–96.

Freidenfelt, T., 1904: Der anatomische Bau der Wurzeln in seinem Zusammenhang mit dem Wassergehalt des Bodens. (Studien über die Wurzeln krautiger Pflanzen. II.). – Bibl. Bot. Heft *61*.

Geiger, D. R., 1975: Phloem loading – Encyclopedia of Plant Physiology. Vol. 1, I (Ed. M. H. Zimmermann & J. A. Milburn), pp. 395–431. Springer, Berlin – Heidelberg – New York.

Goller, H., 1977: Beiträge zur Anatomie adulter Gramineen-

wurzeln im Hinblick auf taxonomische Verwendbarkeit. – Beitr. Biol. Pflanzen *53*: 217–307.

Goosens, A. P., 1936: Notes on the anatomy of grass roots. – Trans. Roy. Soc. South Afr. *23*: 1–21.

Greenway, H. & C. B. Osmond, 1972: Salt responses of enzymes from species differing in salt tolerance. – Plant Physiol. *49*: 256–259.

Gunning, B. E. S., J. S. Pate & L. G. Briarty, 1968: Specialized "transfer cells" in minor veins of leaves and their possible significance in phloem translocation. – J. Cell Biol. *37*: C7–12.

Gutierrez, M., V. E. Gracen & G. E. Edwards, 1974: Biochemical and cytological relationships in C_4 plants. – Planta (Berl.) *119*: 279–300.

Guttenberg, H. von, 1943: Die physiologischen Scheiden. – Handb. d. Pflanzenanatomie, 1, 2 Bd. V. Gebrüder Borntraeger, Berlin.

Hansen, D. J., P. Dayanandan, P. B. Kaufman & J. D. Brotherson, 1976: Ecological adaptations of salt marsh grass, *Distichlis spicata* (Gramineae), and evironmental factors affecting its growth and distribution. – Amer. J. Bot. *63*: 635–650.

Harris, W. M., 1971: Ultrastructural observations on the mesophyll cells of pine leaves. – Can. J. Bot. *49*: 1107–1109.

Hatch, M. D., T. Kagawa & S. Craig, 1975: Subdivision of C_4-pathway species based on differing C_4 acid decarboxylating systems and ultrastructural features. – Aust. J. Plant Physiol. *2*: 111–128.

Hattersley, P. W. & L. Watson, 1976: C_4 grasses: An anatomical criterion for distinguishing between NADP-malic enzyme species and PCK or NAD-malic enzyme species. – Aust. J. Bot. *24*: 297–308.

Henríci, M., 1929: Die Struktuur van die Bas en Graswortels in die Droë Streke van Suid-Afrika. – Wetensk. Pamflet *85*, Dept. van Landbou, Pretoria.

Jensen, W. A., 1962: Botanical Histochemistry. – Freeman, San Francisco.

Johnson, Sr. C. & W. V. Brown, 1973: Grass leaf ultrastructural variations. – Amer. J. Bot. *60*: 727–735.

Kaufman, P. B., L. B. Petering & J. G. Smith, 1970: Ultrastructural development of cork-silica cell pairs in *Avena* internodal epidermis. – Bot. Gaz. *131*: 173–185.

Kroemer, K., 1903: Wurzelhaut, Hypodermis und Endodermis der Angiospermenwurzel. – Bibl. Bot. Heft *59*.

Kuo, J., T. P. O'Brien & M. J. Canny, 1974: Pit-field distribution, plasmodesmatal frequency, and assimilate flux in the mestome sheath cells of wheat leaves. – Planta (Berl.) *121*: 97–118.

Levering, C. A. & W. W. Thomson, 1971: The ultrastructure of the salt gland of *Spartina foliosa*. – Planta (Berl.) *97*: 183–196.

Liphschitz, N. & Y. Waisel, 1974: Existence of salt glands in various genera of the Gramineae. – New Phytol. *73*: 507–513.

Matile, Ph., 1975: The lytic compartment of plant cells. – Cell Biology Monographs, Vol. 1. Springer, Berlin.

Mazia, D., P. A. Brewer & M. Alfert, 1953: The cytochemical staining and measurement of protein with mercuric bromphenol blue. – Biol. Bull. *104*: 57–67.

McWilliam, J. R. & K. Mison, 1974: Significance of the C_4 pathway in *Triodia irritans* (Spinifex), a grass adapted to arid environments. – Aust. J. Plant Physiol. *1*: 171–175.

Metcalfe, C. R., 1960: Anatomy of the Monocotyledons. I. The Gramineae. – Clarendon Press, Oxford.

Mollenhauer, H. H., 1974: Poststaining sections for electron microscopy. – Stain Techn. *49*: 305–308.

O'Brien, T. P. & D. J. Carr, 1970: A suberized layer in the cell walls of the bundle sheath of grasses. – Aust. J. biol. Sci. *23*: 275–287.

– J. Kuo, 1975: Development of the suberized lamella in the mestome sheath of wheat leaves. – Aust. J. Bot. *23*: 783–794.

Olesen, P., 1974: Leaf anatomy and ultrastructure of chloroplasts in *Salsola kali* L. as related to the C_4-pathway of photosynthesis. – Bot. Notiser *127*: 352–363.

– 1975: Plasmodesmata between mesophyll and bundle sheath cells in relation to the exchange of C_4-acids. – Planta (Berl.) *123*: 199–202.

– 1978: Structure of chloroplast membranes as revealed by natural and experimental fixation with tannic acid: Particles in and on the thylakoid membrane. – Biochem. Physiol. Pflanzen *172*: 319–342.

Pate, J. S. & B. E. S. Gunning, 1969: Vascular transfer cells in angiosperm leaves. A taxonomic and morphological survey. – Protoplasma *68*: 135–156.

Pickett-Heaps, J. D., 1967: The effects of colchicine on the ultrastructure of dividing plant cells, xylem wall differentiation and distribution of cytoplasmic microtubules. – Develop. Biol. *15*: 206–236.

Raju, M. V. S., T. A. Steeves & J. M. Naylor, 1964: Developmental studies on *Euphorbia esula* L.: Apices of long and short roots. – Can. J. Bot. *42*: 1615–1628.

Ruthsatz, B., 1977: Pflanzengesellschaften und ihre Lebensbedingungen in den Andinen Halbwüsten Nordwest-Argentiniens. – Dissertationes Botanicæ *39*: 1–168. – Cramer, Vaduz.

Schnepf, E., 1973: Mikrotubulus-Anordnung und -Umordnung, Wandbildung und Zellmorphogenese in jungen *Sphagnum*-Blättchen. – Protoplasma *78*: 145–173.

Sharman, B. C. & P. A. Hitch, 1967: Initiation of procambial strands in leaf primordia of bread wheat, *Triticum aestivum* L. – Ann. Bot. *31*: 229–243.

Sievers, J., 1971: Basic two-dye stains for epoxy-embedded 0.3–1 µ sections. – Stain Techn. *46*: 195–199.

Spurr, A. R., 1969: A low-viscosity epoxy resin embedding medium for electron microscopy. – J. Ultrastruct. Res. *26*: 31–43.

Smith, C. G., 1974: The ultrastructural development of spherosomes and oil bodies in the developing embryo of *Crambe abyssinica*. – Planta (Berl.) *119*: 125–142.

Stelzer, R. & A. Läuchli, 1977: Salz- und Überflutungstoleranz von *Puccinellia peisonis* II. Strukturelle Differenzierung der Wurzel in Beziehung zur Funktion. – Z. Pflanzenphysiol. *84*: 95–108.

Tanton, T. W. & S. H. Crowdy, 1972: Water pathways in higher plants III. The transpiration stream within leaves. – J. Exp. Bot. *23*: 619–625.

Thomson, W. W., 1975: The structure and function of salt glands. – Ecological Studies. Vol. 15 (Ed. A. Poljakoff-Mayber & J. Gale), pp. 118–146. Springer, Berlin.

Volkens, G., 1887: Die Flora der Ägyptisch-arabischen Wüste auf Grundlage anatomisch-physiologischer Forschungen. – Berlin.

Werner, D. J., 1972: Campo Arenal (NW-Argentinien). Eine Landschafts-ökologische Detailstudie. – Biogeografica *1*: 75–86.

– 1974: Landschaftsökologische Untersuchungen in der argentinischen Puna. – Deutscher Geographentag, Kassel, 1973. Tagungsber. u. wissensch. Abh., S. 508–528.

Wiebe, H. H. & H. A. Al-Saadi, 1976: The role of invaginations in armed mesophyll cells of pine needles. – New Phytol. *77*: 773–775.

Zee, S.-Y. & T. P. O'Brien, 1971: Vascular transfer cells in the wheat spikelet. – Aust. J. biol. Sci. *24*: 35–49.

Zemke, E., 1939: Anatomische Untersuchungen an Pflanzen der Namibwüste. – Flora N.F. *33*: 365–416.

Zimmermann, M. H., P. B. Tomlinson & J. Le Claire, 1974: Vascular construction and development in the stems of certain Pandanaceae. – Bot. J. Linn. Soc. *68*: 21–41.

Indleveret til Selskabet 5. maj 1978,

Færdig fra trykkeriet december 1978.

Plates I–XI

a. Secreting epidermal cells of root tip between cap and root hair zone. Vacuoles with fibrillar or granular contents on both sides of the large, central nucleus. Dense cytoplasm with mitochondria (M), endoplasmic reticulum (ER), and starch-containing proplastids (P). Actively secreting dictyosomes are concentrated along the conspicuously thickened outer wall (arrows). (TEM × 13,800). – *b.* Details of cytoplasm adjacent to outer wall showing rough endoplasmic reticulum (ER), mitochondria (M) and numerous dictyosomes giving off vesicles (V) containing dense, fibrillar material. The outer wall shows transfer-cell-like invaginations apparently formed by discharge of the dictyosome vesicles into the wall; microtubules (arrows) are preferentially distributed between the invaginations. Numerous dense ribosomes bound to ER cisternae or free in the cytoplasm (R). (TEM × 69,000).

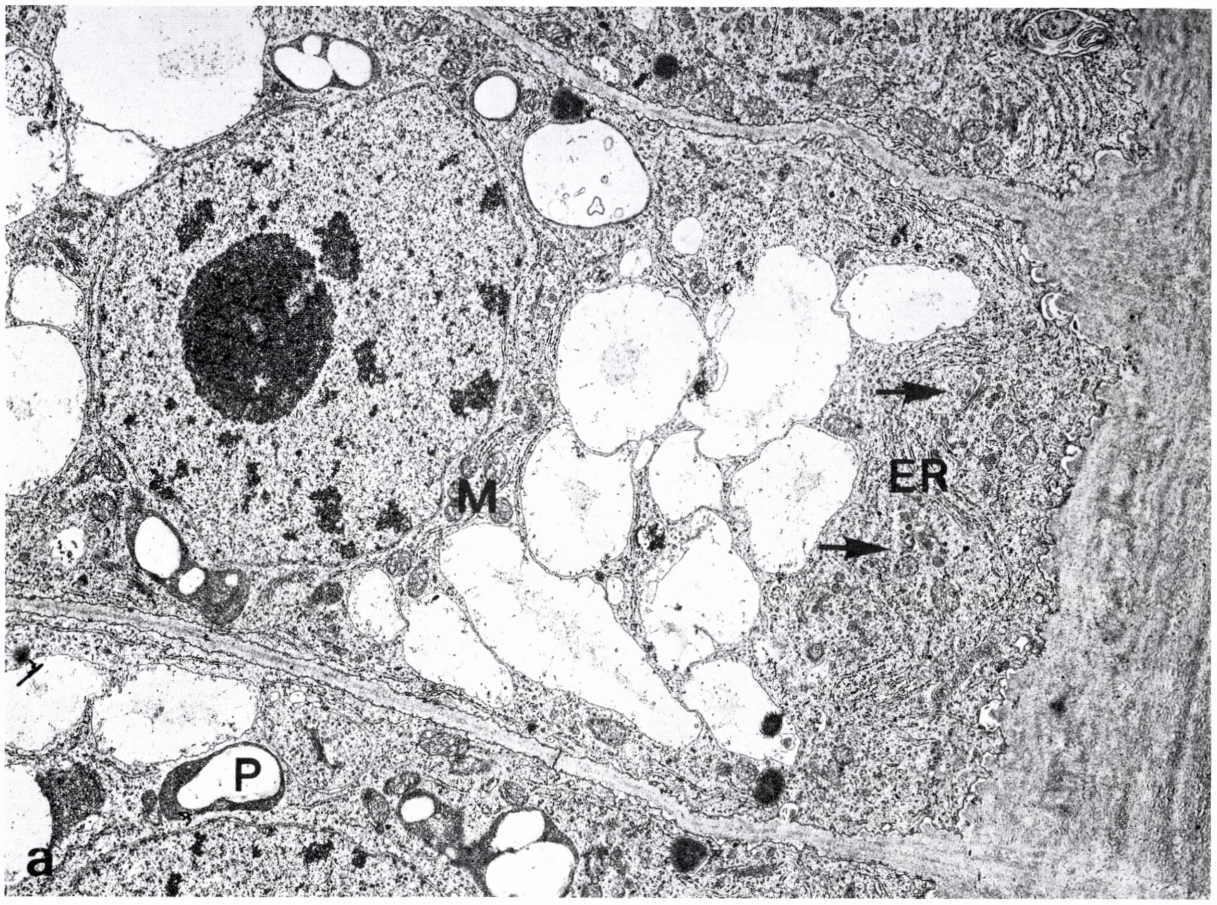
M
ER
P
a

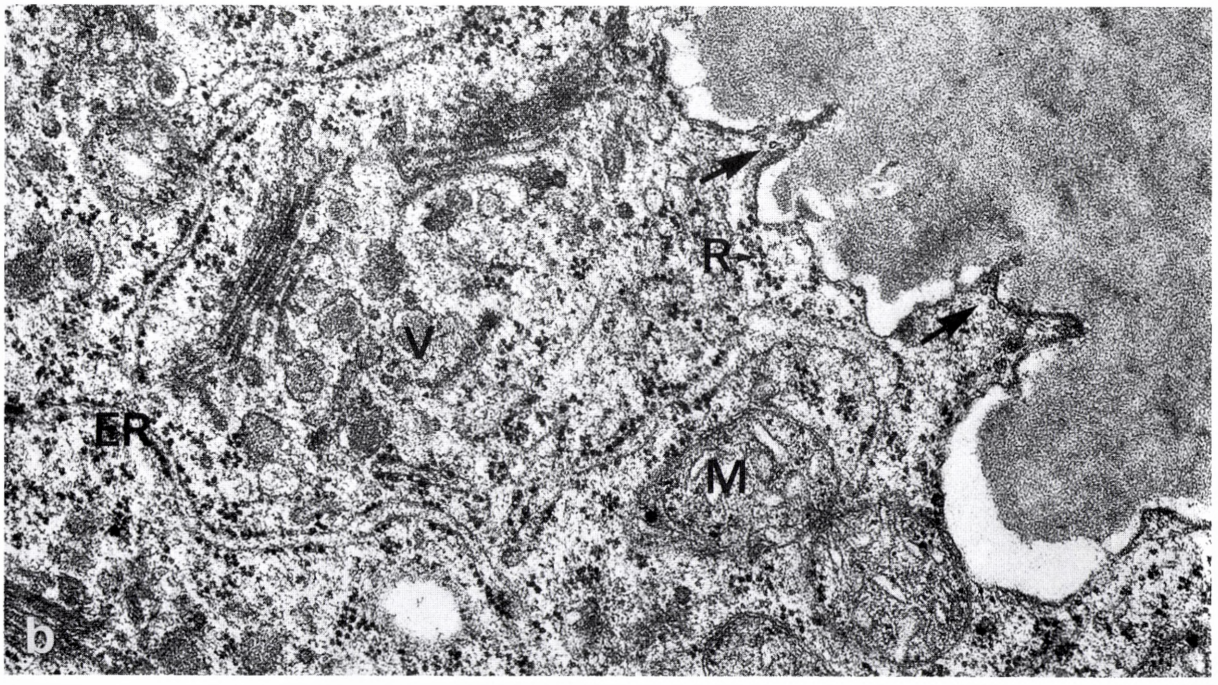
R
V
ER
M
b

Stages in the differentiation of chloroplasts in the two cell types in the chlorenchyma, TEM. – *a*. Survey of young mesophyll (MS) and bundle sheath (BS) cells. Small starch-containing proplastids (P) are scattered in both cell types; in mesophyll cells the first signs of developing air spaces and internal ridges are found (arrows). (× 4,200). – *b–e*. Starch grains (S), thylakoid development and grana formation in young bundle-sheath chloroplasts (b × 41,000; c × 38,000) and mesophyll chloroplasts (d × 30,000; e × 34,000).

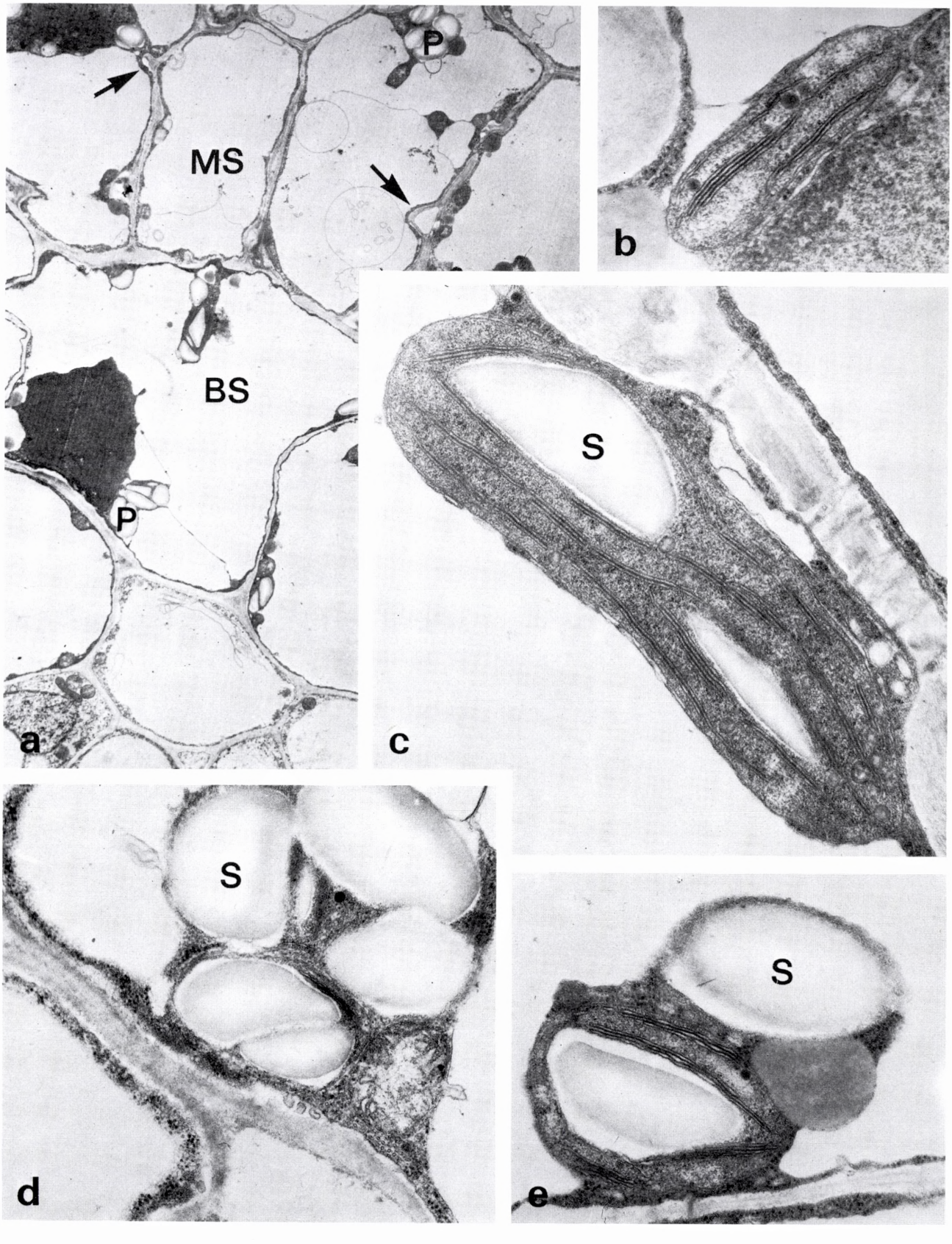
P
MS
BS
P
a
b
S
c
S
d
S
e

Mature chloroplasts in bundle-sheath (a, b) and mesophyll cells (c, d), TEM. – *a*. Transverse section of leaf showing tightly packed chloroplasts separated by cytoplasm and mitochondria (M); the elongated chloroplasts project into the central vacuole. (× 19,000). – *b*. Numerous well-developed grana are separated by relatively few stroma thylakoids. Arrow points to narrow band of cytoplasm with ribosomes between the two chloroplasts. (× 25,400). – *c*, *d*. Well-developed peripheral reticulum (PR) and semicrystalloid aggregates of electron-dense tubules (T). (c × 33,000; d × 25,800).

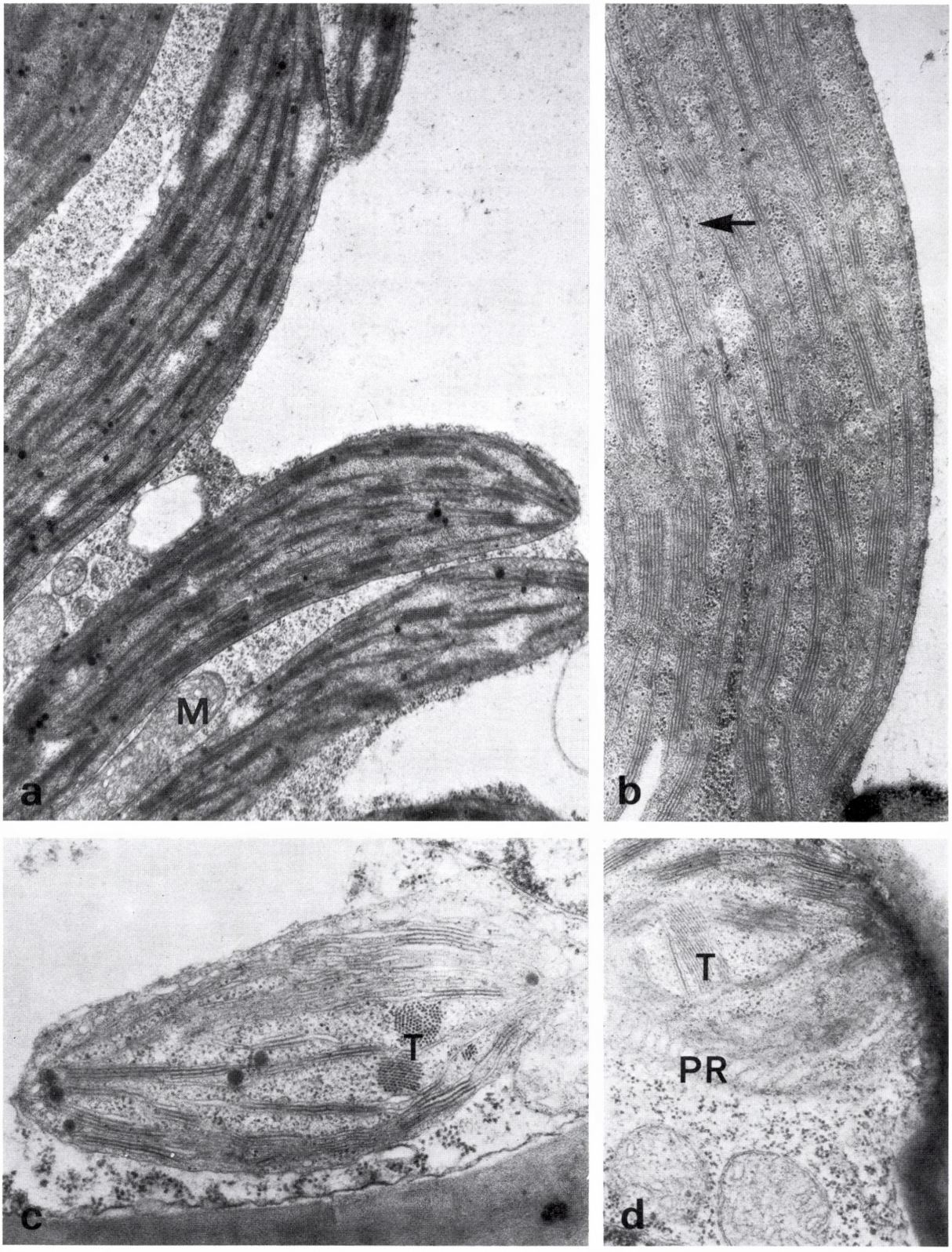
M
a
b
T
c
T
PR
d

Differentiation of arm cell mesophyll, TEM. – *a*. Oblique, paradermal section showing the uneven development of air spaces which starts around the substomatal chambers (on the right). (× 3,780). – *b*. At sites of air space formation a local dissolution of the middle lamella (*) is accompanied by two opposite bands of microtubules (arrows) "pulling" the wall halves apart. (× 48,000). – *c*. Developing internal ridges on the mesophyll side of the wall between mesophyll and bundle sheath cell. The ridges are covered by bands of microtubules (arrows) and the cytoplasm appears active with dictyosomes (D), mitochondria (M) and dilated endoplasmic reticulum cisternae (ER). (× 21,800). – *d*. Developing air spaces separated by young pit fields in areas of contact between the arms in later stages. (× 11,760). – *e*. Continuous microtubules associated with developing internal ridge around part of mesophyll cell. (× 19,000).

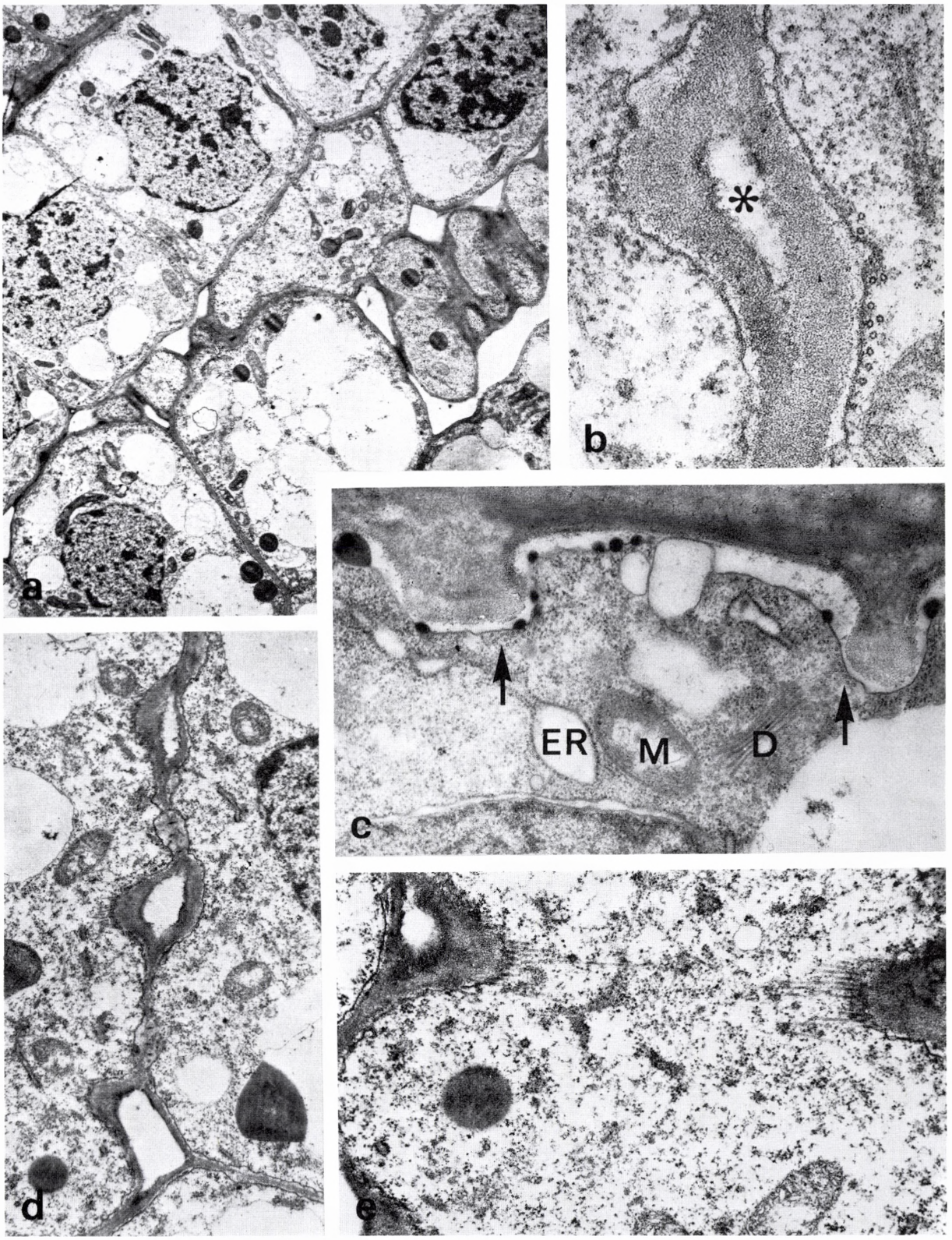
a
b
*
c
ER
M
D
d
e

Development of stomata and epidermal salt gland short cells, TEM. – *a*. Paradermal section showing survey of young stomatal complexes and alternating short and long cells in the epidermis. (× 3,000). – *b*. Transection of stomatal complex before extensive thickening of guard cell walls takes place; note continuous outer ledges (arrow). (× 5,600). – *c*. Mature stomatal complex: slightly oblique, paradermal section showing rather thin-walled subsidiary cells and thickened, bulbous ends of the guard cells. The latter with starch-containing chloroplasts (arrow). (× 3,000). – *d*. Young salt gland cell with dense cytoplasm between highly vacuolated epidermal (E) and mesophyll cells (MS). (× 3,600).

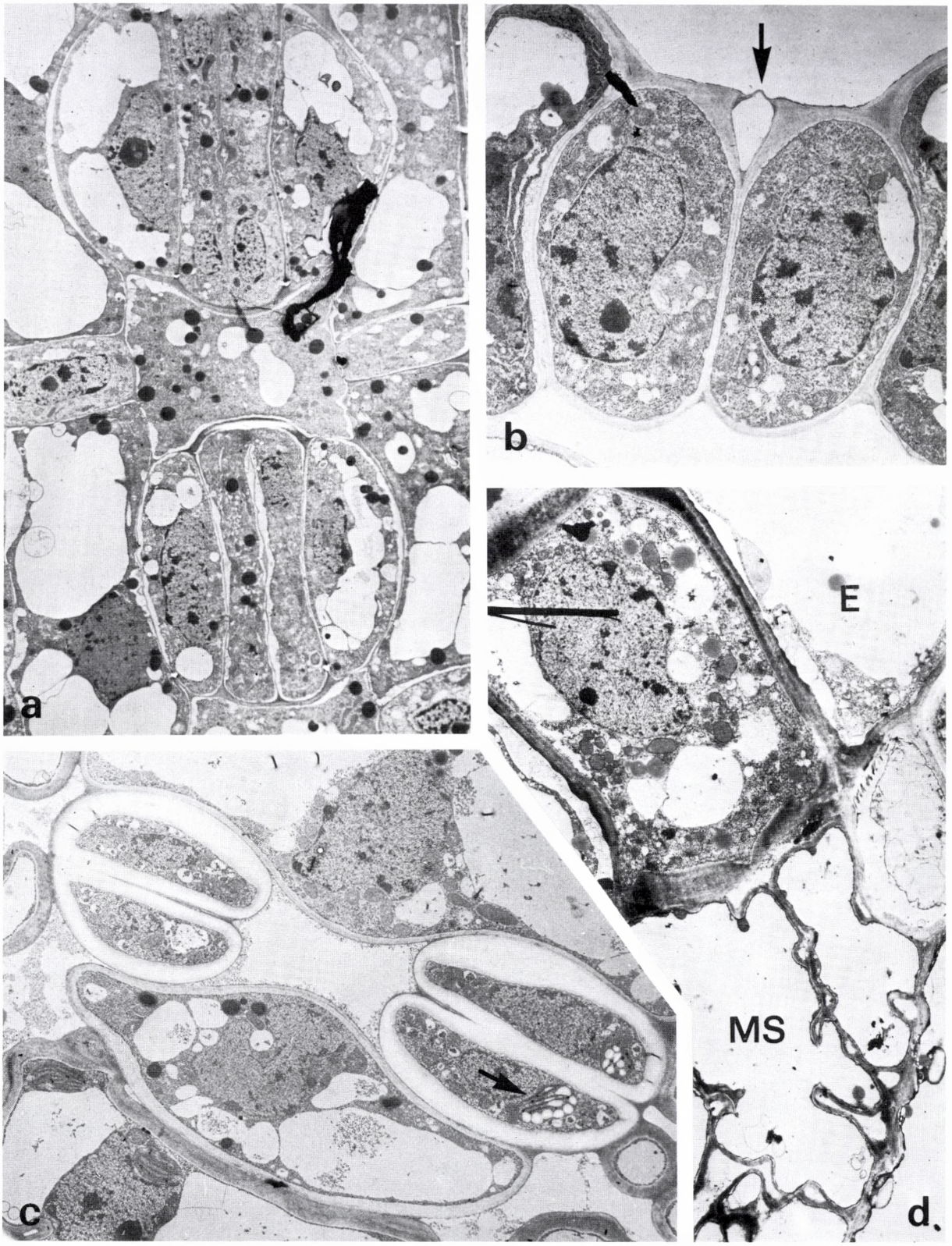
a
b
E
MS
c
d

Transections of specialized epidermal short cells possibly functioning as salt glands, TEM. – *a*. Dense, cutinized layer in anticlinal wall separated from the cytoplasm by electron-transparent (and strongly PAS-positive) layer. (× 40,000). – *b*. Survey of immature gland showing pit connections to epidermal and mesophyll cells. In the epidermal cell to the right a pit penetrates the inner part of the outer wall but stops at the cuticular layer. Similar texture and density in outer, continuous cuticular layer and inner, cutinized layer around gland cell; central depression of gland cell not included in the section. (*) point to areas where complex lamellar structures develop in a mature gland, see c. (× 4,280). – *c*. Mature gland with complex lamellar structure between anticlinal wall (W) and central nucleus (N). (× 26,400). – *d*. Outer wall of mature gland showing depression resulting from decrease in thickness of cuticular layer; the central area of the wall (which is characterized by strong affinity for Toluidine Blue and Ruthenium Red) appears rather empty. The two black lines are folds in the section. (× 9,800). – *e*. Part of young gland cell (detail of Plate Vd) showing strongly stainable plastids (P) and mitochondria. (× 20,000).

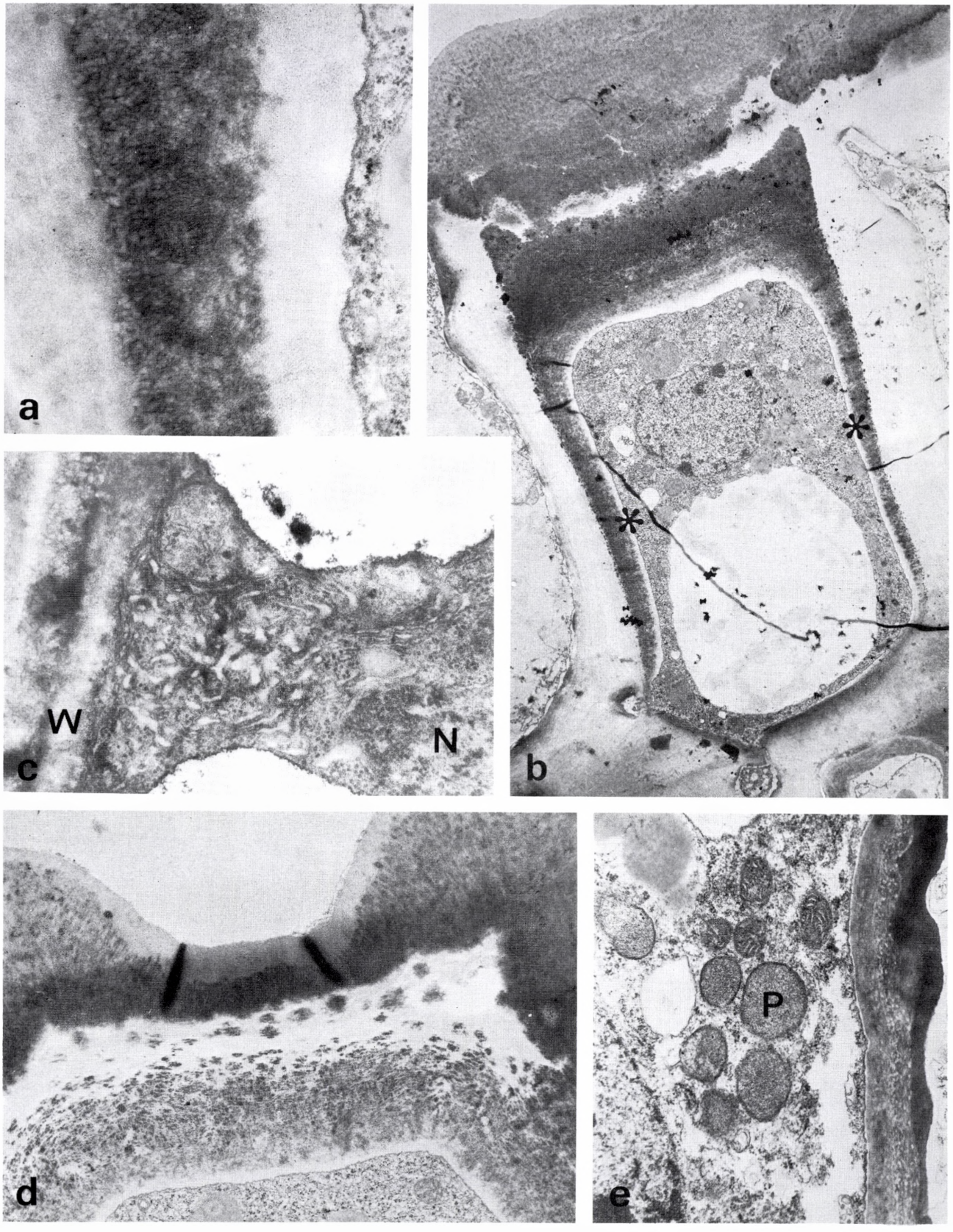
a
b
c
W
N
d
e
P

Vascular tissue, mestome sheath and transfer cells, TEM. – *a*. Longitudinal survey showing armed mesophyll (MS), bundle sheath tightly packed with chloroplasts and mitochondria, and mestome sheath (*) adjacent to sieve element (SE). (× 3,200). – *b*. Longitudinal section of minor bundle. Transfer cell (T) with numerous pit fields; sieve element (SE) with callose plugs around the pores in lateral sieve area; mestome sheath (*) on the opposite side of the bundle; bundle sheath cells on both sides. (× 4,200). – *c*. Transection of transfer cell adjacent to three phloem parenchyma cells, bundle sheath cell (BS) and one xylem element (XY). (× 6,400). – *d*. Layered suberin lamellae between two adjoining mestome sheath cells (bundle side to the right). (× 51,000). – *e*. Transection of plasmodesmata in pit field between mesophyll and bundle sheath cell. (× 48,000).

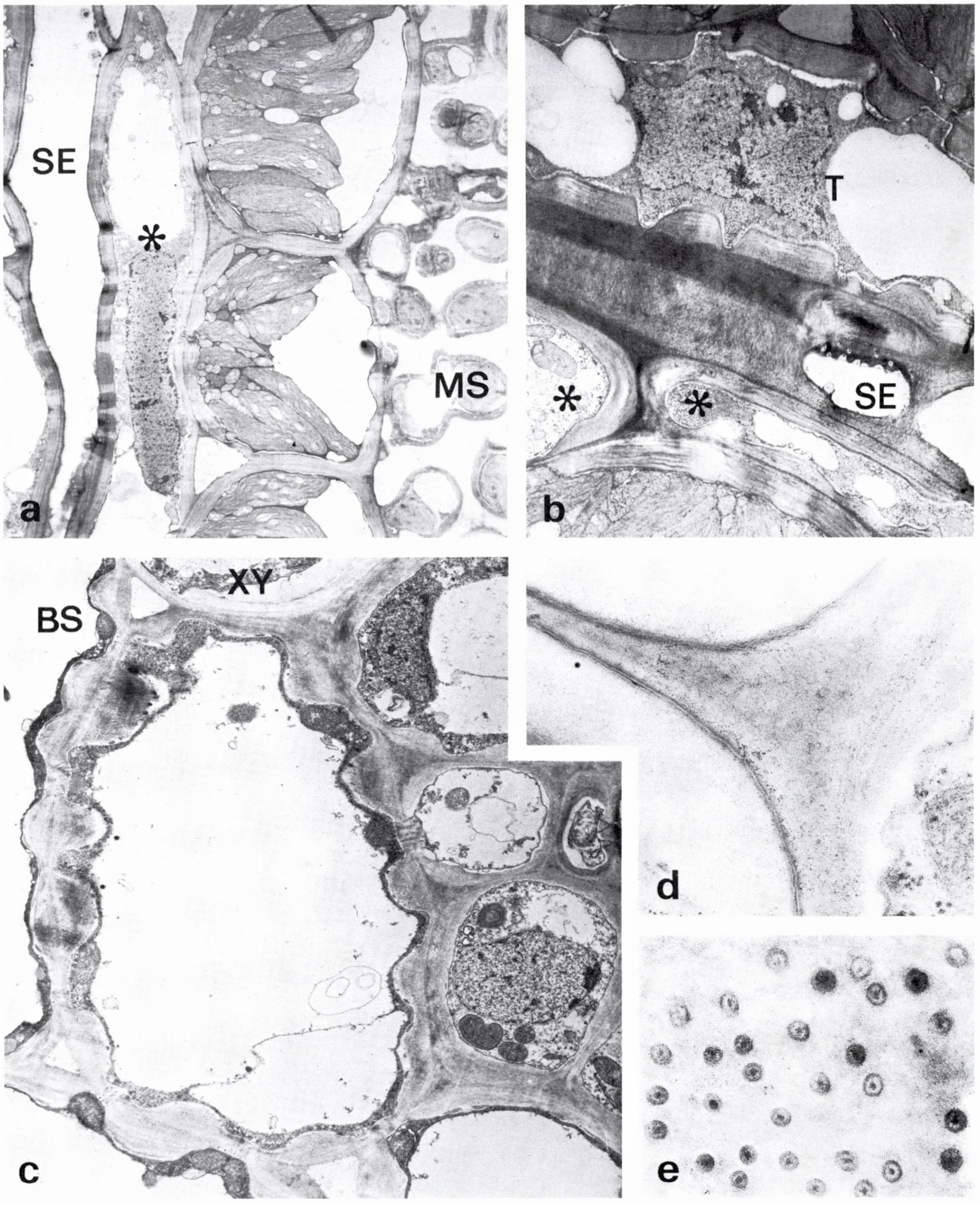
SE
*
MS
a
T
*
*
SE
b
BS
XY
c
d
e

Senescence and degeneration (stage 6) of chloroplasts in mesophyll cells, TEM. – *a*, *b*. Disorganization of grana configurations: the thylakoids are placed in parallel, curved clusters. Arrows indicate aggregates of hexagonally packed tubules. (a × 11,760; b × 47,600). – *c*, *d*. Longitudinal (c) and transverse (d) sections of the tubules which increase in number. (c × 160,000; d × 100,000). – *e*. High magnification of the tubules from chloroplast fixed with tannic acid: a subunit structure in the tubules is evident. (× 280,000).

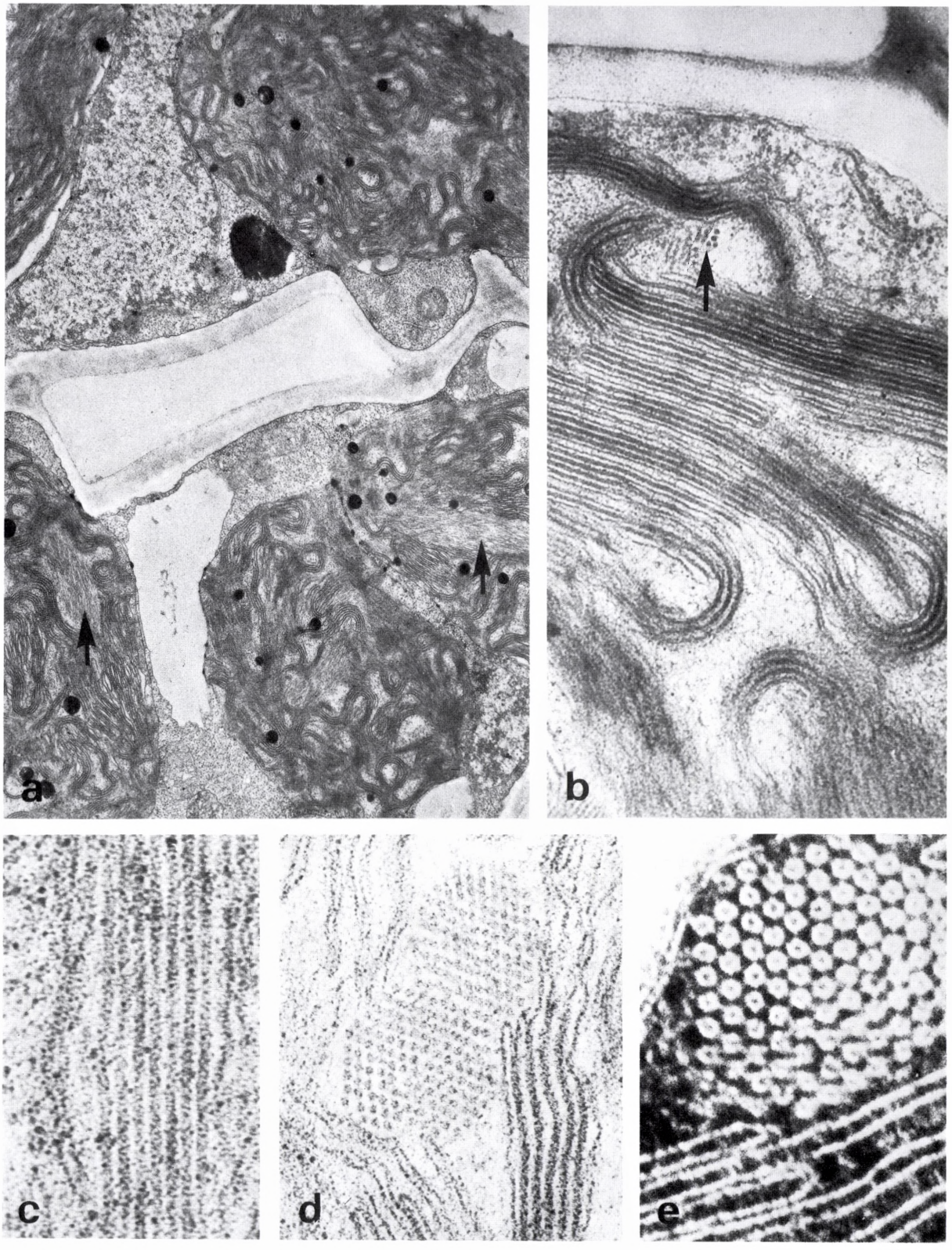
a
b
c
d
e

Senescence and degeneration (stage 6) of chloroplasts in bundle sheath cells, TEM. – *a*. Early stage of senescence: swollen mitochondria (M) and microbody (*); increased density of plastoglobuli and electron-dense deposits along the chloroplast envelope (arrows). (× 19,800). – *b*. Incipient swelling of stromathylakoids which become filled with dense, granular material. (× 70,000). – *c*, *d*. Grana are dissolved and many thylakoids form long lamellae parallel to the chloroplast surface (c), the plastoglobuli increase in size and number (d) and show varying degrees of electron-density. Very dense lamellae (arrows) appear often in contact with plastoglobuli. (c × 33,000; d × 27,500). – *e*. Chloroplast debris after rupture of the envelope: dense lamellae and large, irregular plastoglobuli. (× 30,000).

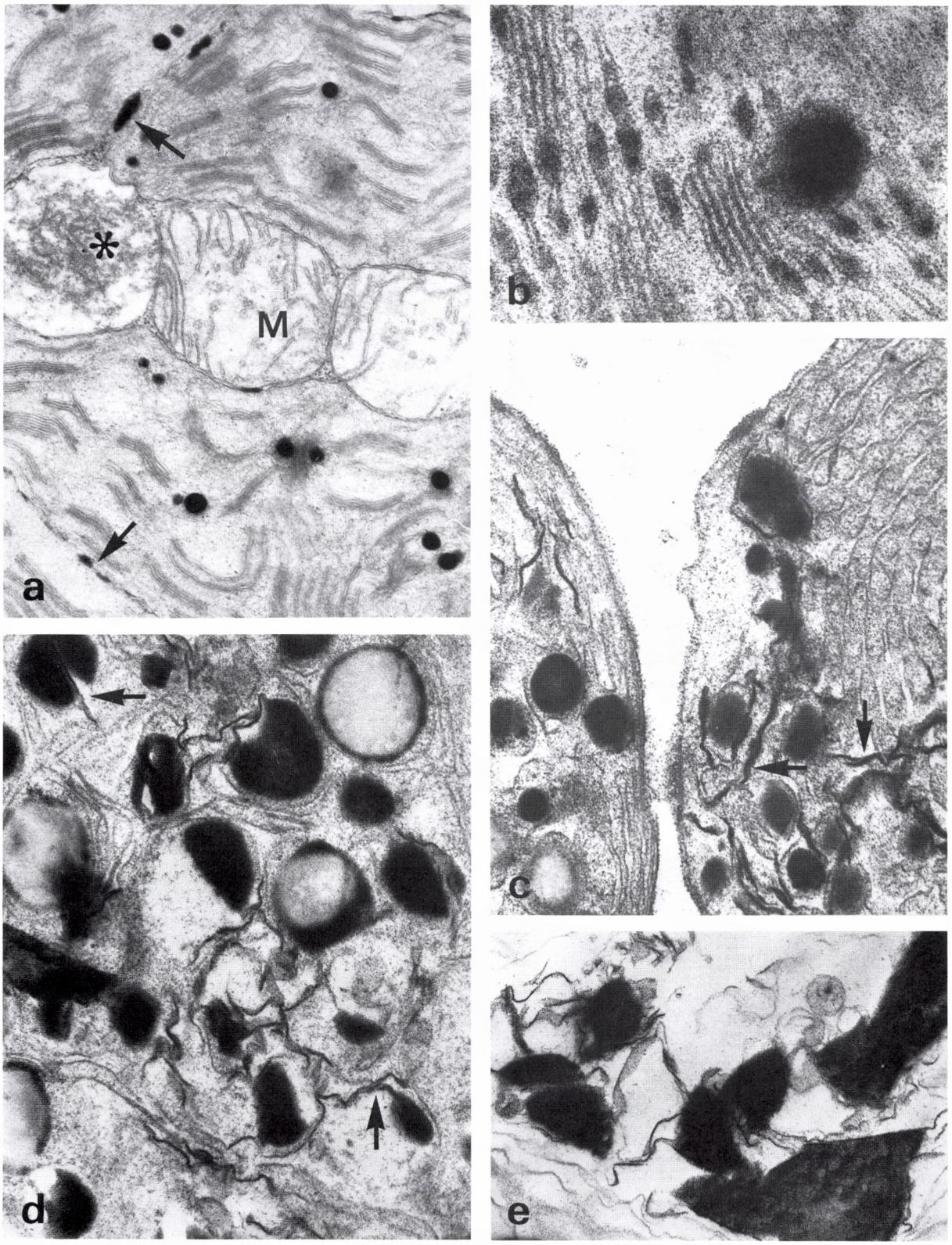
a
M
b
c
d
e

Development of vacuolar bodies in senescing bundle sheath cells, TEM. – *a*, *b*. Two-phase bodies appear in the cytoplasm, presumably derived from spherosomes. Note conspicuous pit field with numerous plasmodesmata between bundle sheath and mesophyll cell. (× 24,200). – *c*. A small two-phase body in the cytoplasm and a much enlarged similar body associated with the vacuole. The interior phase of the large vacuolar body comprises several separate compartments with granular, possibly lytic, contents. (× 12,400). – *d*. Strongly lobed (amoeboid?) vacuolar bodies in contact with three chloroplasts; no signs of a separating tonoplast. (× 19,000). – *e*. Enlarged vacuolar body with thickened exterior phase and dilute, granular interior phase. (× 12,400).

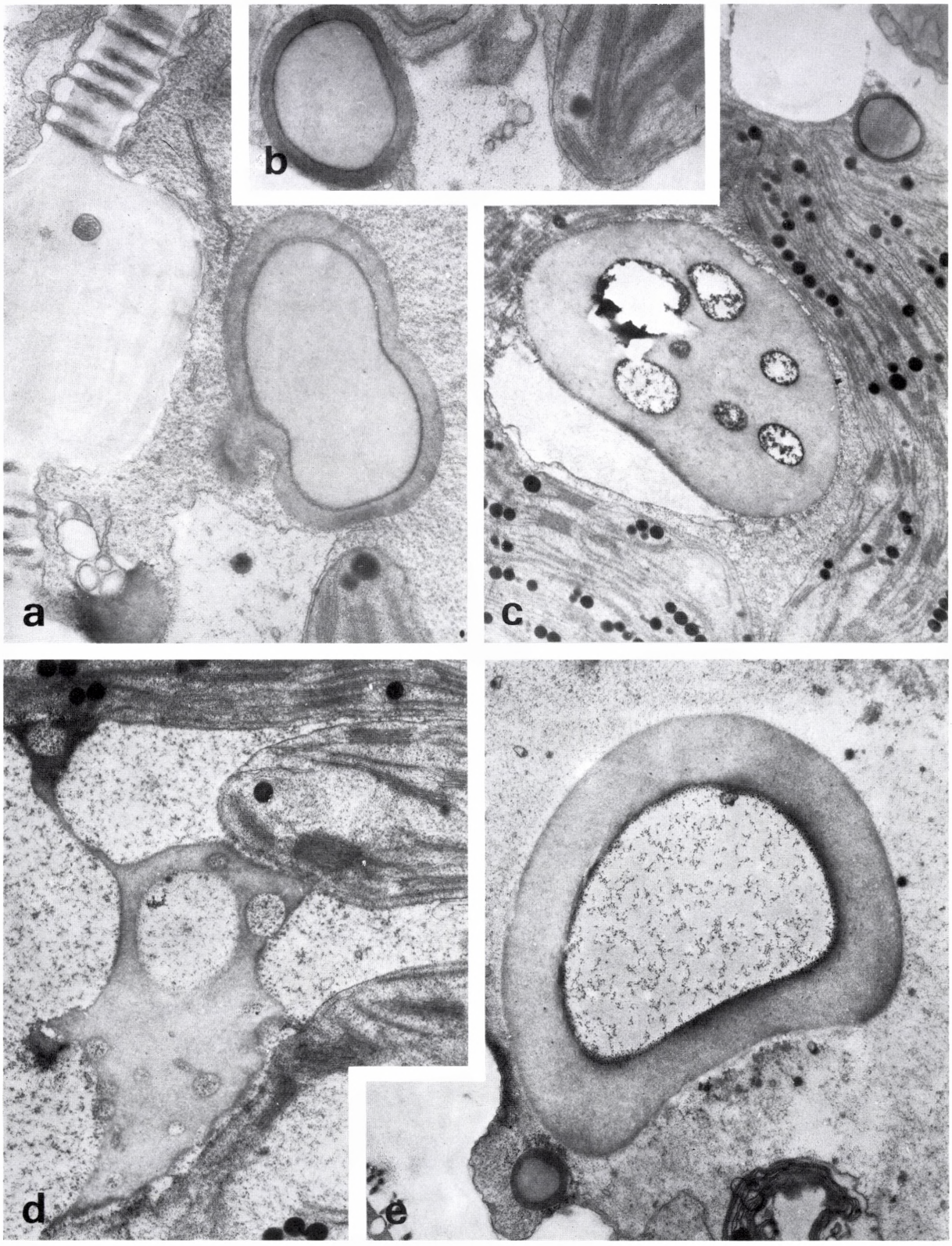
a
b
c
d
e

Late stages in the development of vacuolar bodies in bundle sheath cells, TEM. – *a*. Enlarged body with dilute, interior phase; the section is slightly damaged. Note abundant plasmodesmata in pit field between mesophyll and bundle sheath cell. (× 7,500). – *b*, *c*. Similar bodies with intimate contact between exterior phase and chloroplast. Arrow points to remains of the tonoplast. (b × 9,900; c × 24,100). – *d*. Very dense exterior phase of mature vacuolar body in contact with senescing chloroplast. (× 10,700).

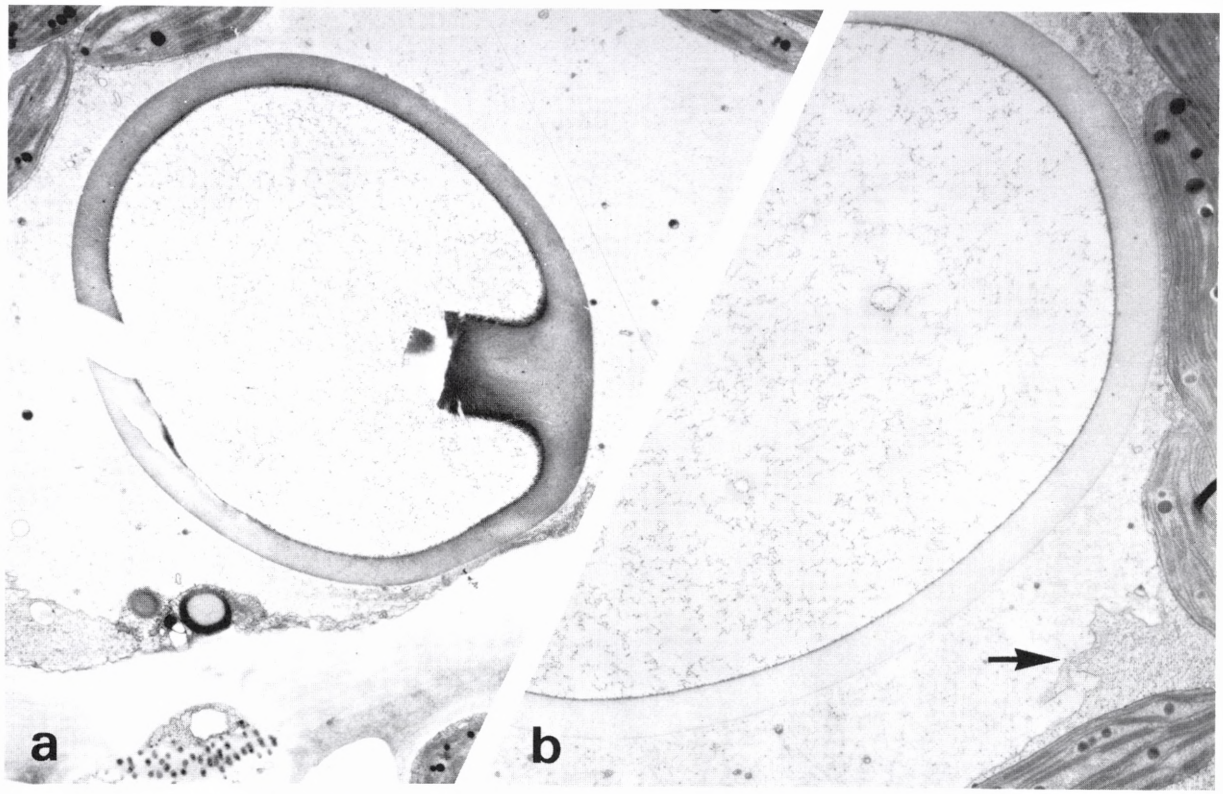
a
b


c

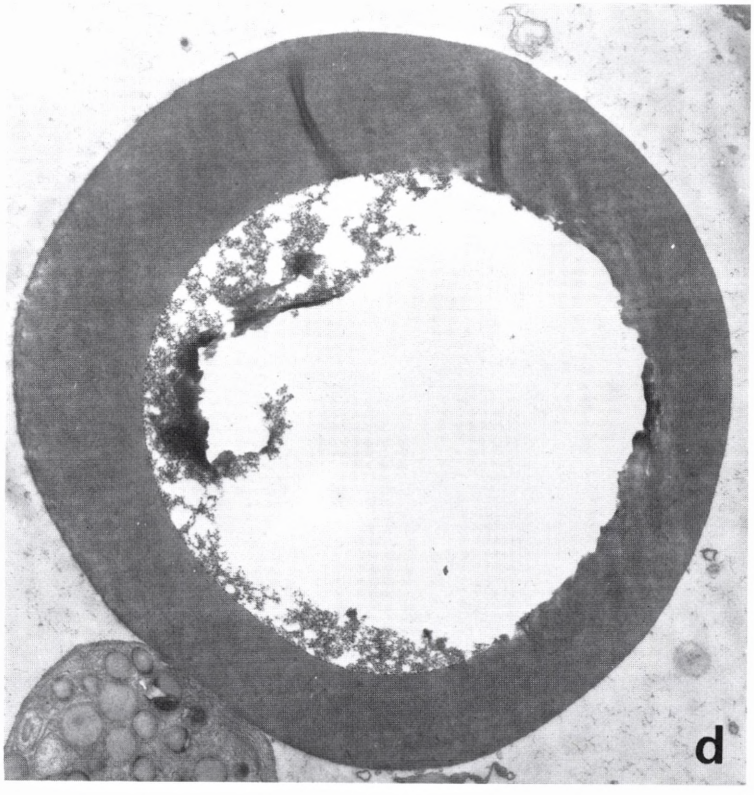
d

Biologiske Skrifter

Biol. Skr. Dan. Vid. Selsk.
Priser excl. moms

Vol. 17 (DKr. 330.–)

1. Degerbøl, Magnus, and Fredskild, Bent: The Urus (*Bos primigenius* Bojanus) and Neolithic Domesticated Cattle (*Bos taurus domesticus* Linné) in Denmark. With a Revision of *Bos*-Remains from the Kitchen Middens. Zoological and Palynological Investigations. 1970... 200.–
2. Hansen, Hans Jørgen: Electron-Microscopical Studies on the Ultrastructures of some Perforate Calcitic Radiate and Granulate Foraminifera. 1970..... 50.–
3. Mathiesen, Fr. J.: Palaeobotanical Investigations into some Cormophytic Macrofossils from the Neogene Tertiary Lignites of Central Jutland. Part II: *Gymnosperms*. 1970..... 80.–

Vol. 18 (DKr. 450.–)

1. Hansen, Georg Nørgaard: On the Structure and Vascularization of the Pituitary Gland in some Primitive Actinopterygians (*Acipenser*, *Polyodon*, *Calamoichthys*, *Polypterus*, *Lepisosteus* and *Amia*). 1971..... 70.–
2. Dyck, Jan: Structure and Spectral Reflectance of Green and Blue Feathers of the Rose-faced Lovebird (*Agapornis roseicollis*). 1971..... 60.–
3. Perch-Nielsen, Katharina: Elektronenmikroskopische Untersuchungen an Coccolithen und verwandten Formen aus dem Eozän von Dänemark. 1971... 160.–
4. Böcher, Tyge W., and Lyshede, Ole B.: Anatomical Studies in Xerophytic Apophyllous Plants. II. Additional Species from South American Shrub-Steppes. 1972..... 160.–

Vol. 19 (DKr. 410.–)

1. Humphreys, William F., and Lützen, Jørgen: Studies on Parasitic Gastropods from Echinoderms. I. On the Structure of the Parasitic Gastropod Megadenus cantharelloides n. sp., with Comparisons on Paramegadenus n. g. 1972..... 30.–
2. Surlyk, Finn: Morphological Adaptations and Population Structures of the Danish Chalk Brachiopods (Maastrichtian, Upper Cretaceous). 1972..... 60.–
3. Hammer, Marie: Tahiti. Investigation on the Oribatid Fauna of Tahiti, and on some Oribatids found on the Atoll Rangiroa. 1972..... 80.–
4. Wingstrand, Karl Georg: Comparative Spermatology of a Pentastomid, *Raillietiella Hemidactyli*, and a Branchiuran Crustacean, *Argulus Foliaceus*, with a Discussion of Pentastomid Relationships. 1972..... 80.–
5. Böcher, Tyge W., and Jørgensen, C. A.: Jyske dværgbuskheder. Eksperimentelle undersøgelser af forskellige kulturindgrebs indflydelse på vegetationen. With an English Summary. 1972..... 50.–
6. Lützen, Jørgen: Studies on Parasitic Gastropods from Echinoderms. II. On *Stilifer* Broderip, with Special Reference to the Structure of the Sexual Apparatus and the Reproduction. 1972..... 30.–
7. Rasmussen, H. Wienberg: Lower Tertiary Crinoidea, Crinoidea, Asteroidea and Ophiuroidea from Northern Europe and Greenland. 1972..... 80.–

Vol. 20 (DKr. 490.–)

1. Blom, Lars: Ridge Pattern and Surface Ultrastructure of the Oviducal Mucosa of the Hen (*Gallus domesticus*). 1973..... 30.–
2. Jensen, Poul Vagn: Structure and Metamorphosis of the Larval Heart of *Calliphora erythrocephala*. 1973.. 30.–
3. Hammer, Marie: Oribatids from Tongatapu and Eua, the Tonga Islands, and from Upolu, Western Samoa. 1973..... 80.–
4. Gooding, Richard U., and Lützen, Jørgen: Studies on Parasitic Gastropods from Echinoderms. III. A Description of *Robillardia Cernica* Smith 1889, Parasitic in the Sea Urchin *Echinometra* Meuschen, with Notes on its Biology. 1973..... 30.–
5. Manton, I., and Leadbeater, B. S. C.: Fine-structural Observations on six Species of *Chrysochromulina* from Wild Danish Marine Nanoplankton, including a Description of *C. campanulifera* sp. nov. and a Preliminary Summary of the Nanoplankton as a Whole. 1974..... 40.–

6. Birkelund, Tove, and Hansen, Hans Jørgen: Shell Ultrastructures of some Maastrichtian Ammonoidea and Coleoidea and their Taxonomic Implications. 1974 ..... 50.–
7. Poulsen, Chr.: Silurian Pelecypoda, Monoplacophora, and Gastropoda from the Reefy Facies of the Offley Island Formation of Washington Land and Offley Island (Northwest Greenland). 1974..... 30.–
8. Böcher, Tyge W.: Structure of the Multinodal Photosynthetic Thorns in *Prosopis Kuntzei* Harms. 1975 ..... 60.–
9. Mathiesen, Fr. J.: Palaeobotanical Investigations into some Cormophytic Macrofossils from the Neogene Tertiary Lignites of Central Jutland. Part III: Angiosperms. 1975..... 80.–
10. Bromley, R. G.; Schultz, M.-G., and Peake, N. B.: Paramoudras: Giant Flints, Long Burrows and the Early Diagenesis of Chalks. 1975..... 60.–

Vol. 21 (DKr. 650.–)

1. Nygaard, Gunnar: New or Interesting Plankton Algae. 1977..... 150.–
2. Peel, John S.: Systematics and Palaeoecology of the Silurian Gastropods of the Arisaig Group, Nova Scotia. 1977..... 150.–
3. van der Land, Jacob, and Nørrevang, Arne: Structure and Relationship of Lamellibrachia (Annelida, Vestimentifera). 1977..... 200.-
4. Hammer, Marie: Investigations on the Oribatid Fauna of the North West Pakistan. 1977..... 150.–

Vol. 22 (*uafsluttet/unfinished*)

1. Wingstrand, K. G.: Comparative Spermatology of the Crustacea Entomostraca 1. Subclass Branchiopoda. 1978..... 150.–
2. Alexandersen, Verner: Sūkās V. A Study of Teeth and Jaws from a Middle Bronze Age Collective Grave on Tall Sūkās. 1978. (Publications of the Carlsberg Expedition to Phoenicia 6. The other reports from this expedition are printed in the *Historisk-filosofiske Skrifter*, including no. 5, *Hist.-fil. Skr.* 10:1, with the report of the excavation in question: Henrik Thrane: Sūkās V, 1978, 100 DKr.) 80.–
3. Böcher, Tyge W. and Olesen, Peter: Structural and Ecophysiological Pattern in the Xero-Halophytic C_4 Grass, *Sporobolus rigens* (Tr.) Desv..... 100.–

Printed in Denmark by Bianco Lunos Bogtrykkeri A/S. ISBN 87-7304-063-0